2001

The Chemical Mechanism of a Brown-Rot Decay Mimtic System and its Application in Paper Recycling Processes

Yuhui Qian

THE CHEMICAL MECHANISM OF A BROWN-ROT DECAY MIMETIC SYSTEM AND ITS APPLICATION IN PAPER RECYCLING PROCESSES

By

Yuhui Qian

B.S. Nanjing Forest University, 1991

M.S. Nanjing Forest University, 1994

A THESIS

Submitted in Partial Fulfillment of the

Requirements for the Degree of

Master of Science

(in Forestry)

The Graduate School

The University of Maine

December, 2001

Advisory Committee:

Barry S. Goodell, Professor of Wood Science and Technology,
Co-operating Professor of Chemical Engineering and the Advanced Engineered Wood Composites Center, Advisor

Joseph M. Genco, Professor of Chemical Engineering,
Calder Professor of Pulp and Paper Science and Engineering

Jody Jellison, Professor of Molecular Plant Pathology
Co-operating Associate Professor of Forestry and Microbiology

THE CHEMICAL MECHANISM OF A BROWN-ROT DECAY MIMETIC SYSTEM AND ITS APPLICATION IN PAPER RECYCLING PROCESSES

By Yuhui Qian

Thesis Advisor: Dr. Barry S. Goodell

An Abstract of the Thesis Presented
in Partial Fulfillment of the Requirements for the
Degree of Master of Science
(in Forestry)
December, 2001

This work is aimed at improving our current knowledge of the non-enzymatic mechanisms involved in brown-rot decay, as well as the exploration of potential applications of a brown-rot mimetic model system in paper recycling processes. The study was divided into two parts. The first part focussed on the chemical mechanisms involved in chelation and reduction of iron by a low molecular weight chelator (isolated from the brown-rot fungus *Gloeophyllum trabeum*) and its model compound 2,3-dihydroxybenzoic acid (2,3-DHBA). Chelation as well as free radical generation mediated by this system were studied by ESR measurement. The results indicate that the effects of the chelator/iron ratio, the pH, and other reaction parameters on hydroxyl radical generation by a Fenton type system could be determined using ESR spin-trapping techniques. The results also support the hypothesis that superoxide radicals are involved in the chelator-mediated Fenton process. In the second part of the study, the effect of a chelator-mediated Fenton system for the improvement of deinking efficiency and the

modification of fiber and paper properties was studied. For the deinking study, copy paper was laser printed with an identical standard pattern. Then repulping and flotation operations were performed to remove ink particles. Under properly controlled deinking conditions, the chelator mediated treatment (CMT) resulted in a reduction in dirt count over that of conventional deinking procedures with no significant loss of pulp strength. To study the effect of the chelator system treatment on the quality of pulp with different fines content, a fully bleached hardwood kraft pulp was beaten to different freeness levels and treated with the chelator-mediated free radical system. The result shows that virgin fiber and heavily beaten fiber respond differently to the free radical treatment. Unbeaten fibers become more flexible and easier to collapse after free radical treatment, while beaten fibers show a reduction in fines and small materials after mild free radical treatment.

ACKNOWLEDGEMENTS

Many thanks to Dr. Barry Goodell, my major advisor, for his continual academic guidance, moral encouragement and support in the past three years of study. I have benefited greatly from his innovative suggestions and academic resourcefulness. I would also like to extend my sincere thanks to the other members of my advisory committee, Dr. Joseph Genco and Dr. Jody Jellison for their time spent on the manuscript and constructional comments and suggestions.

I would like to thank Dr. Heok Kwon and Dr. Donna Johnson in the Department of Chemical Engineering, for their assistance and patience during my experiments.

Sincere thanks to Dr. Christopher Felix and his co-workers in the National Biomedical EPR Center at the Medical College of Wisconsin, for their assistance during the ESR experiments.

My appreciation goes to all the faculty and graduate students of Wood Science and Technology, for their effort of making this program so active and fruitful.

Thanks, Grandma, for being my inspiration throughout my life. All I did is for you.

TABLE OF CONTENTS

LIST OF TABLES

LIST OF FIGURES

PREFACE

This work focuses on iron binding, iron reduction, and free radicals that are generated in a process related to a non-enzymatic mechanism employed by brown-rot fungi in the decay of wood. UV/VIS spectroscopy, direct electron spin resonance (ESR), and ESR spin trapping techniques were used in the investigation. A mediated Fenton system was developed to mimic the early stages of non-enzymatic brown-rot activity. This bio-mimetic system was also evaluated for its application in paper recycling process and its effect on fiber characteristics.

The work in this thesis includes four chapters. Chapter 1 covers: 1) A general review of the non-enzymatic brown-rot decay mechanism. 2) An introduction to ESR, and ESR- spin trapping techniques and their application to wood decay. 3) A review of the basic steps in paper recycling, enzymatic deinking, and enzymatic modification of fiber and paper properties. This section also covers biological substitutes for some of the chemicals used in the paper making process with the goal of minimizing the environmental impact involved with the use of pulping chemicals, and also the goal of reducing operating costs. The effect of the chelator system on iron binding, reduction, and free radical generation as studied by ESR measurement is summarized in Chapter 2. In Chapters 3 and 4, the use of the mediated Fenton system in deinking of laser printed copy paper and in modifications of fiber and paper properties are studied respectively.

Chapter 1

LITERATURE REVIEW

1.1. Brown-rot Decay of Wood

Serious microbiological deterioration of wood can be caused by fungi. Brown-rot decay is the most common type of decay found in softwoods and it is the most destructive type of decay seen in wood products because it can cause rapid structural failure. Wood attacked by brown-rot fungi, in advanced stages, darkens and breaks into cubically shaped pieces that crumble easily into a brown powder. Brown-rot fungi rapidly utilize the hemicelluloses and cellulose of the cell wall, leaving the lignin modified but essentially undigested (Cowling, 1961; Illman *et al.*, 1989; Kirk *et al.*, 1991).

1.1.1. Non-enzymatic Mechanisms Involved in Brown-rot Decay

Historically, the degradation of wood by brown-rot fungi was considered a pure enzymatic process (Reese *et al.*, 1950). But later it was recognized that even the smallest cellulases are too large to penetrate the pores of the wood cell wall (Cowling *et al.*, 1969). Halliwell *et al.* (1965, 1984) reported that cotton cellulose could be degraded by Fenton's reagent (H_2O_2/Fe^{2+}), which generates hydroxyl radicals or a similar oxidizing reagent. Kirk *et al.* (1991) compared pure cellulose degraded by brown-rot fungi with cellulose treated with different oxidants. Agosin *et al.* (1989) also studied the changes in lignin during brown-rot degradation. It was found that changes in cellulose and lignin caused by brown-rot decay are consistent with an oxidative mechanism. Based on these observations, Halliwell (1965, 1988) proposed the possible existence of a non-enzymatic system involving peroxide and iron. Koenigs (1972, 1974) also found that brown-rot fungi produce extracellular hydrogen peroxide, and wood may contain enough iron, and

thus lended support to Halliwell's hypothesis. Cobb (1981) demonstrated direct evidence for a non-enzymatic decay mechanism. In his experiments, liquid cultures of *Gloeophyllum trabeum* were incubated in an apparatus with two chambers where ^{14}C labeled cellulose was separated from the fungus by an ultrafiltration membrane. The membrane prevented the passage of enzymes between the two chambers. Under these conditions, $^{14}CO_2$ and other radioactive water-soluble products were still detected in the growth chamber. These observations directly support the hypothesis that a non-enzymatic mechanism is involved in brown-rot decay caused by *G. trabeum*.

1.1.2. The Role of Low Molecular Weight Decay Agents

Many researchers have demonstrated that Fenton chemistry (Eq. 1) is the most likely candidate for the non-enzymatic decay mechanism (Highley, 1980; Schmidt *et al.*, 1981; Cohen, 1985):

$$Fe^{2+} + H_2O_2 \rightarrow Fe^{3+} + HO^{\bullet} + HO^{-} \quad (1)$$

One potential problem with the Fenton system is that virtually all iron in oxygenated environments exists in various oxidized forms rather than as Fe^{2+}. Winterbourn (1991) showed that iron in aqueous environments tends to aggregate as insoluble oxygen-bridged polymeric complexes at physiological pH. Therefore, in order for the Fenton reaction to occur, there must be a mechanism to first extract iron from its oxyhydroxide forms, and then reduce the oxidized ferric iron to Fe^{2+}. It has been suggested that a low-molecular-weight decay agent may be involved in brown-rot decay, at least in its initial stages. The agent must be small enough to penetrate the cell wall, and it must have iron reduction capability as well. Recently, extensive research has been focused on the isolation and characterization of the low-molecular-weight decay agents

involved in brown-rot decay (Goodell *et al.*, 1997; Tanaka *et al.*, 1994; Jellison *et al.*, 1991a; Paszczynski *et al.*, 1999; Kerem *et al.*, 1999; Shimada *et al.*, 1994; Green *et al.*, 1991; Hyde and Wood, 1995).

Oxalic acid was proposed by Schmidt *et al.* (1981) to play a role in reduction of Fe^{3+} to Fe^{2+}, which increased cellulose decomposition by the Fenton reaction. However, Tanaka *et al.* (1994) reported that at higher concentrations of oxalic acid, cellulose degradation by the Fenton's system is inhibited. Furthermore, it was observed that iron reduction by oxalic acid is a light-dependent reaction (Zepp *et al.*, 1992; Sulzberger and Laubscher, 1995) and wood decay occurs primarily in the dark.

Hyde and Wood (1995) proposed a model for attack at a distance from the hyphae of the brown-rot fungi *Coniophora puteana*, based on the formation of H_2O_2 by autoxidation. *C. puteana* produces cellobiose dehydrogenase (CDH), which reduces Fe^{3+} to Fe^{2+}. Diffusion of Fe^{2+} away from the hyphae in a low pH environment promotes conversion to Fe^{2+}-oxalate and autoxidation with H_2O_2 as the product. The critical Fe^{2+}/H_2O_2 combination could therefore be formed at a distance. A weakness of this hypothesis as outlined by Paszczynski *et al.* (1999) is that the reaction rate of iron with CDH is very low, and CDH is produced by few brown-rot fungi.

The brown-rot fungus *T. palustris* (Hirano *et al.*, 1995) has been shown to produce a glycopeptide of MW 1000 – 1500, which is capable of reducing Fe^{3+} to Fe^{2+} but which binds the Fe^{2+}. The composition of the "glycopeptide" has not been reported, nor has a mechanism for its function been described.

It has been found that the brown-rot fungus *G. trabeum* produces extracellular iron-binding metabolites (termed Gt-chelator), which have been proposed to catalyze the

Fenton reaction during initial wood decay stages (Jellison *et al.*, 1991a; Goodell *et al.*, 1997). Low molecular weight phenolate derivative chelators (< 1000 MW) have been isolated and partially purified from the brown-rot fungus *G. trabeum* cultures (Fekete *et al.*, 1989; Lu, 1994; Goodell *et al.*, 1994, 1997), and it has been shown that Gt-chelators have a high affinity for Fe^{3+} and a strong Fe^{3+} reducing capability. It was also observed that Gt-chelator promotes the redox cycling of iron, which consequently promotes the Fenton reaction because of very limited iron levels in some wood (Goodell *et al.*, 1997; Jellison *et al.*, 1997).

Paszczynski and co-workers (1999) extracted *G. trabeum* culture supernatant with methylene chloride, and analyzed the concentrated extract by GC-MS. Several benzene derivatives were detected, including a dimethoxycatechol (4,5- dimethoxycatechol) and a quinone (2,5-dimethoxyhydroquinone). The purification of these compounds is consistent with the work done with partially purified preparation from *G. trabeum* as outlined previously by Goodell *et al.* (1997).

Based on current study on the iron chelation and reduction by the phenolic chelators, a mechanism of chelator redox process is proposed in Figure 1.1.

1.2. ESR Technology and Its Application in Wood Decay Studies

1.2.1. ESR and ESR Spin-trapping Techniques

Electron Spin Resonance (ESR), also known as Electron Paramagnetic Resonance (EPR), is an attractive technique for the identification and study of species containing unpaired electrons (radicals and certain transition metal species). ESR spectroscopy involves the flipping of electron spins between two different energy levels, an act that is

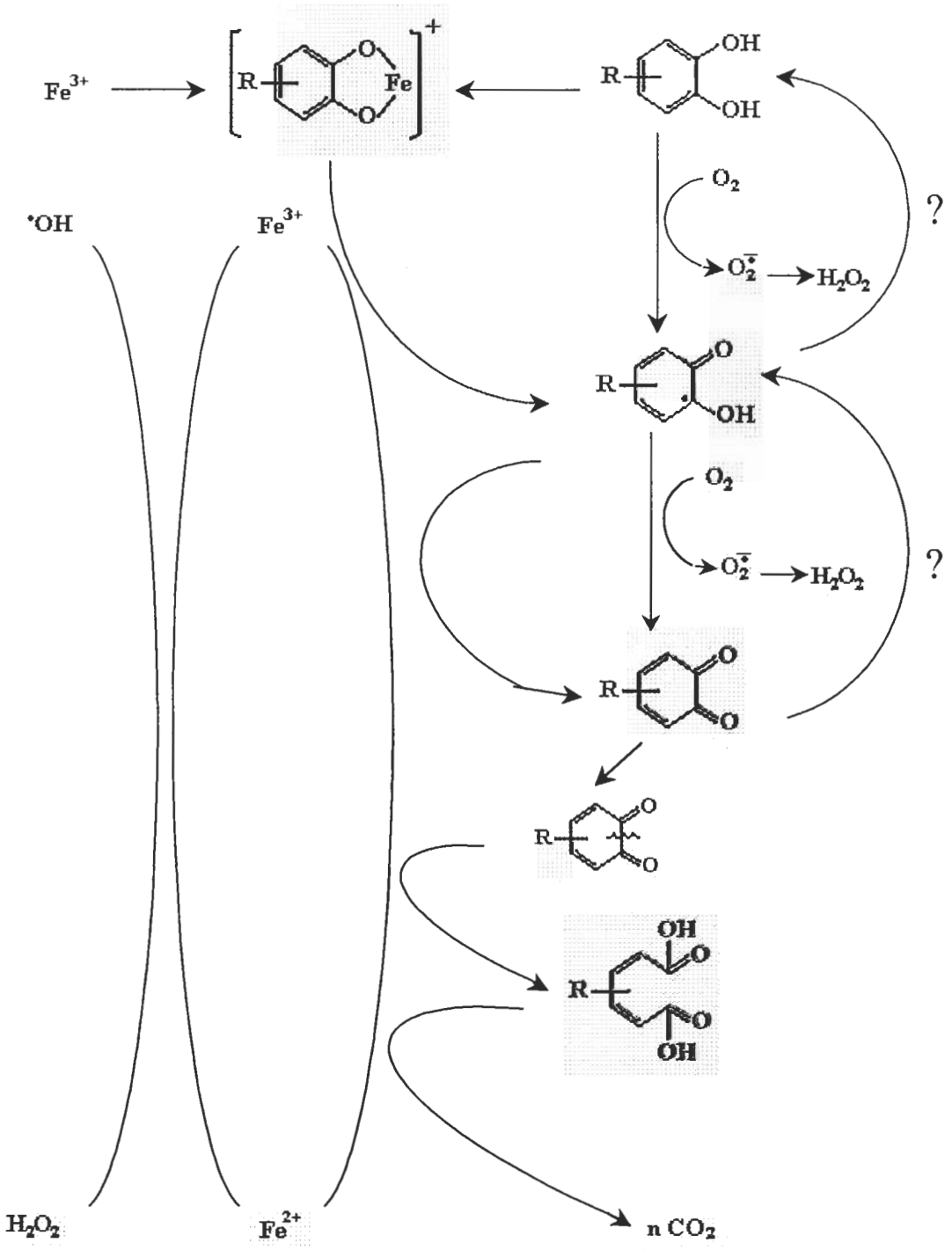

Figure 1.1. Proposed Mechanism for Chelator Redox and Free Radical Generation Processes Involving Ferric Iron and Catechol-like Phenolic Compounds.

caused by the absorption of microwave radiation (Wertz and Bolton, 1972). ESR was discovered by Zavoisky in 1944. Since then, a wide range of applications of ESR in chemistry, physics, biology, and medicine have been published. ESR usually requires microwave-frequency radiation (GHz), and only those samples with at least one unpaired electron can be detected. Basically, ESR is conducted in the presence of a static magnetic field, samples containing unpaired electrons will show a resonant absorption when the frequency of the microwave radiation is appropriate to the energy difference between two spin states of the electrons in the sample (Weil *et al.*, 1996).

ESR is considered to be the least ambiguous method for the detection of free radicals. However, for most short-lived free radicals, especially oxygen-based free radicals, ESR spectrum are difficult to observe directly, especially under physiological conditions. This is due either to the very short relaxation time of the radical resonance, or because the radicals are not present at a high enough concentration to be detected by standard ESR spectrometers. A decrease in sample temperature may redress this effect, but this usually reduces any physiologically significant aspects of the ESR spectrum (Chopard, 1992). However, spin trapping allows the formation of relatively stable free radical products, thereby allowing their detection at room temperature. The technique of spin trapping was first developed by Janzen and Blackburn (Janzen *et al.*, 1969). Perkins (1980) presented a very detailed review of the development of ESR spin-trapping techniques. In the spin trapping procedure, a very reactive short-lived free radical reacts with a diamagnetic compound (the spin trap) to produce a relatively long-lived free radical product (the spin adduct), which can be detected by standard ESR spectrometry. Compared with other free radical determination methods, spin trapping often reveals

more information about the production of free radicals in biochemical and biological systems.

Frequently used spin traps include Nitroso compounds (2-nitroso-2-methylpropane), PBN(*N-tert*-butyl-α-phenylnitrone), and DMPO (5,5-dimethylpyrroline-*N*-oxide). Among them, DMPO is perhaps the most popular spin trap currently in use (Buettner, 1985).

1.2.2. ESR Study of Iron Chelation and Free Radical Generation Systems

Iron is an essential element in the chemistry of living systems. Although the metal is relatively abundant in the earth's crust, it is inaccessible to microorganisms under normal conditions due to the formation of insoluble hydroxides (Hartwig and Loepper, 1993). In many woods, only a very limited amount of iron exists, and it has been found in the 0-2 μM range in non-decayed wood (Jellison *et al.*, 1992). As an evolutionary response to this stress, microbes produce low molecular weight organic ligands (siderophores or chelators), which effectively solubilize ferric ion for transport into the cell (Neilands, 1974). Siderophore activity has not been demonstrated in wood degrading fungi but some chelators produced by these fungi not only have high affinity for iron, but also demonstrate strong iron reduction ability (Goodell *et al.*, 1997; Chandhoke, 1991). In the wood degradation process this iron reduction ability would be very important for hydroxyl radical production via Fenton reactions. This reaction has been hypothesized to be essential in early stages of wood degradation by brown-rot fungi.

Iron chelation and free radical generation can be studied by using ESR and ESR-spin trapping techniques respectively. Kalyanaraman *et al.* (1991) studied the interactions between the adriamycin semiquinone, hydrogen peroxide, iron-chelators, and radical

scavengers by using direct ESR and spin trapping techniques. In the presence of iron-chelators, semiquinone appears to react with peroxide, forming the hydroxyl radical. In direct ESR spectroscopy, a signal at g = 4.3 is typical of high-spin ferric iron in a low-symmetry environment (Beinert, 1972). This type of signal is found in a wide variety of organic and inorganic materials, and it's intensity usually depends on the presence of chelators. In some cases, the relative amount of ferric ions bound to chelators has been determined by measuring ESR signal intensities of characteristic iron chelator complexes (Zareba, 1995). Illman (1988) and her co-workers used ESR spin trapping to detect the presence of hydroxyl radicals during the growth of the brown-rot fungus *Postia placenta*.

1.3. Paper Recyclingfor MOW

The pulp and paper manufacturing industry is one of the largest wood consumers today. Along with increasing world economic growth, a substantial increase in paper consumption is expected. This means that more trees will be harvested and more solid waste will be created as paper products are consumed and disposed of. Because of the environmental and economic concerns associated with the consumption of our forest resources the paper industry could well experience a limited raw material resource with concurrent reduction of industry growth. Therefore, "recycling" as a solution to this problem is attracting more and more attention since it is an effective way to preserve forest resources, and save energy and landfill space.

1.3.1. Basic Steps in Paper Recycling

A primary objective of recycling processes is to decrease the amount of residual ink specks in deinked paper and increase the brightness of the final products. Traditional

deinking process steps include swelling, repulping, screening, flotation, and washing operations (McKinney, 1995). Repulping is the first step of secondary fiber utilization. Depending on their design or function, secondary-pulping devices may be used as dispergers, fiberizers, or deflakers. The objective of screening and cleaning is the removal of non-fibrous contaminants, with minimal losses of useful fiber. Actual deinking is by two methods, washing and flotation. During repulping, ink is broken into particles, which are suspended in the pulping liquid. Deinking is the process of separating these particles from fiber material. After repulping, small ink particles are effectively removed by subsequent washing stages with the wash filtrate. Flotation is the most important operation in deinking, especially for the removal of electrostatic toners. Basically, ink particles are more hydrophobic than paper fibers, which is the basis of separation by flotation. To increase the deinking efficiency, different chemicals are used in the deinking processes. A typical chemical deinking treatment consists of 0.5% NaOH, 3.0% Na_2SiO_3, 0.4% H_2O_2, and 0.5% DTPA (Hamilton *et al.* 1987).

1.3.2. Enzymatic Deinking

The growing use of various coated papers and laser-printed or photocopied papers has created special recycling problems that conventional deinking processes handle poorly. These types of inks contain plastic polymers that melt together and bond to the fibers. Conventional repulping with chemicals does not effectively remove the cured toner from the fiber surface (Jeffries, 1994). In order to improve the deinking of laser-printed paper, additional dewatering, dispersion steps, and more washing and flotation are needed. Some specific mechanical devices such as kneaders and dispergers have been developed to deink mixed office waste (MOW) (McBride 1994). Because of technical

and economic problems, less than 10% of laser printed papers are recycled back into printing and writing grades. There would be significant benefit if an effective means were found to release toners from office waste. Biotechnology may provide some potential solutions to these problems, and enzymatic deinking has received increasing attention in this regard. Many types of hydrolytic enzymes (especially cellulase and hemicellulase) have been investigated for their ability to improve deinking performance with non-impacted printed paper (Heitman, 1992; Zollner, 1997; Jobbins, 1997). However, the mechanism of enzyme-enhanced deinking is still not entirely clear. In some references, the effect of enzymatic deinking is thought to be the result of a peeling effect. Cellulases can peel away cellulose microfibrils from the fiber surface, which aids in the release of ink particles. Other researchers attribute the increase of deinking efficiency to the removal of fines (Jackson, 1993). The improved drainage of the pulp can increase the efficiency of flotation significantly.

1.3.3. Enzymatic Modifications of Fiber and Paper Properties

The application of biotechnology in the manufacture of pulp and paper is receiving increasing attention. Enzyme technology has been investigated in various processes in the pulp and paper field (Daniels, 1992). These include enzymatic bleaching, pretreatment of mechanical pulp (enzymatic refining), modification of pulp properties such as drainage and fiber flexibility, and facilitation of contaminant removal from recycled fibers. Some enzymes are specific for cellulose, which is the dominant component of the fiber surfaces. Although the degradation of carbohydrates may lead to the loss of fiber strength, we still can take advantage of this reaction in paper manufacture if the reaction can be controlled. Previous work has shown that selected mixtures of

enzymes can increase the freeness of pulp under certain conditions with little or no loss in physical properties (Jackson, 1993; Pommier *et al.*, 1989). Laboratory investigations also confirmed that cellulase treatment of coarse fibers can result in both enhanced fiber flexibility and collapsibility, which consequently improves sheet consolidation (Mansfield *et al.*, 1998). Therefore, it should be possible to apply enzymatic reactions specific to holocellulose in papermaking, especially in paper recycling. Increasing interest has been generated in this area since, compared to chemical processes, biotechnology has apparent environmental and economic advantages.

Chapter 2

THE EFFECT OF LOW MOLECULAR WEIGHT CHELATORS ON IRON CHELATION AND FREE RADICAL GENERATION AS STUDIED BY ESR MEASUREMENT

2.1. Abstract

Gt-chelator is a partially purified mixture of low molecular weight compounds isolated from the brown rot fungus *Gloeophyllum trabeum,* it was previously shown to have a high affinity for iron and also a strong iron reducing ability (Goodell *et al.*, 1997). These characteristics suggest that Gt-chelator plays a role in non-enzymatic wood decay process, especially in a Fenton type free radical system. Gt-chelators were identified as catecholate phenolics in the previous studies (Jellison *et al.*, 1991a; Chandhoke *et al.*, 1992). Therefore, 2,3–dihydroxybenzoic acid (2,3-DHBA) was used as a model compound for the Gt-chelator in the ESR studies. In this work, the binding between a chelator model compound and ferric iron was studied by ESR spectroscopy. The effects of the chelator model compound, Fenton reagents, as well as the reaction conditions on free radical generation were also studied using ESR spin-trapping techniques. The results indicate:

1. The relative amount of ferric iron bound to chelators is directly related to the chelator / iron ratio in the system. The relative quantity of the chelator-iron complex can be determined by measuring the intensities of the characteristic g4.3 ESR signal.

2. The effects of the chelator/iron ratio, pH, and other reaction parameters on hydroxyl radical generation in a Fenton type system could be determined using ESR spin-trapping techniques.

3. Data support the hypothesis that superoxide radicals are involved in the chelator mediated Fenton processes.

2.2. Introduction

While many wood decay fungi produce highly active enzyme systems, non-enzymatic depolymerization systems have also been proposed to have a role in fungal wood decomposition processes (Reese, 1977). Previous research has suggested that highly reactive free radicals such as the hydroxyl radical (·OH), produced via the Fenton reaction or other one electron reactions, are responsible for the cleavage of wood components at least in early stages of wood decay (Illman, *et al.*, 1989; Backa, *et al.*, 1992). Hydroxyl radicals have been detected in both white rot and brown rot fungi (Backa, *et al.*, 1993; Koenigs, 1972; Koenigs, 1974). Therefore, it is possible that in wood degradation, the wood structure is opened up by the attack of free radicals in early degradation stages to permit easier penetration of relatively larger enzymes at later stages.

Goodell *et al.* (1997) has studied the mechanisms related to the biodegradation of wood by brown-rot fungi, especially *Gloeophyllum trabeum*. They present data which suggest that hydroxyl radicals generated by a chelator mediated Fenton reaction may be responsible for the biodegradation of wood by brown rot fungi, at least in initial stages of degradation. In their work, low molecular weight phenolic compounds (termed Gt-chelators) were isolated and characterized using GC/MS and LC/MS. Gt chelators were identified as catecholate phenolics that could reduce ferric iron to efficiently catalyze Fenton reactions. Although much of the mechanism involved in Gt chelator catalyzed

$^{\bullet}OH$ production has been worked out, a redox cycling mechanism may promote the production of multiple moles of hydroxyl radical per mole of iron. This mechanism has not yet been explored adequately and must still be studied for greater understanding of wood biodegradation.

Recently, Pracht (2000) demonstrates a "breakdown" mechanism during the redox process between ferric iron and catechol or guaiacol etc. phenolic substances. Their work shows that catechol and guaiacol will be effectively oxidized to CO_2 by reducing ferric iron, which may explain the multiple iron reduction observed in the redox process involving ferric iron and phenolic chelators. In their work, the molar ratio between the resultant Fe(II) and catechol is around 6:1, and a corresponding CO_2 production is detected, this implies that the breakdown phenolic compounds are the possible electron sources for the multiple iron reduction during the redox process.

Iron plays an essential role in fungal growth. Many microorganisms have an efficient system to sequester ferric iron and other transition metal ions (Smith, *et al.*, 1990; Lopez, *et al.*, 1992). In some systems, reducing agents such as ascorbic acid, caffeic acid, and gallic acid etc. are involved to accelerate hydroxyl radical formation by reducing Fe^{3+} to Fe^{2+} (Moran, 1997; Halliwell, *et al.*, 1989). Therefore, the catalytic properties of iron in a Fenton type system will greatly depend on the nature of the chelator binding the iron (Aust, *et al.*, 1991; Gelvan, *et al.*, 1991). In previous work by Goodell *et al.* (1997), Gt-chelators were shown not only to have strong affinity for ferric ions, but also were capable of reducing multiple ferric ions to ferrous ions. Structural data indicated that catecholate phenolics are the components of the Gt chelator partially

purified fraction. Therefore, in this thesis, 2,3-dihydroxybenzoic acid (2,3-DHBA) was used as a model compound of Gt-chelator in iron binding and reduction study.

The iron chelating ability of some phenolic compounds is usually attributed to the high nucleophilic aromatic rings or the presence of chelating groups such as pyrogallol, catechol, or ortho-hydroxy-carbonyl groups (Moran, 1997; Laughton, 1989). Many of these phenolic compounds are also capable of reducing Fe^{3+} to Fe^{2+}, which will react with H_2O_2 to give hydroxyl radical and other highly reactive species (Halliwell and Gutteridge, 1988).

Electron spin resonance (ESR) is a particularly powerful method for studying molecular species that possess unpaired electrons, such as transition metal ions and some free radicals (Cowan, 1993). In this thesis, the binding of iron with Gt chelator and its model compound (DHBA) was studied by ESR methodology. Iron reduction was quantitatively measured by ferrozine assay, and the effect of these iron chelators on hydroxyl radical formation was determined by ESR - spin trapping. DMPO was used as a spin trap since it produces an easily identifiable spin adduct with hydroxyl radicals and it usually has high solubility and superior trapping efficiency (Buettner, 1985).

2.3. Materials and Methods

2.3.1. Chemicals Preparation

A Gt-chelator mixture of phenolic compounds was isolated from the brown rot fungus *Gloeophyllum trabeum* by ultrafiltration (< 1000 dalton) and extraction with ethyl acetate as previously described (Goodell *et al.*, 1997). The concentration of Gt-

chelator was determined by Arnow and Rioux assay and 2,3-dihydroxybenzoic acid (DHBA) was used to develop a standard curve.

Purchase of 2,3 – dihydroxybenzoic acid, $FeCl_3$, and hydrogen peroxide was from Sigma Chemical (St. Louis, MO). Purchase of 5,5–dimethyl-1-pyrroline-1-oxide (DMPO) and superoxide dismutase (SOD) was from Aldrich Chemical (Milwaukee, WI). In order to avoid iron or other metal ion contamination, deionized water was used to make all solutions, and all material was disposable (plastic) or acid washed (glass).

2.3.2. Iron Chelation Study

The binding of iron by Gt-chelator or 2,3-DHBA was examined via electron spin resonance spectroscopy. The relative amount of ferric ion bound to the chelator could be assessed by comparing the ESR signal intensities of the high spin ferric complex to that of the uncomplexed chelator. ESR measurements were carried out on an IBM-Bruker ER200D ESR spectrometer at the National Biomedical ESR Center, Medical College of Wisconsin, Milwaukee, USA. A field modulation of 100 kHz was employed and the spectrometer was operated in the X-band region. Ferric complex samples were run as frozen solutions at both liquid nitrogen (77K) and liquid helium (15K) temperatures. Unless specifically mentioned, ESR spectra were measured under the conditions shown in Table 2.1. Figure 2.1 shows the direct ESR spectra of the iron/Gt-chelator complexes. The peak at g 4.3 is typically assigned to high spin ferric complexes (Shinde, 1991) indicated the binding of ferric iron by the Gt-chelator.

Table 2.1. Direct ESR Parameters

ESR parameters	
Temperature	77 K
Sweep field	2,500 ± 2,500 G
Scan time	300 sec
Time constant	1 sec
Modulation frequency	100 kHz
Modulation amplitude	5 G
Microwave power	4.9 mW
Overall receiver gain	1.25×10^5

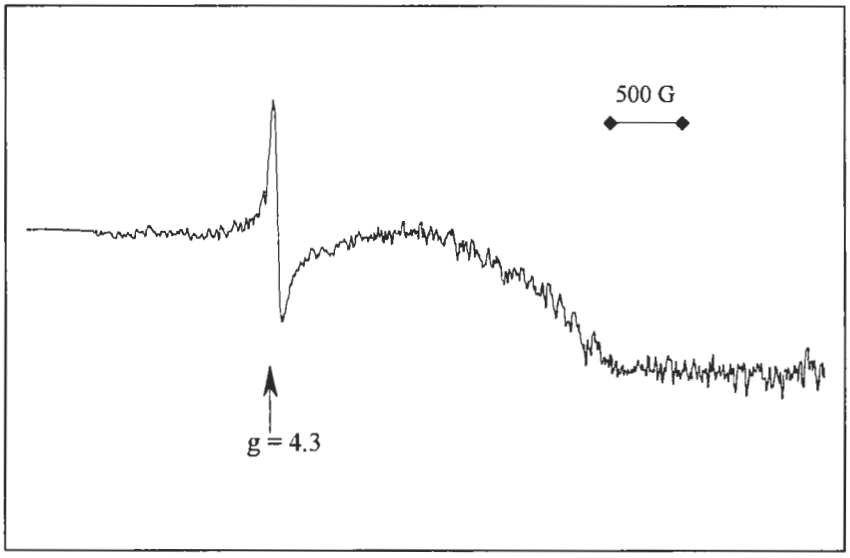

Figure 2.1. ESR Spectra of Gt-chelator / Fe(III) Complexes (recorded at 77 K). Sample contains: 62.5 μM Gt chelator, 3.1 mM Fe(III), and 20 mM pH 4.0 acetate buffer. After incubation at room temperature for 2 minutes the solution was frozen and transferred to an ESR cell for analysis.

2.3.3. Iron Reduction Study

The reduction of ferric iron in aqueous solutions was determined by the ferrozine assay (Goodell *et al.*, 1997; Stookey, 1970; Gibbs, 1976). The ferrozine reagent, 3-(2-pyridyl) 5,6-bis (4-phenylsulfonic acid)-1,2,4-triasine, complexes with ferrous ions to form a strongly colored complex, which can be conveniently measured in the spectrophotometer with molar absorptivity of 2.79×10^4 (Stookey, 1970). The calibration curve for Fe(II) determination (concentrations 0-200 μM of $FeCl_2$) by the ferrozine assay (1.0 mM ferrozine reagent in pH 4.0 acetate buffer, 100 mM) is shown in Appendix A. Ferrozine reagent was added into assay solutions and incubated for 5 minutes before readings at 562 nm was taken. Ferrozine reacts with Fe(II) and therefore can pull the equilibrium between Fe(II) and Fe(III) over long periods of time. Care was therefore taken read the reactions consistently at 5 minutes reaction time.

2.3.4. Determination of Hydroxyl Radical by ESR - Spin Trapping

Hydroxyl radicals were generated by a Fenton type system in a reaction mixture consisting of ferric ions, reducing chelators, and hydrogen peroxide. The pH tested was 2.4 and 4.0. Hydrogen peroxide was added to the system last to trigger the reaction, and the reaction mixture was then rapidly introduced into an aqueous flat cell and ESR observations were begun. ESR spectra were recorded at room temperature after incubation for a specified time. The yield of the free hydroxyl radicals was determined by the formation of characteristic DMPO-OH spin adducts, using DMPO as the spin trap reagent. A typical incubation mixture consisted of: 10 mM DMPO, 20 mM pH 4.0 (2.4) buffer, 1 mM Fe(III) (as ferric chloride), 1 mM H_2O_2, and 2,3-DHBA (at concentrations

ranging from 0.05 mM to 5 mM) in a final volume of 1.0 ml. Solutions of iron salts, DMPO, and H_2O_2 were made up freshly just before use. Superoxide dismutase (SOD) was also used in the experiments to study the involvement of superoxide radicals in this redox system.

Unless listed separately, the ESR settings used in the ESR-spin trapping experiments were as shown in Table 2.2. Distinct ESR spectra were observed for all Fenton based reactions when the DMPO spin trap was present in the system (Figure 2.2). The relative amount of DMPO-OH adducts formed in the system could be compared by integrating the peak area or by measuring the height of the signals.

Table 2.2. ESR Settings for Spin Trapping Measurement

ESR parameters	
Temperature	Room temperature
Sweep field	3,465 ± 100 G
Scan time	200 sec
Time constant	0.5 sec
Modulation frequency	100 kHz
Modulation amplitude	1 G
Microwave power	4.9 mW
Overall receiver gain	5.0×10^4

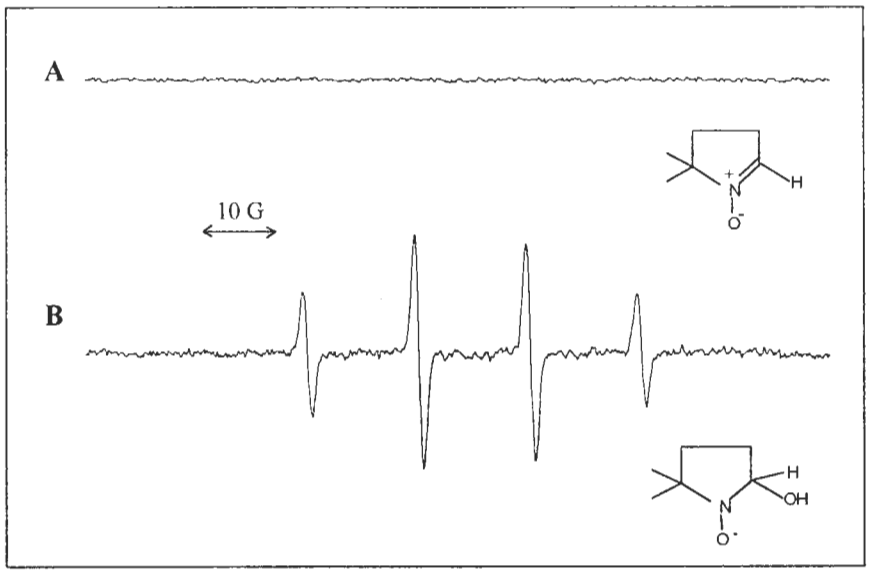

Figure 2.2. ESR Spectra of DMPO-Spin Adducts. Samples containing: **A)** 10 mM DMPO, 20 mM pH 4.0 acetate buffer, **B)** 10 mM DMPO, 20 mM pH 4.0 acetate buffer, 1 mM Fe(III), 1 mM H_2O_2, and 1 mM DHBA. The samples are incubated at room temperature for 5 minutes before recording the spectra.

2.4. Results

2.4.1. The Effect of DHBA / Iron Ratio

Because Gt-chelator is a mixture of phenolic compounds, to simplify analysis, we used the model compound 2,3 – dihydroxybenzoic acid (DHBA) that has previously been used as a model siderophore chelator and which is known to reduce iron similarly to the Gt chelator (Goodell *et al*, 1997). The iron binding and reducing ability of the model compound was studied as a function of chelator/iron ratio. The effect of chelator/iron ratio on free radical generation was also studied by ESR-spin trapping. Figure 2.3 shows the intensity change of g4.3 signal over time at different DHBA / iron ratios (mol / mol). It was observed that initial iron binding strength was directly related to the availability of chelators in the solution, with greater concentrations of DHBA promoting proportionally

greater DHBA/iron binding. Different binding kinetics were also observed for different iron/chelator ratios. At low DHBA iron ratios (DHBA:iron = 0.05:1), the g 4.3 signal increased over two hours incubation, indicating an increase in the binding of ferric iron by DHBA. When the DHBA/iron ratio was increased to 1:1 and 3:1, the intensity of g4.3 signal reached a maximum after 10 minutes incubation, then the strength of the signal decreased gradually (Figure 2.3).

These phenomena may be explained in terms of competition between the ability of DHBA to reduce ferric ions and to bind them. It has been proposed that ferric iron species react with catecholate derivatives through a two-step mechanism with the formation of an intermediate semiquinone radical (Mentasti *et al.,* 1997). Xu and Jordan (1988) studied the reduction of ferric iron by DHBA and concluded that the initial step involved a rapid binding of one Fe^{3+} to DHBA between the acid group and a neighboring hydroxyl group, forming a DHBA-iron complex. The complex then subsequently reduces additional Fe^{3+} and concurrently is oxidized to form a semiquinone intermediate. In the current work (low DHBA/iron ratios with iron in excess), the binding capacity was dependant on the available DHBA in the system. In previous work Goodell *et al.* (1997) proposed that at low pH's, DHBA may undergo "redox cycling" to cycle between the semiquinone and the hydroquinone state. In relatively high DHBA concentration (DHBA excess), more ferric iron binds to DHBA initially, and less free iron may be reduced. The ferrozine assay (Figure 2.4) and ESR-spin trapping results (Figure 2.5) confirm that excessive chelator may actually inhibit the iron reduction as the first formed iron chelate complex is produced. As a consequence, hydroxyl radical generation is reduced at high initial chelator concentration relative to the amount of iron present.

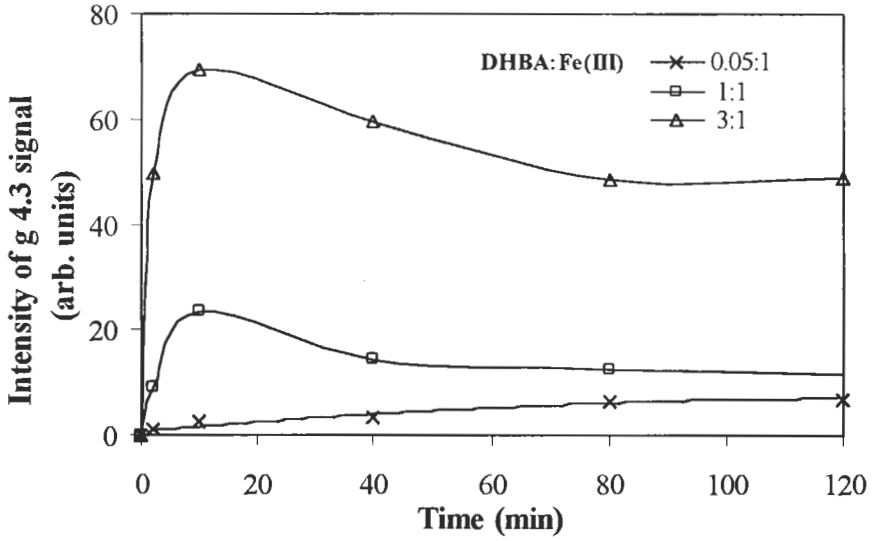

Figure 2.3. Time Course Study of the g 4.3 Signal Intensity at Different DHBA/Iron Ratios. Samples contains: (0.25 mM ~ 15 mM) 2,3-DHBA, 5 mM Fe(III), and 20 mM pH 4.0 acetate buffer. After incubation at room temperature from 2 minutes to 120 minutes, the solution was frozen and transferred to an ESR cell for analysis.

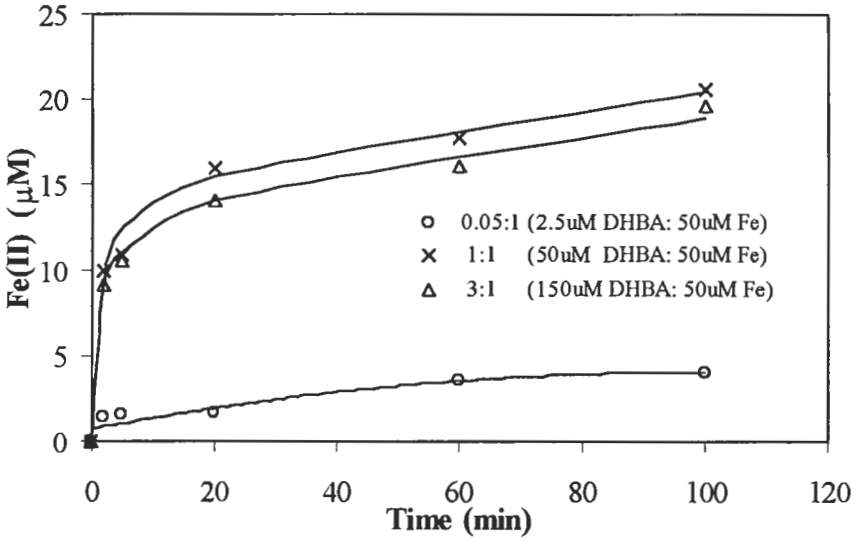

Figure 2.4. Effect of the DHBA/Fe Ratio on Ferric Iron Reduction Kinetics. Iron reduction was measured by using the ferrozine assay. 50 μM Fe(III) was incubated with (2.5 ~ 150 μM) DHBA at pH 4.0 acetate buffer (100 mM) for different time periods in the dark. Readings were made at 562 nm 2 minutes after adding ferrozine reagent (1.0 mM).

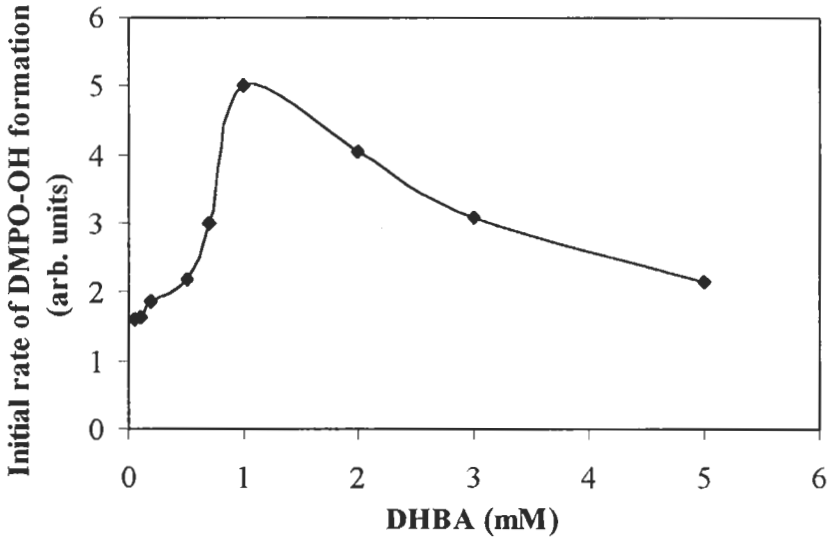

Figure 2.5. The Initial Rate of DMPO-OH Spin Adduct Formation as a Function of DHBA Concentration. Experimental conditions: DMPO 10 mM, pH 4.0 acetate buffer 20 mM, Fe(III) 1 mM, H_2O_2 1 mM. The relative rate of DMPO-OH production was set as an arbitrary unit. Samples were incubated at room temperature for 5 minutes before ESR measurements were taken.

Figure 2.5 shows the effect of the concentration of DHBA on the production of DMPO-OH adducts. The relative amount of free hydroxyl radical formed in the system can be determined by spin trapping techniques. In this work we measured the intensities of the DMPO-OH signals as DHBA concentrations were varied in the presence of Fenton reagents. The maximum formation rate of the DMPO-OH adduct in the initial stages is at about a DHBA/Fe^{3+} ratio of equivalence. Addition of greater or lesser amount of DHBA inhibited the initial rate of formation of free hydroxyl radicals significantly. One possible reason is that at the equivalent ratio with iron, DHBA has the most efficient reducing ability in the initial reaction stage.

The characteristic Fe^{3+}-DHBA binding signal is readily detected at liquid nitrogen temperatures (77 K), however, in a high magnetic field, the signal becomes broader and unclear. Lower temperature analysis was tested as a means to help alleviate this

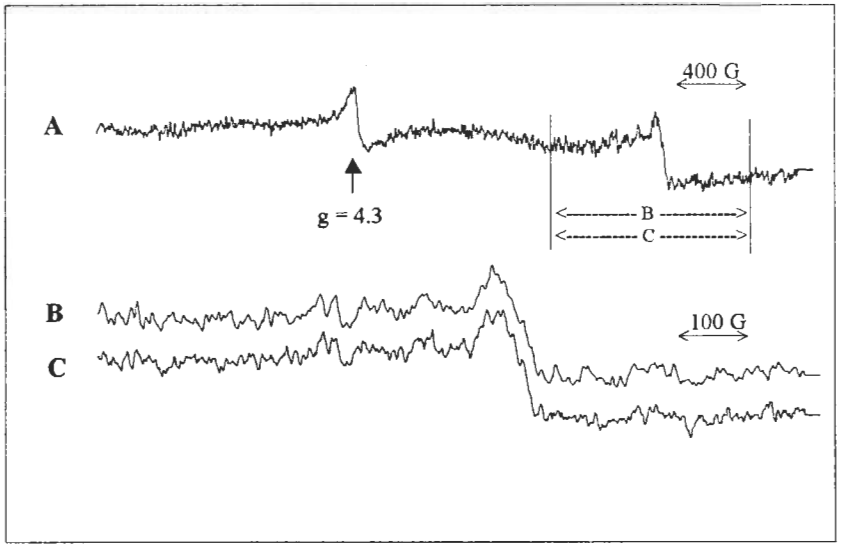

Figure 2.6. ESR Spectra of 2,3-DHBA / Fe(III) Complex (recorded at liquid helium temperature 15 K). Sample contained: 1 mM 2,3-DHBA, 1 mM Fe(III) and 20 mM pH 4.0 acetate buffer. ESR settings: **A)** sweep field 2,000 ± 2,000G overall receiver gain $1.25x10^4$. **B)** sweep field 3,200 ± 500G, overall receiver gain $2.5x10^4$. **C)** same sample and same ESR setting as B), except that the ESR cell was rotated 120°.

problem. Figure 2.6A shows the ESR spectra of the DHBA-Fe^{3+} complex in liquid helium (15 K). At this temperature many small peaks were resolved in the high magnetic field. In order to determine whether those signals represented data or just system noise, two more detailed scans (Figure 2.6B and 2.6C) were conducted in the high magnetic field (2,700 ~ 3,700 G). Measurement B and C are the same sample with the same ESR setting, except that the ESR cell was rotated 120° in run C. Comparison showed that the small peaks in the high magnetic field were real signals rather than system noise since the ESR spectra of measurement B and C were essentially identical. Typically, signals of this

type are assigned to microcrystalline iron, indicating the existence of particulate iron in solution. This was useful in helping us understand iron binding and reduction by chelators at different pH conditions because only dissolved iron will be bound and reduced by model chelators.

2.4.2. The Effect of pH

Figure 2.7 demonstrates that the binding of DHBA to ferric iron and the formation of microcrystalline iron are pH dependent.

Samples were prepared at pH 4.0 (Figure 2.7A) and at pH 2.4 (Figure 2.7B) respectively. At the lower pH, the g 4.3 signal increased and the signal for micro-crystalline iron was reduced. This was because of the better solubility of iron in the lower pH environment.

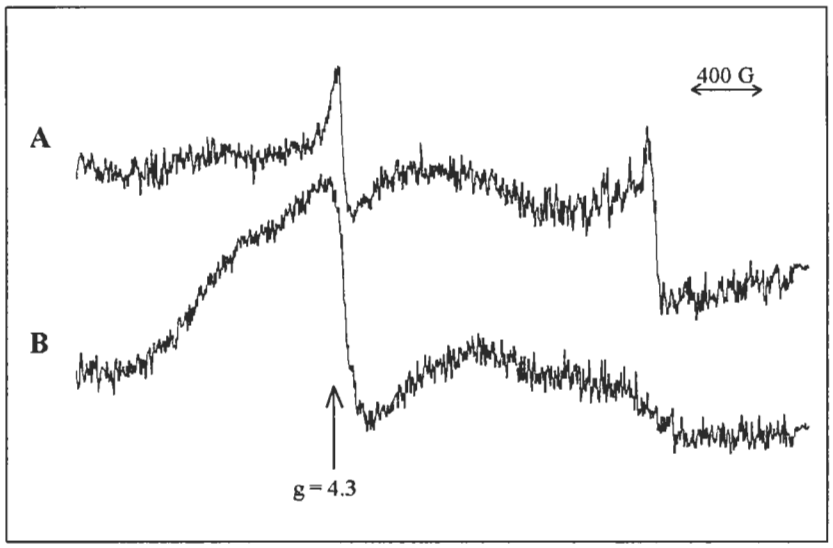

Figure 2.7. ESR Spectra of 2,3-DHBA / Fe(III) Complexes under Different pH Conditions. The spectra were recorded at liquid helium temperature (15 K). Samples contained: 1 mM 2,3-DHBA, 1 mM Fe(III), and **A)** 20 mM pH 4.0 acetate buffer, **B)** 20 mM pH 2.4 KCl-HCl buffer. After incubation at room temperature for 2 minutes, the solution was frozen in an ESR cell for analysis. ESR setting: sweep field 2,000 ± 2,000G, microwave power 20 mW, overall receiver gain 1.25×10^4, time constant 0.128 second, scan time 4 minutes.

The effect of the DHBA/Fe(III) ratio on the formation of free hydroxyl radicals was also investigated at different pH conditions (Figure 2.8). It was observed that at both pH 2.4 and 4.0 conditions, the maximum initial DMPO-OH production occurred at around a 1:1 DHBA/Fe^{3+} ratio. Greater or lesser ratios inhibited the formation of free hydroxyl radicals in the initial reaction stages. In the lower pH environment (2.4), an inhibition of •OH production at higher iron ratios was apparent.

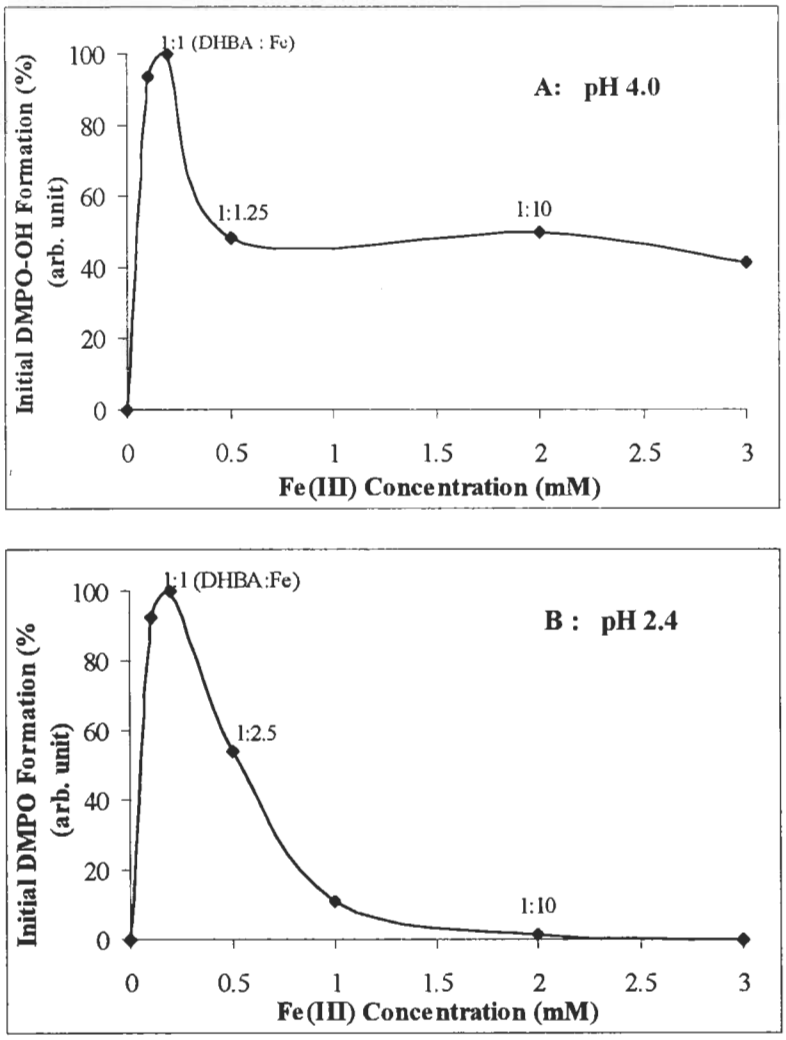

Figure 2.8. Initial DMPO-OH Production as a Function of DHBA/Fe Ratio. The samples contained: 10 mM DMPO, 0.2 mM DHBA, 1 mM H2O2, and **A)** 20 mM pH 4.0 acetate buffer, **B)** 20 mM pH 2.4 HCl-KCl buffer. Since the intensity of the DMPO-OH signal at pH 2.4 is much greater than that at pH 4.0, different ESR settings were used, and the percentage of DMPO-OH formation at 1:1 DHBA/Fe ratio was set to 100% arbitrarily for both pH conditions.

The effect of pH and DHBA/iron ratio on hydroxyl radical formation was also studied in a similar spin-trap experiment, which employed the same ESR settings (Figure 2.9). At a lower pH (2.4) and a 1:0.5 DHBA/iron ratio, the DMPO-OH signal was very strong, indicating greater Fenton reaction activity. It is possible that at lower pH the 2,3-

DHBA has a stronger reducing ability, and iron has better solubility. Therefore, more reduced iron would be available for Fenton reactions. However, at pH 2.4, excessive iron will inhibit the formation of the DMPO-OH adduct and in addition the DMPO-OH signal is relatively unstable and decays faster at pH 2.4 than at pH 4.0.

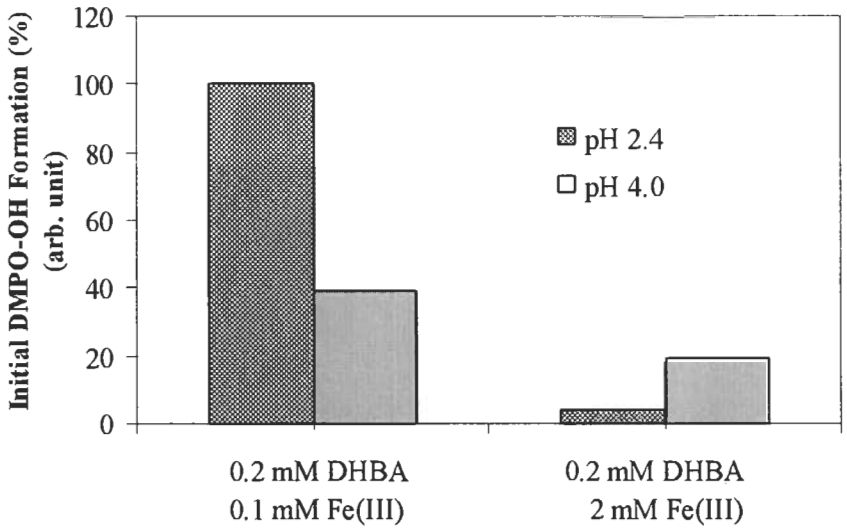

Figure 2.9. The pH and DHBA/Iron Ratio Dependent Generation of Free Hydroxyl Radicals during Initial Reaction Stage. Samples containing: 10 mM DMPO, 20 mM pH 2.4 (4.0) buffer, 1 mM H_2O_2, 200 μM DHBA, and 100 μM (2 mM) Fe(III). The samples are incubated at room temperature for 5 minutes before recording the spectra. ESR setting: center field 3,465 Gauss, sweep range 100 Gauss, modulation amplitude $10x10^{-1}$ Gauss, microwave power 4.9 mW, overall receiver gain $1.25x10^{4}x10$, time constant 0.5 second, scan time 200 s.

2.4.3. The Involvement of Superoxide Radicals in Redox Cycling

The specificity of superoxide dismutase (SOD) in reaction with $O_2^{\cdot}$ has frequently been used as a probe for the involvement of this radical in biochemical systems (Buttner, 1985). Specifically, SOD will cause the dismutation of superoxide to form peroxide.

Figure 2.10 shows the effect of SOD on the generation of free hydroxyl radicals in a Fenton type system containing a 2,3-DHBA/iron complex. In contrast to results from work with other systems in which SOD is believed to inhibit the generation of ·OH in Fenton type reactions (Rowley *et al.,* 1983; Gutteridge *et al.,* 1986), the results of the present experiment showed that SOD stimulated the formation of DMPO-OH adducts. The ESR signal of the DMPO-OH adduct detected in our system with SOD is much larger than the one without SOD addition. This implies that the superoxide radical is produced in this system, since SOD will specifically react with O_2^- (Fridovich, 1976). It is well known that superoxide is produced in the redox cycling of catechols when exposed to oxygenated environments (Appel 1993, Berenbaum 1995). The data in our work also show that O_2^- was not a major reductant of Fe(III) since SOD would otherwise inhibit reactions involving O_2^-. Therefore, in this system O_2^- is more likely related to the redox cycling of iron chelator following Eq. 2 (Halliwell *et al.,* 1989):

$$\text{Quinone} + O_2^- \leftrightarrow \text{semiquinone} + O_2 \qquad (2)$$

Spin trapping of the hydroxyl radical was also studied in the absence of H_2O_2, with or without SOD (Figure 2.11). No DMPO-OH signal was observed in the absence of SOD, while a weak DMPO-OH signal formed in the system containing SOD. This is a strong indication that the superoxide radical is produced in this system because SOD catalyzes reactions converting O_2^- to H_2O_2 (Halliwell, 1989), thus explaining the formation of low amounts of free hydroxyl radicals in the system even without the addition of H_2O_2.

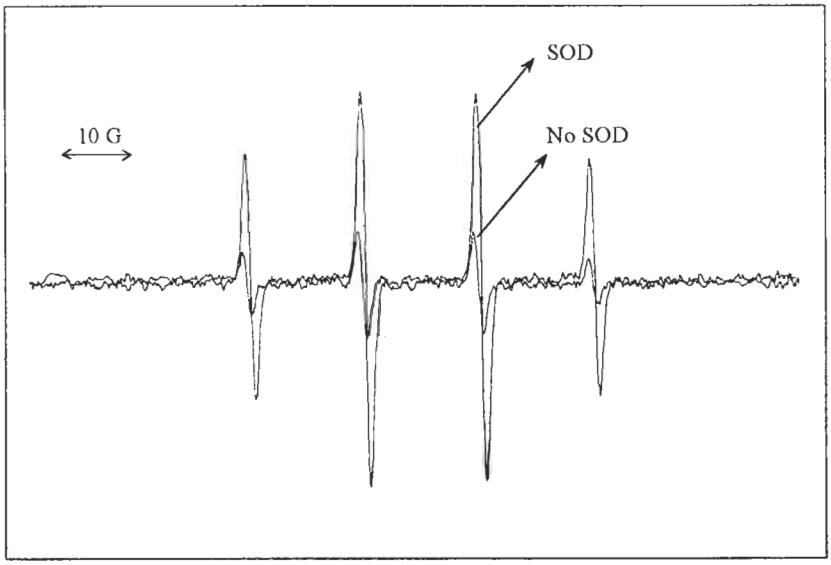

Figure 2.10. The Effect of SOD on the Generation of Free Hydroxyl Radical. The experiment conditions were:10 mM DMPO, 20 mM pH 4.0 buffer, 1 mM H_2O_2, 1 mM Fe(III), 500 μM 2,3-DHBA, with and without SOD 50 μl (about 100 units) in a total of 1 ml final solution. The samples were incubated at room temperature for 5 minutes before recording the spectra.

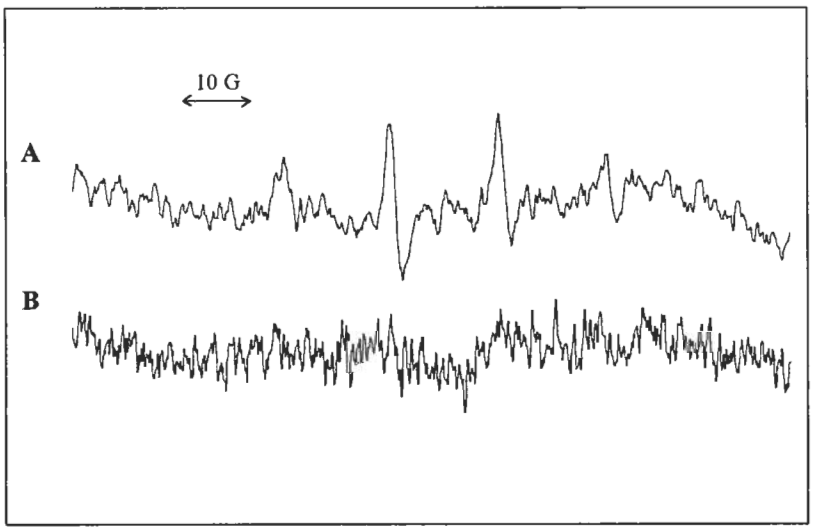

Figure 2.11. The Involvement of Superoxide Radical in the DHBA-Iron Complex Redox System. Experiment conditions: 10 mM DMPO, 20 mM pH 4.0 buffer, 1 mM Fe(III), 500 μM 2,3-DHBA, **A)** SOD 50 μl (about 100 units), **B)** without SOD, in total 1 ml final solution. The samples were incubated at room temperature for 5 minutes before recording the spectra. ESR settings: Center field 3,465 Gauss, sweep range 100 Gauss, modulation amplitude 2 x 1 Gauss, microwave power 4.9 mW, overall receiver gain $1.60 \times 10^5 \times 10$, time constant 0.5 second, scan time 200s.

2.5. Discussion

The results of this study confirmed that iron chelation by the Gt-chelator model, 2,3-DHBA occurred. The binding affinity was related to reagent concentration, incubation time and pH. In the ESR spectra, we find in general the g 4.3 signal, which reflects chelation of iron, increasing as the iron and chelator concentration increases.

The status of iron in the reducing chelator system is very complicated. Iron is able to exist as bound iron, reduced iron, or crystalline iron. At liquid helium temperatures, the ESR spectra clearly show the micro-crystalline iron signals in the system. Comparing the ESR spectra at pH 2.4 and pH 4.0, there is less crystalline iron and more bound iron at the lower pH. One possible reason is that the solubility of iron is greater under the more acidic conditions, therefore, more Fe(III) can be reduced at lower pH's when the DHBA/iron ratio is about equivalent. Spin trapping experiments also showed that, compared with the DMPO-OH signal obtained at higher pH's, at lower pH's the DMPO-OH signal is larger but relatively unstable and decays more rapidly. A possible reason for this is that ferric ions form complex hydroxide mixtures above pH 3.0 (Koppenol and Butler, 1985). Previous reports show that Fe^{3+} starts to hydrolyze to $Fe(OH)^{2+}$ (Eq. 3) at pH 2 and is 90% converted at pH 3 (James and Healy, 1972).

$$Fe^{3+} + H_2O \leftrightarrow Fe(OH)^{2+} + H^+ \qquad (3)$$

When 2,3 DHBA-Fe(III) complexes were used to catalyze the generation of free hydroxyl radicals, the DHBA/iron ratio was one of the factors that affected the formation of the DMPO-OH adduct. At low DHBA/iron ratios, the amount of the DMPO-OH adduct increased when the DHBA concentration was increased. However, after reaching a maximum at about a 1:1 DHBA/iron ratio, further increasing the DHBA concentration

had an inhibitory effect. At low pH's, this inhibition effect was more apparent. These results suggest a competition between the ability of 2,3-DHBA to reduce ferric iron, and to bind it. But other explanations may be possible.

In contrast to previous work, spin trapping of ·OH in the DHBA enhanced Fenton system showed that superoxide dismutases (SOD) stimulated the formation of the DMPO-OH adduct (Figure 2.10). The results indicate that the superoxide radical exists in this system since SOD enzymes are specific for O_2^- as substrates (Halliwell *et al.*, 1989). SOD are metalloenzymes, which can catalyze the reaction (Eq. 4):

$$O_2^- + O_2^- + 2H^+ \rightarrow H_2O_2 + O_2 \qquad (4)$$

It is possible that other oxygen-based radicals may also be present in the system but a specific spin trap for these radicals was not used.

In the natural environment, a number of enzymes have been discovered that can reduce oxygen to O_2^- (Patriarca *et al.*, 1971; Puntarulo *et al.*, 1988). It has previously been shown that O_2^- can reduce quinones to semiquinones (Halliwell *et al.*, 1989), and in addition can reduce metal ions (Fe^{3+} or Cu^{2+}) that then react with H_2O_2 to form free hydroxyl radicals. If Fe(III) is mainly reduced by O_2^- in the present Fenton system, the production of ·OH should be inhibited by adding SOD. But in the work presented here, SOD does not prevent the ·OH production, it even stimulates the formation of ·OH. This could be explained in terms of competition. In the actual reaction environment however, the situation is complicated and all chemical species such as DHBA, O_2^-, ·OH, and SOD can potentially react with each other affecting free radical production.

The existence of the superoxide radical in the system under study was also confirmed by another spin-trapping experiment (Figure 2.11), which was conducted

under similar conditions as the above experiment with SOD except that there was no H_2O_2 in the system. The DMPO-OH signal was formed although this was not a complete Fenton system. As discussed previously, catechols can undergo redox cycling to produce peroxide which dismutates to hydrogen peroxide, and SOD can also convert $O_2^{\cdot-}$ to H_2O_2. This explains the formation of small amounts of $^{\cdot}OH$ in the system without exogenous H_2O_2.

This work helps to explain how free radicals are produced by fungi, particularly the brown rot fungi, in the process of degradation of wood. However, additional work must still be carried out to further explore the mechanisms involved in the enhanced Fenton reaction observed when the Gt chelator and certain model catechols are used to mediate these reactions in vitro.

Chapter 3

DEINKING OF LASER PRINTED COPY PAPER WITH A MEDIATED FREE RADICAL SYSTEM

3.1. Abstract

In recent years, the use of hydrolysis enzymes in paper recycling processes has received increasing attention. This part of the thesis reports on the effect of chelator-mediated bio-mimetic free radical treatment on repulping and flotation operations during the deinking of laser printed copy paper.

Office copy paper was laser printed with a standard pattern that covered approximately 30% surface of the page. Repulping and flotation operations were then conducted under varied conditions. Chelator-mediated free radical treatment was carried out at two different chemical levels. A two-step repulping method was also developed, which combined conventional alkaline repulping as well as free radical treatment. The first step was the repulping of printed sheets in the presence of caustic and a surfactant using a process commonly used in conventional deinking. Then the pulp was diluted and neutralized to suit the needs of the subsequent free radical treatment. Flotation trials were performed on each of these treated samples to separate ink particles. Results from image analysis and paper physical properties testing are presented, and the deinking efficiency for these different treatments is also compared. Results indicate that under properly controlled conditions, free radical treatment can perform better than the conventional chemical deinking methods.

3.2. Introduction

The paper industry has been investigating biological replacements for the chemicals used in the papermaking processes in hopes of reducing operating costs and minimizing environment impact. Applications that have been investigated include modification of pulp properties such as improved fiber flexibility and fibrillation, improved drainage of recycled fibers, enzymatic pulping and bleaching of chemical pulp, enzymatic pitch removal, and contaminant removal from recycled fibers. Some new technologies that use enzymes to enhance deinking, bleaching and pitch removal have already been commercialized (Heise *et al.*, 1996). Enzymatic fibrillation during beating has long been recognized as a practical process, and the use of enzymes to increase drainage rates for recycled fibers likewise is a useful and economic means to increase paper machine throughput (Rutledge-Cropsey *et al.*, 1998). The technology for enzyme applications in the pulp and paper industry has previously been reviewed (Jeffries and Viikari, 1996).

3.2.1. Enzymatic Deinking

In the recycling area, research on the use of enzymes to replace or enhance traditional deinking chemicals has been reported with the results indicating enzymatic treatment can achieve similar or better deinking results without affecting the physical properties of final paper products (Yang *et al.*, 1996, Vidotti *et al.*, 1993). Industrial scaleup experiments with enzymatic deinking have been reported (Heise, 1996), and an enzyme enhanced deinking technology has been developed that can be applied on a commercial scale (Knudsen *et al.*, 1998; Yang *et al.*, 1996).

It was previously noted that laser printed white copy papers are difficult to deink with conventional deinking methods (Vidotti *et al.,* 1992). The reduced efficiency is due primarily to the strong adherence of polymeric toner particles to the fiber surface. Recycling mills therefore use increasingly costly mechanical devices for breaking down the large, non-impact ink particles to facilitate removal by flotation or washing (Quick *et al.* 1986; McBride 1994). These intensive mechanical forces are energy demanding and shorten the fibers, decreasing the freeness and strength of the paper formed from these fibers. For these reasons, the recycling rate for laser printed high quality fiber is much less than that of laser-free paper, with less than 10% of laser printed papers being recycled back into printing and writing grades (Darlington 1992). There would be significant benefit if an effective means were found to promote the release of toners from office waste. Using chemistry to mimic biological processes may provide some potential solutions to these problems.

The process of enzymatic deinking has been proven to be an effective method for removing non-contact inks from recovered paper. Most of the recent work on enzymatic deinking employed enzymes such as cellulases and hemicellulases (Prasad 1993; Jeffries *et al.* 1994; Zeyer *et al.* 1996; Zollner and Schroeder 1998), since they are believed to react with holocellulose and affect ink detachment. These enzymes are specific for cellulose or hemicelluose, which are dominant components of fibers.

Although there has been considerable research on the application of these enzymes in paper recycling processes, the mechanism involved in the enzymatic deinking is still not entirely clear. In some references, the effect of enzymatic deinking is thought to be the result of a peeling effect. Zeyer and co-workers (1994) found that the

accessibility of enzymes to the cellulose chains that bond the ink particles to the fiber surface is a very important factor for enzymatic deinking. In another report, this group (Zeyer *et al.*, 1996) found the optimal deinking effect was obtained employing both surface friction and cleavage of the glucosidic bonds of fibers by mechanical and enzymatic treatment together. Therefore, they suggested a model where contact between the ink particle and the fiber was exposed by mechanical action, pulling the fibers apart elastically, followed by enzymatic cleavage of the anchoring fibers that stick to the ink particles. Other researchers however have found that cellulase dosages that were effective in deinking activity were too low to affect fiber properties, and it was considered more likely that enzymes enhanced the deinking process by removing cellulosic fines and microfibrils (Pommier *et al.* 1989; Jeffries *et al.* 1994). Jackson (1993) considered that fines would be attacked by cellulases more readily than intact fibers since fines have a higher specific surface area, which results in an increase in freeness. The small microfibril components have a great affinity for water and ink particles, they tend to attach to the toner particles to form "hairy" contaminants, making toner particles more hydrophilic and accounting for the poor efficiency of the flotation operation. Therefore, the removal of fines and microfibrils may lead to more "clean" rather than "hairy" particles after repulping and thereby make toner particles more hydrophobic, to facilitate subsequent washing and flotation steps (Jeffries and Klungness 1994).

In other research, Zollner and co-workers (1997) found that internal and surface sizing significantly influences the deinking process. They suggested a model for α-amylase assisted deinking. In this model, the release of toner particles from paper is enhanced due to enzymatic degradation of the starch present between pulp fibers and ink

particles. This model may be effective for amylase treated pulp but would not apply to pulp treated with cellulases.

3.2.2. Deinking with a Mediated Fenton System

Although there have been considerable advances in the application of biotechnology to paper recycling, enzymatic deinking processes still face problems that have limited their commercialization. First of all, most of the commercially available enzyme products are too expensive to compete with conventional deinking chemicals. Secondly, enzymes are very sensitive to fluctuations in environment. Enzymatic processes usually have a relatively narrow operating range with regard to, pH, temperature, and storage time, and operating conditions must be precisely controlled in order to maintain enzymatic activity. Moreover, enzymatic processes are generally slower and maybe difficult to retrofit into existing pulp and paper mill operations.

In an attempt to avoid these limitations but still take advantage of biotechnological processes, this work investigated the potential of using a bio-mimetic free radical system in the deinking of laser printed copy paper. The work presented here is partially based on the non-enzymatic mechanism employed by some brown rot fungi in the decay of wood, a mechanism that has been studied at the Forest Products Lab at the University of Maine for the past 10 years. While many fungi produce highly active enzymes, non-enzymatic depolymerization systems have also been found to have a role in wood decomposition processes (Reese, 1977). Previous researchers (Goodell *et al.*, 1997; Illman and Highley, 1989; Backa *et al.*, 1992) have shown that highly reactive free radicals such as the hydroxyl radical ($HO^{\bullet}$), produced via the Fenton reaction or other one electron reactions, are responsible for the cleavage of wood components, at least in early

stages of brown-rot wood decay. Hydroxyl radical activity has also been detected in a number of white-rot and brown-rot fungi (Tanaka *et al.*, 1999; Barr *et al.*, 1992; Backa *et al.*, 1993). Other work has shown that in initial wood degradation stages, enzymes can not diffuse into fiber cell walls due to the size limitations, but certain low molecular substances are small enough to penetrate the fiber cell wall and facilitate the generation of free hydroxyl radicals (Goodell *et al.*, 1997; Tanaka *et al.*, 1994; Paszczynski *et al.*, 1999; Kerem *et al.*, 1999; Shimada *et al.*, 1994; Hyde and Wood, 1995). Low molecular weight phenolic compounds from the brown rot fungus *Gloeophyllum trabeum* have been isolated and structurally identified (Jellison *et al.* 1991a; Fekete *et al.* 1989; Goodell *et al.*, 1997; Paszczynski *et al.*, 1999). The compounds (termed Gt-chelators) were found to be capable of reducing multiple moles of ferric iron, and could therefore promote the production of oxygen-based radical species in the presence of the hydrogen peroxide. It was also found that 2,3-dihydroxybenzoic acid (DHBA) and other chelating compounds with catechol moieties had similar iron reducing kinetic properties to the Gt-chelator (Shao, 1997).

Research on the application of free radicals in pulping and paper processes is just beginning, and most of the studies have been focused on pulp bleaching and waste water treatment. Only limited work has been done in the field of paper recycling. Some studies (Xu 1996; Kang *et al.* 1996; Lind and Merényi 1997) showed that hydroxyl radicals have an ability similar to that of some hydrolytic enzymes for the degradation of cellulose, the dominant chemical component of wood fibers. Walker *et al.* (1995) used three iron-based biomimetic compounds in a polymeric model system (modeling pulp) to evaluate the possible application of these HO• producing systems in pulp and paper processes. Results

showed that all three compounds led to the degradation of both lignin and cellulose models. Hemoglobin exhibited the best selectivity for degradation of lignosulfonate as well as high efficiency in H_2O_2 use. Lind and Merényi (1997) studied the viscosity loss in cellulose induced by hydroxyl radicals during irradiation of pulp. They found that hydroxyl radicals were so reactive that the final viscosity loss was primarily attributed to the radicals generated inside the fiber. We have hypothesized, that by controlling the conditions of a free radical reaction, we could potentially limit free radical reactions to the area where fines or microfibrils are located so that the expected deinking effect can be achieved with minimal affect on fiber physical properties. Since the treatment effects are desired primarily at the outer surface of the fiber, if diffusion of chemicals into the interior of the fiber were limited, then free radical treatment for fiber deinking may have potential. Therefore, in the work presented here. We explore how a chelator-mediated free radical system in a controlled system could potentially be employed in deinking processes as a potential improvement, providing cost savings over conventional and enzymatic deinking processes.

3.2.3. Objectives

The objective of this work was to investigate the possibility of applying a mediated free radical system in deinking processes for laser printed copy papers. The work can be considered an outgrowth of the research on the mechanisms of enzymatic deinking, and the similar effects of enzymatic, and the free radical treatment of carbohydrate material — both can effectively hydrolyze cellulose (the dominant component of fiber surface). In this work, two different free radical repulping processes

were compared to conventional deinking processes for their effect on ink particle size distribution and flotation deinking efficiency.

3.3. Materials and Methods

3.3.1. Paper Furnish

To reduce the variables in comparing repulping and flotation results, one set of "standard" printed sheets was prepared and used for all the trials performed in this work. A standard printed sheet has about 30% print coverage (Appendix B), which is estimated to have approximately nine times the toner area coverage of an average mixed office waste paper. Therefore, the standard printed sheet was used in a 1 printed: 8 white ratio for the experiments. The paper used for printing was Springhill Recycled Relay white (8.5" x 11", 20 lb., 75 g/m^2, 20% post consumer fiber). The filler content of the paper was 11%. All laser printed papers were prepared at the same time, using the same batch of paper, and on the same HP LaserJet 6 laser printer with a new toner cartridge. After printing the paper was randomized to minimize possible bias in print quality over time in the run.

3.3.2. Chemicals

$FeCl_2$, 2,3– dihydroxybenzoic acid, NaOH and hydrogen peroxide were purchased from Sigma Chemical (St. Louis, MO). Surfactant DI-2000 was from High Point Chemical Corp. (High Point, NC). In order to avoid iron or other metal ion contamination, deionized water was used to make pulp slurry and all chemical solutions.

3.3.3. Repulping Procedures

In this work, three repulping processes were investigated. Different treatments were only conducted at repulping stage. The first repulping process, a conventional deinking process (C-1), combined with free radical treatment, was also included as part of the 2nd and 3rd repulping processes (T-1 and T-2). T-1 involved the application of Fenton reagents instead of conventional caustic chemicals during repulping. Because conventional repulping conditions most conducive to cellulose fiber swelling and ink detachment are not necessarily those that promote optimum free radical system performance, a two-step repulping process (T-2) was also studied to avoid this problem when deinking laser printed paper. The strategy was to combine conventional deinking with free radical treatment. The laser printed paper was first pulped in the presence of caustic that promotes ink detachment from cellulose fibers. No Fenton reagent additions were made during the caustic stage. The pH was then reduced to 7 or less, and the chelator-mediated Fenton reagents were added to react with the fiber. Detailed conditions of the repulping trials are shown in Table 3.1.

All samples in this work were repulped using an in-house designed lab scale pulper. The laboratory pulper consists of a Plexiglas cylinder with a removable base and a flat rotor having grooves cut into the surface. Two vertical baffles are mounted on the cylinder wall, and a variable speed motor is attached to the bottom of the pulper (Figure 3.1). The repulper is capable of handling as much as 65 grams of oven dried paper at up to 8% consistency. First, the paper was torn into approximately 1-inch pieces before delivery to the repulper. The temperature of the slurry for repulping was controlled by

Table 3.1. Repulping Operation Conditions.

		C-1	T-1	T-2
Step 1	Mass of paper (o.d.) (g)	65	65	65
	Consistency (%)	8	8	8
	Motor Speed (rpm)	1000	1000	1000
	Chemical Addition*	N/A	DHBA 0.2 mM $FeCl_2$ 0.2 mM H_2O_2 1% Oxalic acid 0.5%	N/A
	pH	10 (NaOH)	5.5 (H_2SO_4)	10 (NaOH)
	Temperature (°C)	40	40	40
	Time (min)	30	30	10
Step 2	Chemical Addition*			DHBA 0.2 mM $FeCl_2$ 0.2 mM H_2O_2 1% Oxalic acid 0.5%
	pH	N/A	N/A	5.5 (H_2SO_4)
	Temperature (°C)			40
	Time (min)			20

* H_2O_2, Oxalic acid dose was based on the weight of o.d. fiber
DHBA and FeCl2 concentration was based on the final volume of pulp slurry
Oxalic acid was added during the last 5 min of treatment

adjusting the temperature of deionized water added to the paper. After the paper, chemicals, and water were added, the repulper was run at around 700 rpm until the paper had partially broken down. The pH was then adjusted with either NaOH or H_2SO_4 and the rotor speed was then increased to 1000 rpm and the slurry further mixed for the desired time. After this first step, the pH of the slurry was adjusted again, and the appropriate chemicals were added to the repulper if a second step was required (T1 or T2). All pulp samples were then subjected to conventional deinking operations: flotation and washing.

For treatments T-1 and T-2, after repulping, the pH of the slurry was also increased to around 7 to inactivate the free radical system.

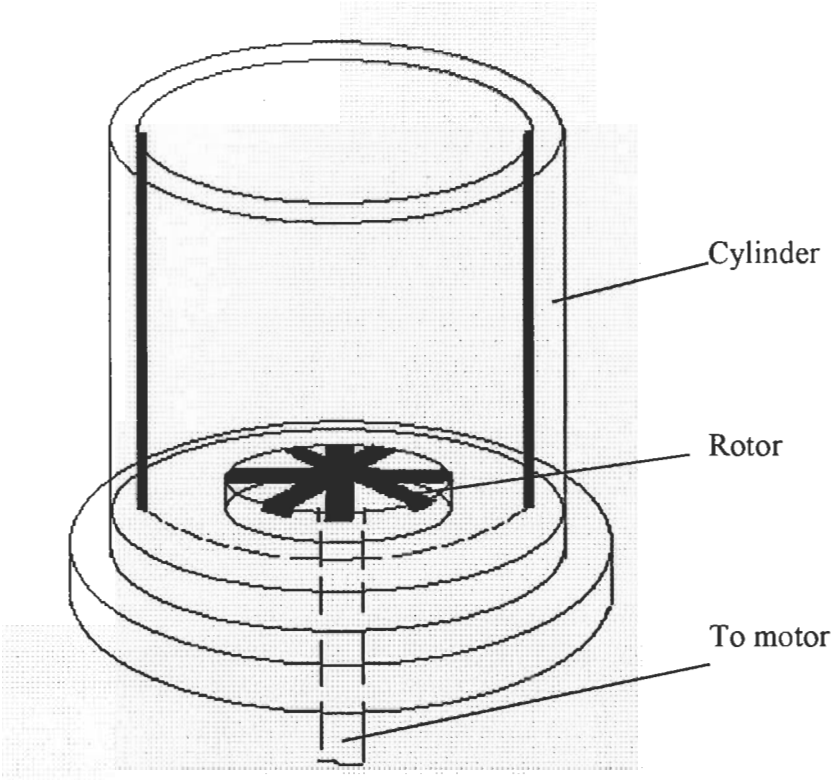

Figure 3.1. View of Laboratory Repulper Assembly.

3.3.4. Flotation Procedures

All flotation trials were performed in a Denver flotation apparatus with a 2.6 L cell. The standard conditions for flotation are listed in Table 3.2.

All diluted pulp slurry was subjected to a 5 seconds pre-mixing without airflow to ensure the thorough mixing of pulp suspension with surfactant. Flotation was performed for 5 min at 1200 rpm with airflow set to 20 L/min. During flotation, foam with ink particles attached was continually skimmed away from the cell surface. After flotation,

the pulp sample was washed in a 200-mesh pulp bag and handsheets were prepared for various TAPPI standard testing as well as image analysis.

Table 3.2. Flotation Operation Conditions

Flotation Cell (liter)	2.6
Stock Amount (liter)	2.6
Rotor Speed (rpm)	1200
Air Flow Rate (liter/min)	20
Stock Consistency (%)	0.75
Stock Temperature (°C)	45
Flotation Time (min)	5
Surfactant DI-2000 (%)	0.2 (based on wt. of fiber)

3.3.5. Handsheet Preparation

Sample handsheets for physical property measurements were prepared following TAPPI standard T-205 om-88. Handsheets used for image analysis were prepared following the same standard except that their basis weight was one-half the standard weight (30 g/m^2). Half-weight handsheets were used in this analysis because the amount of fiber in a standard weight handsheet interferes with the detection and count of particles present in the sheet (Vidotti *et al.* 1993).

3.3.6. Physical Properties and Image Analysis

Measurements of physical properties and optical properties occurred after flotation. Pulp freeness was determined according to TAPPI standard T-227 om-92. Physical testing and brightness of the handsheets was done following TAPPI standard T-220 om-88 and TAPPI standard T-452 om-92 respectively. Ash content was determined according to TAPPI standard T-413 om-85. The average fiber length and fiber length

distribution was measured by using a Kajaani fiber length analyzer according to TAPPI method T-271 pm-91.

To properly evaluate the effectiveness of the deinking process, a combination of several measurement techniques was used in this work. Brightness measurements only give an overall result. It is not possible to determine whether an increase of pulp brightness is caused by ink removal or by the bleaching effect. Therefore brightness is of limited value in evaluating deinking efficiency, and this study used image analysis to determine both ink particle size distribution and the percentage of the sample covered by ink particles.

In the image analysis system used in this study, a HP ScanJet flatbed scanner with an optical resolution of 1200 by 600 dpi was used to digitize the images of the toner particles in the handsheets, and a Spec *Scan® program developed by Apogee Systems, Inc. was used to interface with the scanner and to analyze the acquired images. Appendix C shows the typical output of this image analysis system. To check the consistency of the testing, repeat image analysis was performed. Figure 3.2 shows the results for residual ink measurement of two 'standard' handsheet sets obtained over a period of four weeks. The image analysis results for both handsheet sets showed high repeatability, and the one-way ANOVA tests also confirmed that there was no significant difference between replicate measurements. This indicates that the error related to the image analysis is minimal.

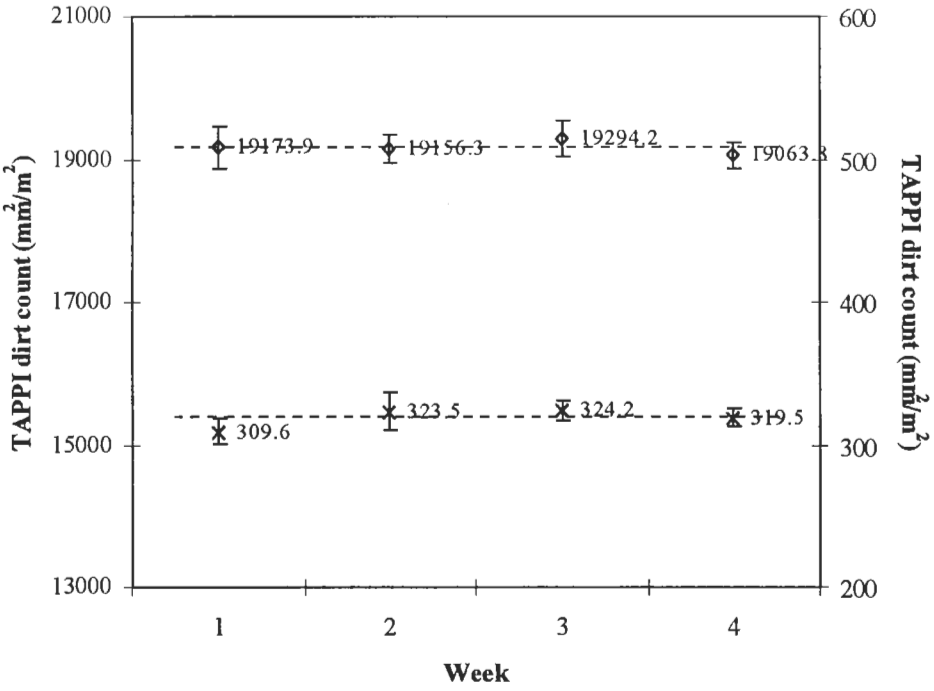

Figure 3.2. Replicated Image Analysis Measurements of Two 'Standard' Handsheet Sets over a Four-week Period. The residual ink was counted based on TAPPI dirt specks (>0.04 mm^2). The dotted line represents the overall mean. The error bar represents the standard deviation of 5 replicated measurements.

3.4. Results and Discussion

For each repulping condition (C-1, T-1 and T-2) the treatment was repeated three times. Unless explicitly mentioned, the results showed below were calculated as the overall mean of triplicate treatments, and the error bar represents the standard deviation of these triplicate treatments.

3.4.1. Deinking Efficiency

The Spec*Scan programs used in this work were 'Dirt Count' and 'Dirt Coverage'. Dirt Count is simply the number of dirt/ink specks detected in the total area scanned (6 inch round), which can also be expressed as count per m^2. Dirt Coverage is the "dirt-covered" area in mm^2 over the total scanned area in m^2, which can also be expressed as PPM. Figure 3.3 shows a comparison of residual ink count between samples prepared before and after flotation for the three treatments. Figure 3.4 compares the ink coverage before and after flotation for the three different deinking processes.

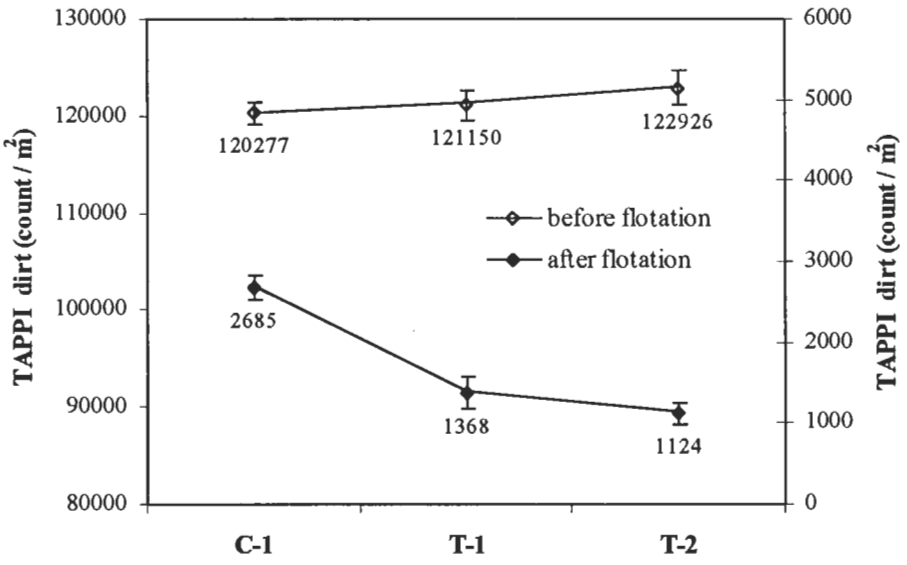

Figure 3.3. TAPPI Residual Ink (>0.04mm^2) Count of Various Samples Before and After Flotation: (C-1) conventional deinking; (T-1) one stage free radical deinking; (T-2) two stage combined alkaline-free radical deinking.

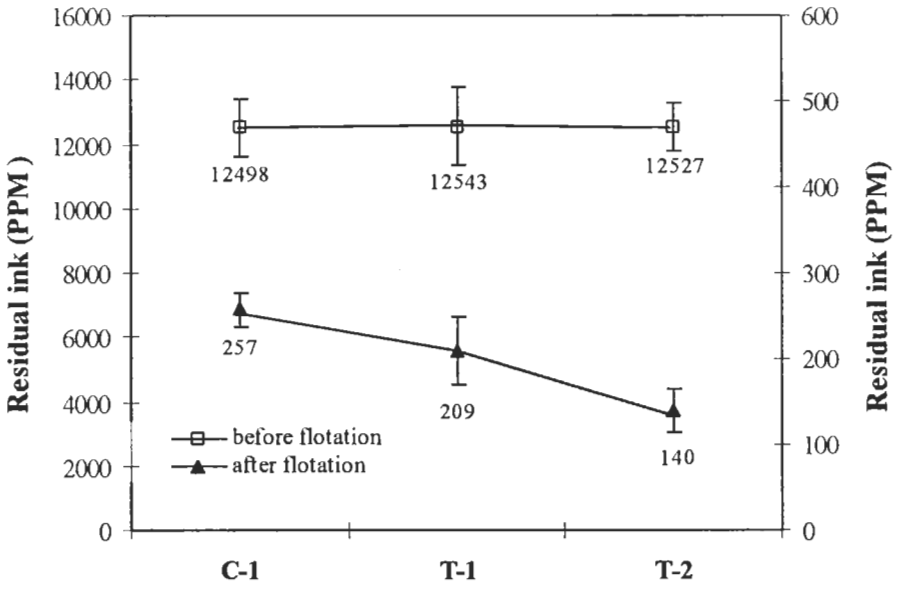

Figure 3.4. TAPPI Residual Ink (>0.04mm^2) Coverage of Various Samples Before and After Flotation: (C-1) conventional deinking; (T-1) one stage free radical deinking; (T-2) two stage combined alkaline-free radical deinking.

The image analysis results indicate that both free radical treatments (T-1 and T-2) resulted in higher toner particle removal efficiency during the flotation step when compared to the conventional repulping (C-1) conducted in this work. Between the two free radical treatments, the combined alkaline-free radical repulping (T-2) displayed a greater deinking efficiency than the one step free radical treatment. The TAPPI dirt count results also showed that T-2 resulted in more TAPPI ink particles (>0.04mm^2) after repulping, which indicated that more reduce-sized toner particles were produced in repulping since the same paper furnish was used in all treatments. This may have been due to the break-up of toner particles held together only by cellulose fibers, leading to the formation of smaller particles. In the following section, ink particle distribution was

measured as a means to provide greater detail on the particle sizes generated in the different deinking processes.

3.4.2. Residual Ink Distribution

One criterion for effective ink removal by flotation is particle size. A comparison of ink particle size profiles from the different deinking processes before and after flotation is illustrated in histogram form in Figures 3.5 and 3.6, respectively.

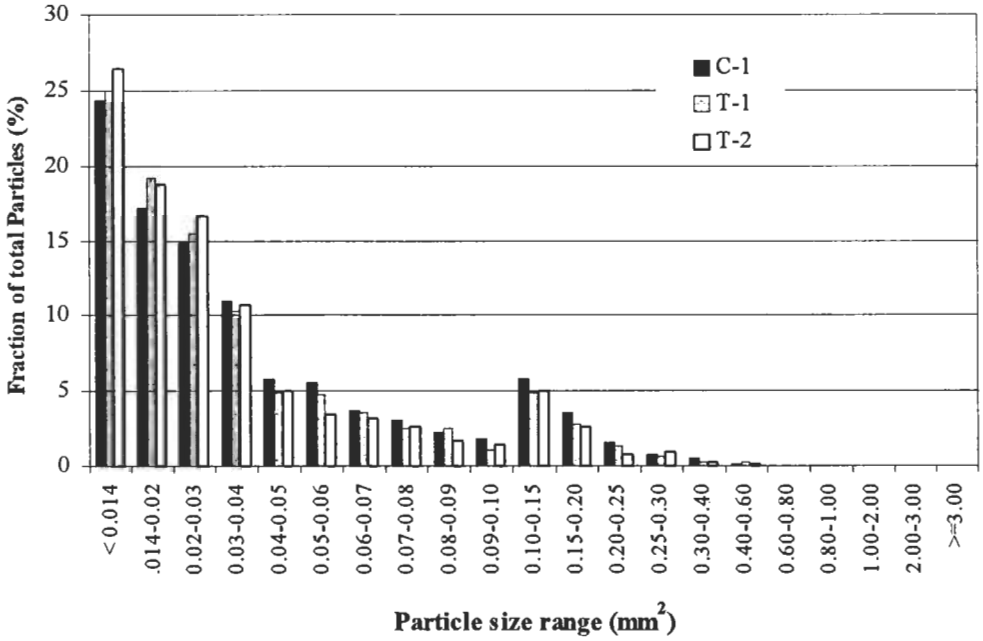

Figure 3.5. Comparison of Toner Particle Size Profiles of Various Samples Before the Flotation Process: (C-1) conventional deinking; (T-1) one stage free radical deinking; (T-2) two stage combined alkaline-free radical deinking.

From Figure 3.5, it can be seen that free radical treatments T-1 and T-2 have more toner particles of size < 0.03 mm^2 and fewer particles in larger size ranges. As mentioned above, one possible cause is the cleavage of cellulose fibers that originally held two toner particles together, which would lead to the formation of smaller particles. Flotation

operations are more efficient when particle sizes are < 225μm (0.04mm^2). Therefore, the smaller toner particles in the free radical treated samples may partially contribute to the higher flotation efficiency.

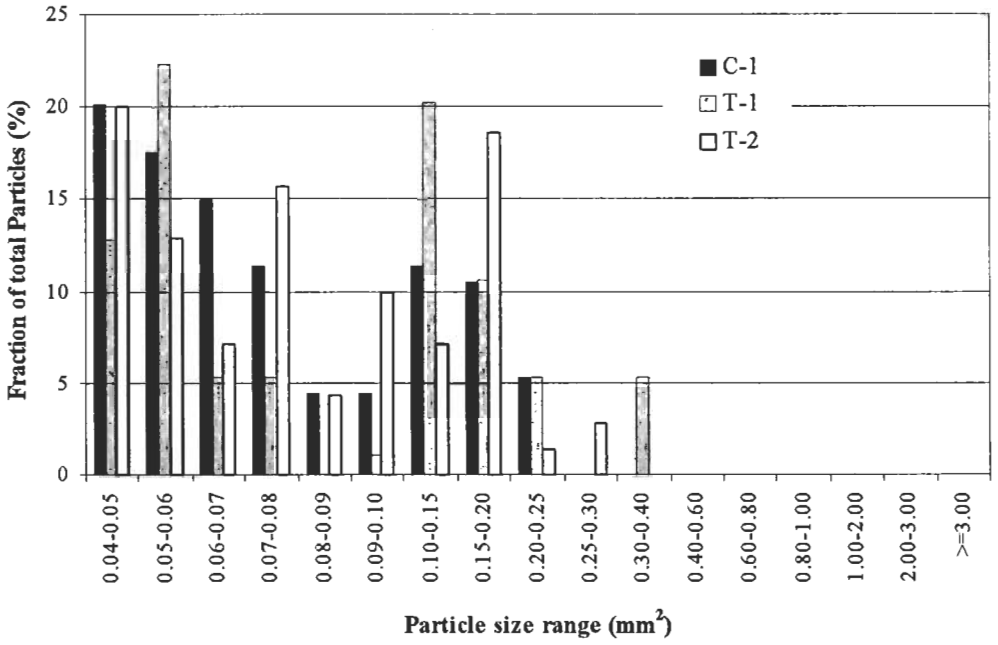

Figure 3.6. Comparison of Toner Particle Size Profiles of Various Samples After the Flotation Process: (C-1) conventional deinking; (T-1) one stage free radical deinking; (T-2) two stage combined alkaline-free radical deinking.

The toner particle distribution after flotation is shown in Figure 3.6. It can be seen that most of the residual ink particles are in 0.04 to 0.20 mm^2 range. Since there is only a small fraction of ink particles left in the deinked pulp, the differences between three treatments are larger and more random.

3.4.3. Pulp Yield

The pulp yields from the repulping and the flotation experiments, and the filler content after treatment are illustrated in Figure 3.7. The free radical treatments led to more apparent material loss, which included fillers, cellulose fibers, and fines. Filler

content did not vary significantly between samples from different treatments. Therefore, the loss of cellulose fibers or fines contributed to most of the yield loss for free radical treated samples.

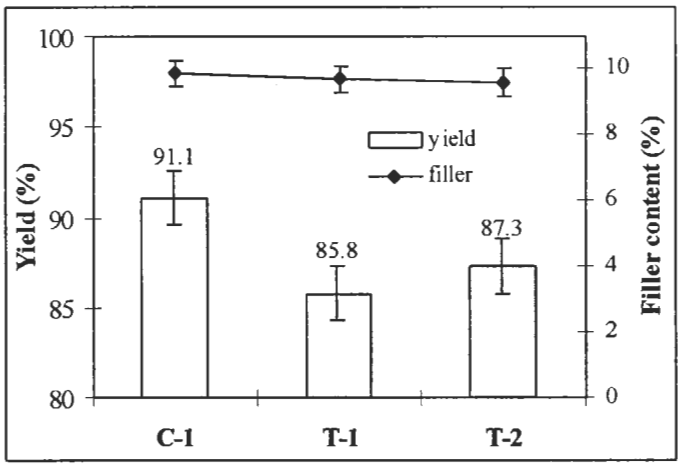

Figure 3.7. Pulp Yield and Filler Content After Deinking Treatments: (C-1) conventional deinking; (T-1) one stage free radical deinking; (T-2) two stage combined alkaline-free radical deinking.

3.4.4. Freeness and Fiber Length Measurement

Pulp freeness was measured for each treatment after the flotation process (Figure 3.8). There is a significant difference between C-1 and T-2 ($p=0.014$) based on ANOVA analysis (Appendix D). Statistical data also show that there is no significant difference between C-1& T-1, and between T-1 & T-2. A possible reason for this is a decrease in the microfibril and fines fractions caused by the free radical reactions. The arithmetic average fiber length and weight/weight average fiber length was measured on a Kajaani FS-100 fiber analyzer (Figure 3.9). The results showed that different treatments had statistically identical effects on the arithmetic average and w/w average fiber length. The raw data and calculations for the kajaani measurements are listed in Appendix D.

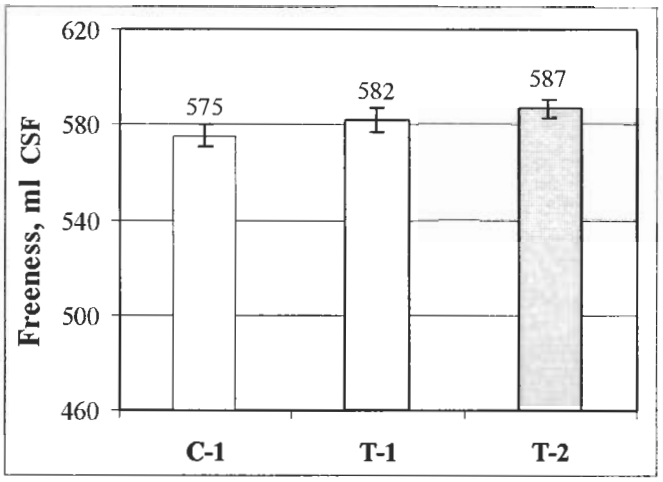

Figure 3.8. Freeness Values of Samples After Flotation: (C-1) conventional deinking; (T-1) one stage free radical deinking; (T-2) two stage combined alkaline-free radical deinking.

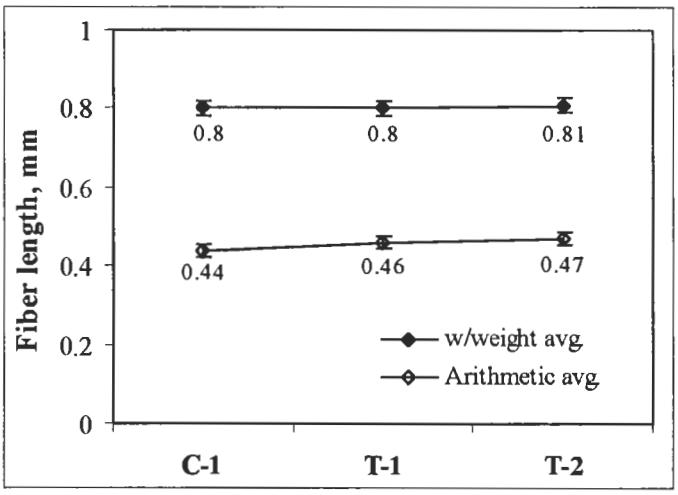

Figure 3.9. The Arithmetic Average and Weight/Weight Average Fiber Length Measured Using a Kajaani Fiber Analyzer : (C-1) conventional deinking; (T-1) one stage free radical deinking; (T-2) two stage combined alkaline-free radical deinking.

3.4.5. Brightness

The brightness of all handsheets produced using the three deinking processes was measured and compared to the brightness of the original copy paper (Figure 3.10).

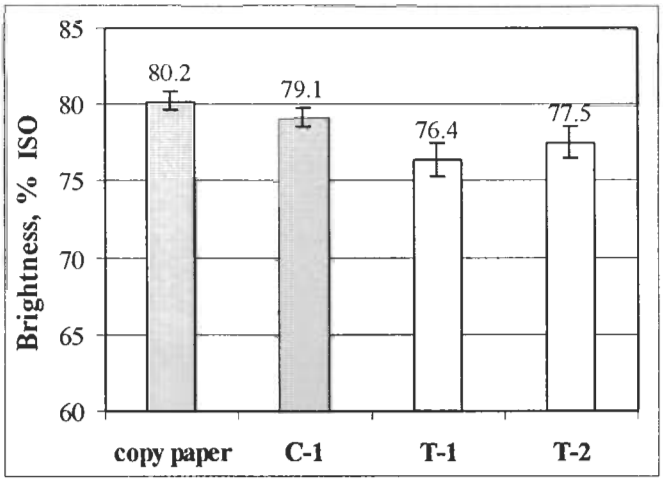

Figure 3.10. Brightness of Various Samples After Deinking: (C-1) conventional deinking; (T-1) one stage free radical deinking; (T-2) two stage combined alkaline-free radical deinking.

The data show that the brightness of conventionally deinked paper (C-1) is in the same range as the original copy paper. The free radical treatment caused about a 4% brightness loss because of the formation of a colored chelator-iron complex during treatment. Previous studies have shown that a 3% oxalic acid extraction can successfully improve the brightness of pulp to its original value. In this work, only 0.5% oxalic acid was applied, therefore, only part of the brightness loss was recovered.

3.4.6. Pulp Physical Properties

The effect of various deinking treatments on the strength properties of pulp was studied, and the results of tensile index, tear index and wet zero-span breaking length are illustrated in Figure 3.11, 3.12, and 3.13 respectively.

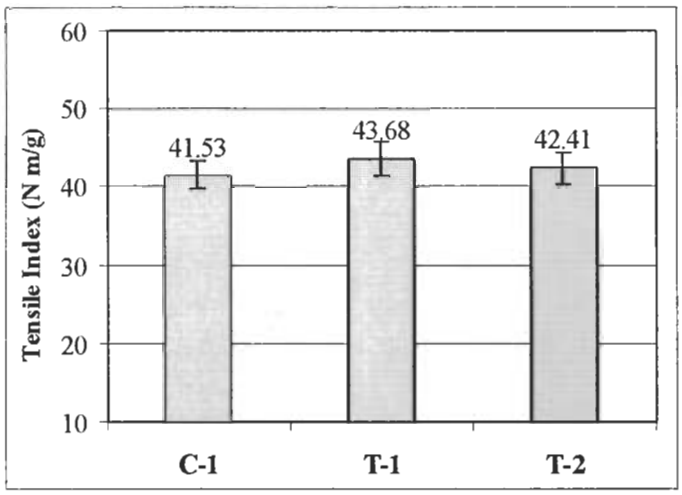

Figure 3.11. Tensile Strength of Various Samples After Deinking: (C-1) conventional deinking; (T-1) one stage free radical deinking; (T-2) two stage combined alkaline-free radical deinking.

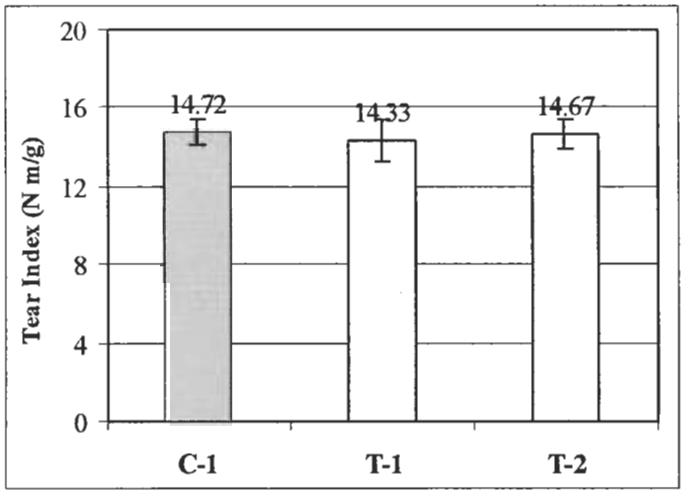

Figure 3.12. Tear Strength of Various Samples After Deinking: (C-1) conventional deinking; (T-1) one stage free radical deinking; (T-2) two stage combined alkaline-free radical deinking.

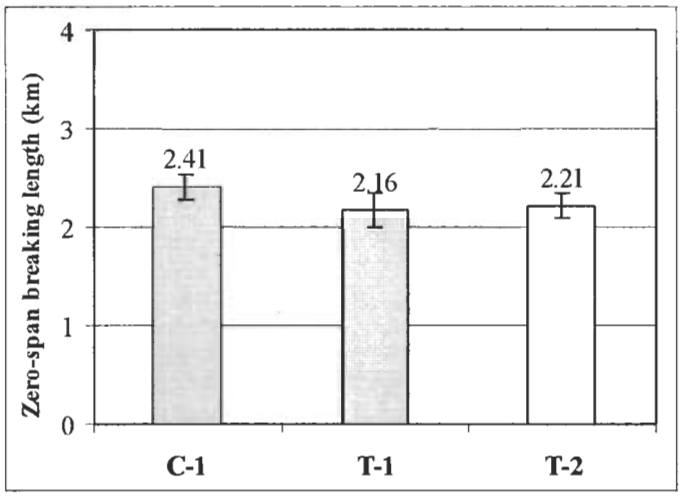

Figure 3.13. Wet Zero-span Tensile Strength of Various Samples After Deinking: (C-1) conventional deinking; (T-1) one stage free radical deinking; (T-2) two stages combined alkaline-free radical deinking.

Although the free radical treatment resulted in slight reductions in intrinsic fiber strength for T-1 (Appendix D), as measured by wet zero-span breaking length (Figure 3.13), the tensile strength (Figure 3.11) and tear strength (Figure 3.12) were basically unaffected by the free radical treatment in this work. Under the current reaction conditions this could potentially be caused by cellulose hydrolysis, promoted by free radical treatment, occurring mainly on fiber surfaces, rather than extending into fiber walls. Consequently, the tear index, tensile index, and individual fiber strength were basically unaffected.

3.5. Conclusions

The work presented here investigated the deinking of a laser printed-paper with a mediated free radical system. The preliminary experiments showed that free radical treatments could potentially be used in deinking laser printed recovered papers. A two-

step deinking process that combined conventional repulping and free radical treatment exhibited higher deinking efficiency than a single step conventional deinking or single step free radical deinking. This may be because free radicals are very active and "short lived", and only easily accessible cellulose chains are subject to the free radical cleavage. Therefore, in a two-step deinking system, mechanical action such as fiber surface friction along with improved fiber swelling under alkaline conditions, increased the accessibility of free radicals to the cellulose chains at the fiber surface that bond to toner particles. Consequently, more toner particles are released from fiber surface in a two-step repulping process. By using free radical repulping, pulp freeness was increased by various degrees, most likely due to free radical defibrillation. An additional reason for increased deinking efficiency during free radical repulping may therefore be the reduction of short fibers and fines, which could potentially facilitate flotation by enhancing or increasing the freeness. Yield reduction could result, however, from losses in cellulose fiber due to free radical activity.

The work presented here is preliminary but offers promise for improved methodology in deinking processes. In future work, to optimize process conditions, the effect of different variables including chemical dose, pulp consistency, pH, operating temperature, and residence time on deinking efficiency and pulp properties should be studied.

Chapter 4

THE EFFECT OF CHELATOR MEDIATED FENTON SYSTEM ON THE FIBER AND PAPER PROPERTIES OF HARDWOOD KRAFT PULP

4.1. Abstract

The effect of a chelator-mediated free radical treatment (CMT) on drainage properties, strength properties, optical properties, and fiber morphology of a fully bleached hardwood kraft pulp was investigated. Beaten and unbeaten pulp fibers were found to react differently to the mediated Fenton system treatment. The nature of the pulp furnish (its fines and microfibril content, and its gross fiber characteristics) had significant effect on the final fiber and paper properties. This was primarily due to the increased specific surface area of small fibers and fines in the beaten pulp fibers. The effects of treatment in general depended on the nature of the pulp furnish as well as the chemical dose of CMT applied. Treatments with high concentrations of Fenton reagents displayed severe damage to the cellulose fibers in both beaten and unbeaten pulp. However, under relatively mild reaction conditions, fiber surface friction and fibrillation of the unbeaten virgin fibers occurred, and this was confirmed through results showing increased pulp tensile strength after treatment. Analysis of heavily beaten pulp showed that overall, fines and fibril removal occurred resulting in freeness gains. Microscopic and ESEM analysis were also carried out to provide more detail on fiber morphology changes during treatment.

4.2. Introduction

Enzymatic treatment of paper making fibers has been a topic of increasing interest. Since researchers first recognized that some enzymes are able to modify or react with cellulose fibers, the use of enzymes with natural fibers has been studied for a variety of processes including pulp and paper operations. To date, cellulases and hemicellulases have been the principle enzymes used in wood fiber modification. Most of the early studies in this area concerned "enzymatic refining", with energy savings being the principle focus (Freiermuth *et al.* 1994). Recently, the use of hydrolysis enzymes in drainage control of recycled fiber has attracted increasing attention (Sarkar *et al.* 1995; Stock *et al.* 1995; Nagarajan *et al.* 1996). It has been shown that under certain conditions, enzymatic treatments promoted an increase in the freeness of recycled pulp with only minimized damage to fiber strength properties (Stork *et al.* 1995; Nagarajan and Sarkar 1996). Researchers have also studied the potential for improving paper properties by a selective enzymatic treatment of coarse pulp fibers (Mansfield *et al.* 1996, 1998). Alteration of fiber morphology by cellulases was observed, resulting in both enhanced fiber flexibility and collapsibility, which improved sheet smoothness and consolidation.

Depending on the fiber source and the enzyme dosage, the literature suggests that hydrolysis enzymes may play different roles during enzymatic modification of cellulose fibers. Because enzymes with cellulolytic activity have shown promise in fiber modification, we have hypothesized that other systems that modify cellulosic materials may also have potential for application in this field. In this work, a mediated Fenton system, which has cellulolytic activity (Goodell *et al.* 1997), has been studied for its interaction with different grades of fibers.

4.2.1. Freeness Control of Recycled Fiber

One area in the paper industry where biological replacement has potential is the paper recycling process. Of particular interest has been the use of hydrolytic enzymes for freeness control of secondary fiber (Stork *et al.* 1995; Eriksson *et al.* 1997; Kantelinen *et al.* 1997). Today, more and more recycled fibers are used in the paper industry. However, a major limitation in paper recycling has been the slower drainage rates on the paper machine caused by fines, colloids, and fillers, etc. This decrease in the pulp freeness results in machine speed limitations, which also limits the refining degree that can be applied to the pulp. Improving freeness would therefore permit faster paper machine speeds, and allow the use of more diluted suspensions in the headbox, resulting in the better paper formation.

Cellulase enzymes are large glycoproteins that can catalytically hydrolyze cellulose. Cellulase enzymes can improve the drainage rate of some grades of fiber (Stork *et al.* 1995). Pommier and his co-workers (1989) have shown that drainage improvement and strength enhancement of secondary fiber can be achieved by enzymatic treatment. They have demonstrated that a mixture of cellulases and hemicellulases can effectively improve the drainage of recycled fiber. Other researchers have investigated different cellulase enzyme sources and doses, attempting to optimize the enzymatic treatment conditions. Many studies have shown that modification of secondary fiber with cellulases and hemicellulases can produce substantial increases in pulp freeness with limited damage to fiber physical properties (Jackson *et al.* 1993; Bhat *et al.* 1991; Nagarajan and Sarkar 1996). Work by Eriksson *et al.* (1997) investigated the effect of different substrates, enzyme doses, and refining levels on drainage improvement with a

commercially available cellulase mixture. They found that lower dosages of enzyme improved freeness in most grades while having little or no effect on the strength properties of the sheet. The higher dosages of enzyme tested did not dramatically improve the freeness, while they did decrease the strength of the resulting paper.

The mechanism of enzymatic action in pulping and paper applications is not yet well understood. Jackson *et al.* (1993) studied enzymatic treatment using bleached softwood kraft pulp focusing on the removal of fines by CMCase enzymes. Their work suggested that enzymes may prefer to attack colloidal cellulose material, and as the quantity of colloidal material decreases, interstitial water flows more readily. Another interpretation of this result is that the enzyme may act on the surface of the fiber removing small components that have a high affinity for water. This would make the fibers less hydrophilic and therefore improve the drainage rate. Stork *et al.* (1995) speculated that drainage improvement during enzymatic treatment did not appear to be due to selective hydrolysis of the fines fraction but was a consequence of the hydrolysis of amorphous cellulose on the surface of the fibers.

4.2.2. Enzymatic Modification of Virgin Fiber

Another important use of biological methods is the reduction of refining energy used in pulping processes. Previous work has shown that enzymes can be used to decrease refining energy in virgin fiber (Freiermuth *et al.* 1994; Moran 1996). Freiermuth *et al.* (1994) found that a commercial cellulase mixture used for treatment between primary and post refining stages on hardwood and softwood kraft pulps resulted in better drainage improvement and decreased refining power consumption. Moran *et al.* (1996) performed similar experiments where the effect of pre-refining and post-refining

enzymatic treatments was studied. Moran's work showed that pre-refining applications resulted in improved refining efficiency, while a post-refining treatment resulted in increased furnish freeness.

4.2.3. Mediated Free Radical System

Although enzymatic applications in the pulp and paper industry have attracted increasing attention over the last twenty years, and intensive effort has been made to study the interactions between cellulase enzymes and fibers, mill-scale application of enzymatic systems has met with limited success for number of reasons. As a natural product, enzyme preparations usually have specific storage and process requirements, which makes their use less feasible in the harsh and dynamic environment of the mill. The cost of enzymes is another factor limiting the commercialization of enzyme technology in the paper industry. Although commercial enzyme prices have fallen significantly over the last decade, most enzymes are still not as cost effective as conventional chemical systems (Daniels 1992). Therefore, in our study a chelator-mediated free radical treatment (CMT) system was used to mimic hydrolytic enzyme activity. Unlike a conventional Fenton system, where high amounts of iron are applied to generate free radicals with hydrogen peroxide, a chelator-based CMT system can work with relatively low amounts of iron by repeated cycling of the iron. This is important because of the potentially deleterious effects of iron on pulp quality. Therefore, more site-specific generation of hydroxyl radicals could be possibly achieved since in the CMT system the presence of the chelator is essential to mediate the reaction. So high concentrations of free radical production mostly occur where the chelator is present. To explore the potential application of this bio-mimetic system in pulp and paper processes,

it was necessary to develop a better understanding of the interaction between the CMT system and cellulose fibers. This work was based partially on the non-enzymatic mechanism employed by some brown rot fungi in the decay of wood, a mechanism which has been studied at the Forest Products Laboratory at the University of Maine for the past 10 years (Goodell *et al.* 1997; Fekete *et al.* 1989).

Previous research has shown that highly reactive free radicals, such as the hydroxyl radical (·OH) produced via the Fenton reaction or other one electron reactions, are responsible for the cleavage of wood components, at least in early stages of wood decay (Backa *et al.* 1993; Tanaka *et al.* 1999; Hyde *et al.* 1997; Goodell *et al.* 1997). In our lab, low molecular weight phenolic compounds from the brown rot fungus *Gloeophyllum trabeum* have been isolated and structurally identified (Jellison *et al.* 1991a, 1991b; Goodell *et al.* 1997). More recent work has isolated and identified two new compounds (4,5-dimethoxy-1,2-benzenediol and 2,5-dimethoxy-1,4-benzenediol) from stationary cultures of *Gloeophyllum trabeum* (Paszczynski *et al.* 1999). A general term Gt-chelator has been used to identify the low molecular weight fraction of chelating compounds isolated from *G. trabeum*. These compounds have the capability to reduce multiple moles of ferric iron, so as to enhance the production of oxygen radical species in the presence of the hydrogen peroxide (Goodell *et al.* 1997). It was also found that 2,3-dihydroxybenzoic acid (DHBA) and certain other chelating compounds had similar iron reduction kinetic properties to the Gt-chelator (Goodell and Jellison 1998).

Many research groups have studied various hydrolytic enzymes (especially cellulase and hemicellulase) for their ability to modify cellulose fibers and it has also been shown that hydroxyl radicals have a similar, but less discriminate, ability to degrade

cellulose (Lind and Merényi 1997). As cellulose is the dominant component of the wood fiber surface, we wished to determine if the application of a CMT could be used as a bio-mimetic system in certain pulp and paper processes where enzyme systems had previously been used with some success.

It is known that hydroxyl radical is very short lived in the environment (half life = 10^{-9} s) and its oxidation potential is only effective within five to ten molecular diameters of potential reactants, diffusion of hydroxyl radical following generation is very limited. Therefore, we hypothesized in this work that if the relatively unselective hydroxyl radical could be limited to the outer portion of the fiber, then we may allow fiber surface modification with less affection on fiber strength properties. This could be potentially be achieved by expose of the fibers to a relatively short CMT, thus limiting the time that CMT reactants could penetrate into the fiber interior.

4.2.4. Objectives

The objective of this research was to study the influence of chelator mediated free radical treatments (CMT) on fiber and paper properties. Both beaten and unbeaten hardwood kraft pulps were investigated. Studies were performed to characterize fiber surface behavior and physical properties following pulp modification with the CMT Fenton system.

4.3. Materials and Methods

4.3.1. Chemicals and Fiber Preparation

$FeCl_2$, 2,3–dihydroxybenzoic acid, NaOH and hydrogen peroxide were purchased from Sigma Chemical (St. Louis, MO). In order to avoid iron or other metal ion contamination, deionized water was used to make all chemical solutions.

A fully bleached hardwood kraft pulp was obtained in dry sheets (8% moisture) from the Chemical Engineering Department Pilot Plant, University of Maine. The pulp sheets were disintegrated in a hydraulic pulper before being beaten with a laboratory Valley beater according to TAPPI Test Method T 200 om-89. In order to produce a fiber sample with a higher fines content, the pulp was beaten for 45 minutes yielding a freeness of 174 ml. To investigate the interactions between the free radical system and pulp of different fines content, three fiber substrates were used in this work (Table 4.1). These were: S-1 - an unbeaten pulp, S-2 - a well-beaten pulp, and S-3 - a mixture of S-1 and S-2 in a 1:1 ratio.

Table 4.1. Pulp Furnish Parameters

	Beating time (min)	*Fines content (%)	C.S.F. (ml)
S-1	0	8.69	592
S-2	45	20.31	184
S-3	(S-1:S-2 @ 1:1)	12.86	388

* Fines content was measured by Bauer-MacNett classifer.

4.3.2. Experimental Design

In this work, each fiber sample was treated using one of three reaction conditions as outlined in Table 4.2. For each reaction condition (Cond2, Cond3 and Cond4), the treatment was performed in triplicate. All test results (except where otherwise indicated) were calculated as the overall mean of triplicate treatments.

Table 4.2. Experimental Conditions

	Cond1	Cond2	Cond3	Cond4
Description	No treatment	H_2O_2 control	Low conc.	High conc.
pH	-	5.0	5.0	5.0
Time (min)	-	60	60	60
Consistency (%)	-	5.0	5.0	5.0
Temperature (°C)	-	50	50	50
*Chemical Addition	-	H_2O_2 1%	DHBA 0.2 mM $FeCl_2$ 0.2 mM H_2O_2 0.5 %	DHBA 2 mM $FeCl_2$ 2 mM H_2O_2 2 %

* H_2O_2 was charged based on the weight of o.d. fiber
DHBA and $FeCl_2$ concentration was based on the final volume of pulp slurry

Based on the experimental design, a total of 27 samples were treated. The treatments were carried out in the polyethylene bags, using a water bath to control the reaction temperature. The pulp slurry was first preheated to the desired temperature and adjusted to the required pH by the addition of sulfuric acid. The measured amount of $FeCl_2$ and DHBA were then added to the slurry. A small amount of filtrate was saved at this time for the COD test. Lastly, Proper amount of hydrogen peroxide was added to trigger the reaction. Some kneading action was performed to ensure the reagents mixed well with pulp fibers. Once the treatment time was reached, the reaction was stopped by soaking the pulp bags in ice-water (0°C). Then a small amount of filtrate was saved again for COD measurement. The treated pulp was washed twice on a Büchner funnel, trying to avoid any loss of fibers. The washed pulp was saved for further measurement.

4.3.3. Analytical Methods

All pulp and paper properties were measured according to TAPPI standards (TAPPI 1992). Pulp freeness was measured at 20°C by TAPPI Test Method T227 om-92

and laboratory handsheets were prepared using TAPPI Test Method T205 om-88. Physical testing and brightness of the handsheets was done following TAPPI standard T220 om-88 and TAPPI standard T452 om-92 respectively. Zero-span breaking length of pulp was measured according to TAPPI Test Method T231 cm-85. Viscosity of pulp samples was determined according to TAPPI Test Method T230 om-89. Fiber length classification was measured using a Bauer-MacNett fiber classifier according to TAPPI Test Method T233 cm-82. Fiber analysis was also performed with a Kajaani FS-100 fiber analyzer to allow detailed fiber distribution measurements. TAPPI Test Method T271 pm-91 provides detail for measurement and calculation of numerical and weighted average fiber lengths as well as fiber length distributions.

TAPPI Test Method T 401 om-88 specifies the procedure used to identify morphological characteristics of pulp fiber under microscope. In this work, digital images of fiber were taken with an Olympus BH-2 optical microscope with phase contrast.

Environmental Scanning Electron Microscopy (ESEM) was also used to provide more detailed information about fiber surface morphological properties.

Reducing sugars released during the free radical hydrolysis can also potentially increase the COD level of the filtrate. Therefore, the chemical oxygen demand (COD) of the pulp filtrates was also measured before and after treatment.

4.3.4. Statistical Analysis

Statistic data on fiber and paper properties were analyzed using *Systat* 9.0 (SPSS, 1999), analysis of variance (ANOVA) procedure. A one-way ANOVA test was used to determine whether any of the population means differed from each other. When only two samples were involved in the comparison, a paired t-test was performed. Comparisons

involving three or more samples were made using a one-way ANOVA since errors in the significance level can result if using a series of t-tests to do this.

An important assumption for ANOVA is the homogeneity of population variances. *Systat* 9.0 performs automatic diagnostics to verify that the data meet the underlying assumptions for ANOVA. Tukey Duncan's multiple range test was also used to test for significant differences among treatment means. The detailed statistic analyses of all data from this work is listed in Appendix E.

4.4. Results and Discussion

All test results presented here (except where otherwise indicated) were calculated as the overall mean of triplicate treatments, and the error bar represents the standard deviation of these triplicate treatments.

4.4.1. Freeness and Fines Content

It is well established that fiber freeness depends heavily on fines content. In this work, a Bauer-MacNett fiber classifier was used to determine the fines content. The results of these fines and freeness analyses for different treatments and fiber furnishes are plotted in Figure 4.1 to Figure 4.3. The resulting freeness and fines content is closely related to the CMT reactants as well as the initial pulp fines content. The freeness change for the S-1 fiber sample (unbeaten pulp) is presented in Figure 4.1. The results show that there is no significant difference between fiber freeness after treatments. The fines content appeared to increase slightly in the Cond4 treatment (high chemical concentration), but the difference was not statistic significant (Appendix E).

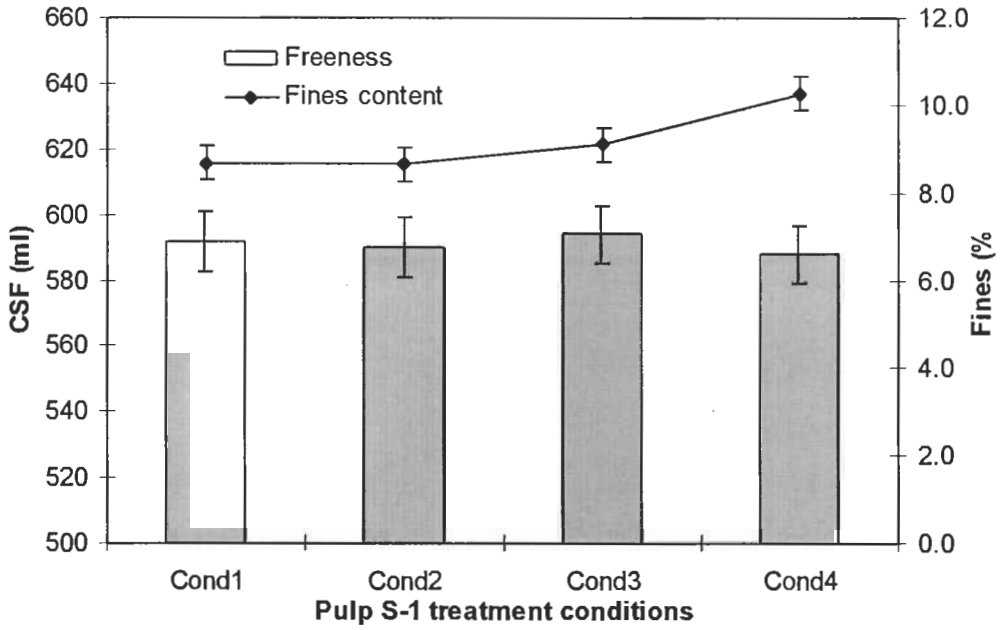

Figure 4.1. Freeness and Fines Content Versus Treatment Conditions for the Unbeaten Pulp S-1. Cond1: untreated; Cond2: H_2O_2 control; Cond3: low chemical concentration; Cond4: high chemical concentration.

Figure 4.2 illustrates the effect of reaction conditions on pulp freeness and fines content for the S-2 well-beaten pulp. There is a significant increase of pulp freeness with treatment Cond3 (low chemical charge). Under Cond3, the unbeaten fiber had an approximate 20-mL freeness increase over the control. Under Cond4 (high chemical charge) however, a decrease in freeness and an increase in fines content was observed. A possible reason for these divergent results is that under relatively mild reaction conditions, the hydroxyl radicals produced by the CMT system may preferentially react with fines and amorphous cellulose, resulting in the observed increase in freeness. At higher chemical charges (Cond4), more free radicals are produced, and the crystalline portion of the cellulose fiber begins to be hydrolyzed, which starts generating fines and leads to the decrease of pulp freeness.

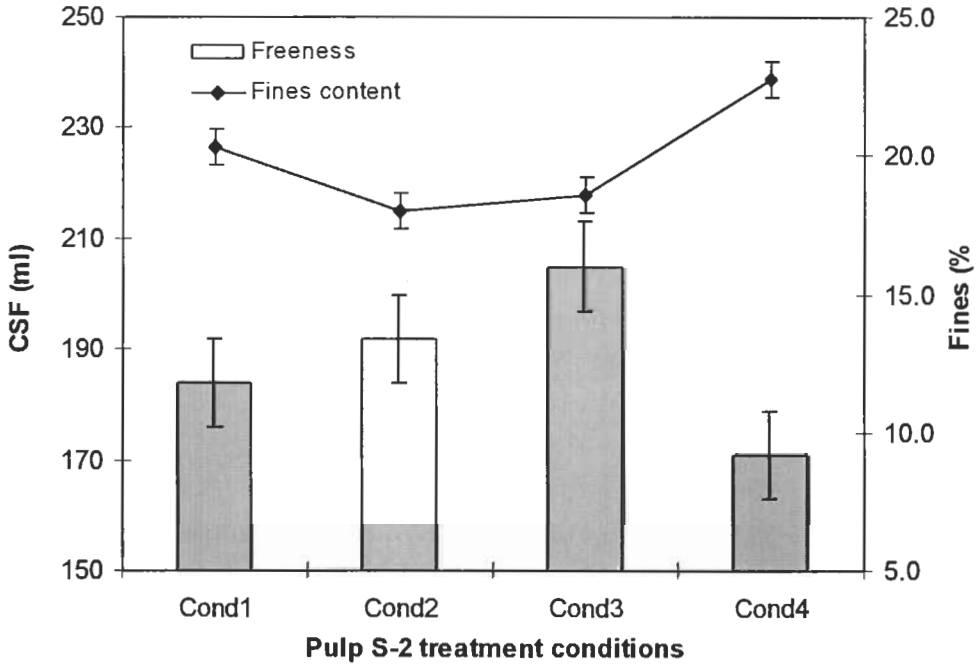

Figure 4.2. Freeness and Fines Content Versus Treatment Conditions for the Well-beaten Pulp S-2. Cond1: untreated; Cond2: H_2O_2 control; Cond3: low chemical concentration; Cond4: high chemical concentration.

The free radical treatment was also conducted on the fiber furnish S-3, which contained the mixture of unbeaten S-1 and the heavily beaten S-2 fiber at a 1:1 ratio. The result (Figure 4.3) shows a similar trend to that shown in Figure 4.2. The pulp freeness change with increased CMT reagent concentration provides further evidence that free radicals tend to react with fines and/or shorter fibers. For the unbeaten pulp (Figure 4.1), treatment Cond4 (high chemical dose) did not change pulp freeness and fines content significantly. Under these conditions a balance between the production of fines and the consumption of fines may be achieved, allowing freeness to remain unchanged. However, in pulp with higher initial fines and short fiber content (Cond4, Figure 4.2 and 4.3), fines

were produced at a greater rate than they could be degraded and a decrease in freeness resulted.

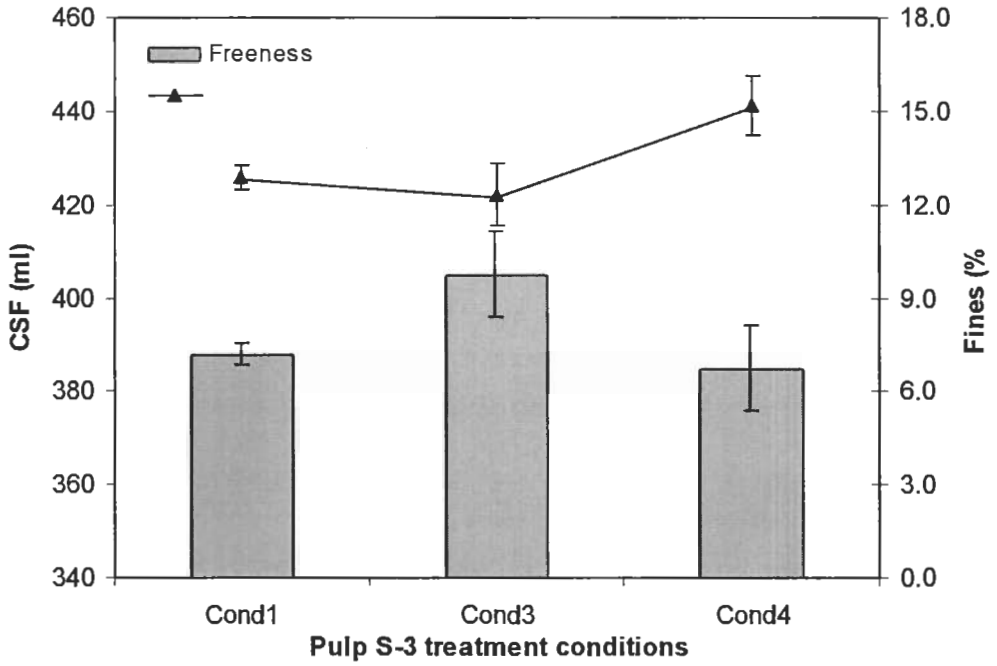

Figure 4.3. Freeness and Fines Content Versus Treatment Conditions for the Mixed Pulp S-3. Cond1: untreated; Cond2: H_2O_2 control; Cond3: low chemical concentration; Cond4: high chemical concentration.

4.4.2. Average Fiber Length and Length Distribution

Figure 4.4 illustrates the effect of CMT on the weighted average fiber length and the arithmetic average fiber length. When treated with low concentration of CMT reagents (Cond3), an increase in the weighted fiber length and a decrease of arithmetic fiber length for series S-1 (unbeaten fiber) occurs. This indicates that the free radical – fiber interaction is limited primarily to the surface of the fibers, which may lead to a separation of surface microfibrils, but the core fiber itself remains intact. Increasing the chemical concentration (Cond4) resulted in a decrease of both w/weighted and arithmetic average fiber length suggesting that, at this level of treatment, fibers were starting to

disintegrate. The fiber physical properties discussed below also confirm that 'over-treatment' with CMT will cause severe damage to cellulose fibers. The arithmetic average fiber length of samples after beating (S-2) remains relatively constant for the different levels of chemical treatments. However, for S-2, a decrease of w/weighted average fiber length could be observed at the most concentrated CMT levels, indicating the hydrolysis of both fibrils as well as longer fibers.

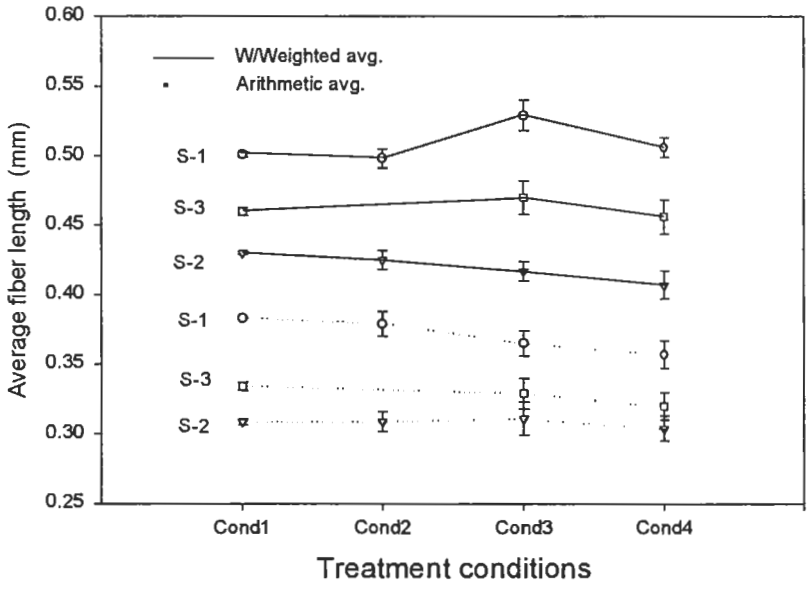

Figure 4.4. Fiber Length (w/weighted avg. and arithmetic avg.) as a Function of Treatment Conditions (for the pulp samples S-1, S-2, and S-3). Cond1: untreated; Cond2: H_2O_2 control; Cond3: low chemical concentration; Cond4: high chemical concentration.

Fiber length distributions of the treated fibers were also calculated to determine any changes in fiber length due to hydrolysis caused by CMT free radical reactions. Figure 4.5 shows the arithmetic fiber length distribution of unbeaten pulp S-1 treated under the different conditions described.

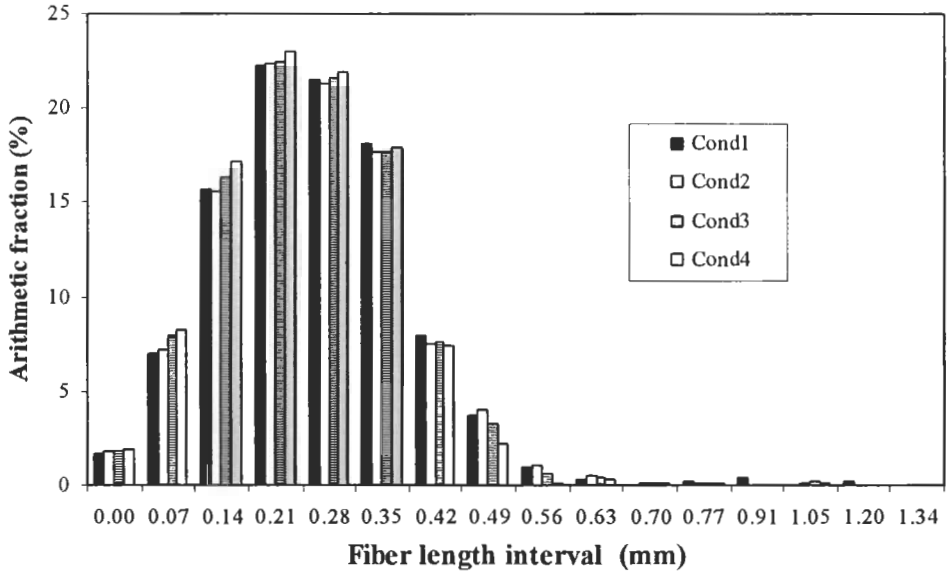

Figure 4.5. Comparison of Arithmetic Fiber Length Distribution after Different Treatments for the Unbeaten Fiber, S-1 samples. Cond1: untreated; Cond2: H_2O_2 control; Cond3: low chemical concentration; Cond4: high chemical concentration.

Changes in the fiber length histogram mainly occurred in the intervals ranging from 0 mm to 0.49 mm. For example, comparing Cond1 (no treatment) to Cond4 (high levels of CMT), the amount of fiber in the 0.14-0.21 mm interval increased from 15.6% to 17.3%, whereas the amount of fiber in the 0.49-0.56 interval decreased from 3.8% to 2.2%. The increase in the short fiber fraction after the free radical treatment may have been the result of fibrils being removed from the surfaces of the large fiber fractions or the disintegration of large fibers. The fiber histogram for well-beaten fiber (S-2) was also determined (Figure 4.6). Fibers treated with different CMT levels showed different length distribution patterns. The short fiber fractions of the heavily beaten pulp decreased at lower chemical concentrations. However, if treated at high CMT levels, the fraction of short fiber increases. For example, compared to 23.3% for the untreated control (Cond1),

the percentage of fiber in the 0.07-0.14 mm interval decreased to 21.5% for Cond2 but increased to 24.5% for Cond4.

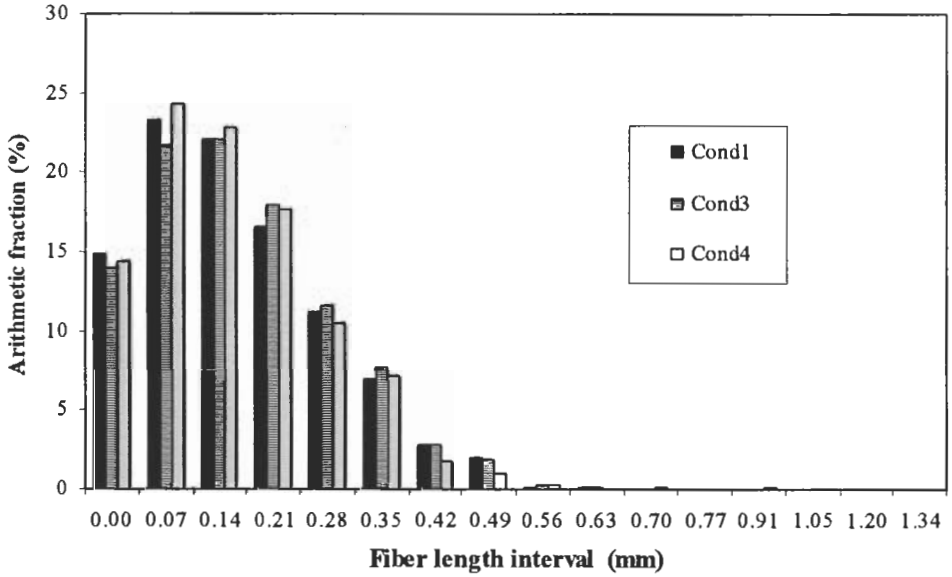

Figure 4.6. Comparison of Arithmetic Fiber Length Distribution after Different Treatments for the Beaten Fiber Sample S-2. Cond1: untreated; Cond3: low chemical concentration; Cond4: high chemical concentration.

It is possible that the small fibers originally present in these intervals were fragmented by the free radical hydrolysis to the point that it was below the sensitivity of the Kajaani FS-100 instrument. For the Cond3 pulp though, there were more short fibers hydrolyzed than generated, resulting in a downward trend in the short fiber profile. For the Cond4 pulp, there were more short fibers generated than hydrolyzed, resulting in an increase in the number of short fibers in the profile.

4.4.3. COD Measurement

As discussed early, small fibers may be further hydrolyzed to water-soluble compounds like sugars during CMT reactions. Therefore, a Chemical Oxygen Demand

(COD) assay of the treatment filtrate was performed to determine the concentration of residual organic material in each sample. Basically, the COD procedure employs a strong oxidant to completely oxidize carbon and hydrogen present in organic matter. The COD results are listed in Table 4.3, and COD gain as a function of chemical dose is plotted in Figure 4.7.

Table 4.3. COD Change of the Filtration During Treatment

	Cond3			Cond4		
	Before treatment	After treatment	Difference	Before treatment	After treatment	Difference
S-1	189.8	300.5	110.7	744.8	799.1	54.3
S-2	220.6	350.0	129.4	895.8	1268.6	372.8
S-3	201.4	325.7	124.3	730.5	896.2	165.7

*Standard deviation for measurement: ± 10 mg/L COD

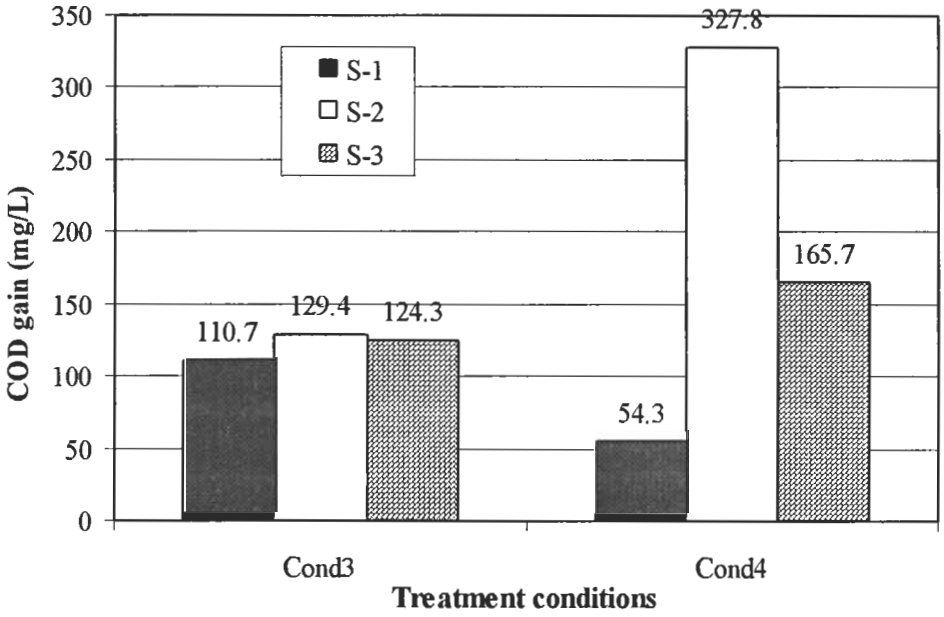

Figure 4.7. COD Gain Versus Different Treatment Conditions. Cond3: low chemical concentration; Cond4: high chemical concentration.

Figure 4.7 indicates that there are more low-MW organics being produced at the higher chemical charge (Cond4) except for the sample S-1, which shows a decrease in COD gain with increasing CMT concentration. Sample S-2 shows the largest overall

COD gain, which is probably due to its greater content of short fibers and fines, which are more subject to free radical hydrolysis than virgin fiber. The COD data provides useful information with regard to the extent of fiber hydrolysis during CMT reactions. However, since hydroxyl radicals are also strong oxidants and can further reduce COD levels in the filtrates, the COD data must be examined together with other results to avoid errors analyzing free radical hydrolysis reactions. For example, sample S-1 has a smaller COD gain when the CMT chemical concentrations are higher. This likely occurs because the oxidation of organic materials is more rapid when the CMT concentrations are higher and therefore, sample S-1 displays an overall decrease in COD gain. Considering both the COD results and the fines content results together, a reasonable hypothesize can be structured showing that fines are more readily attacked by free radicals as compared to intact, larger fibers.

4.4.4. Pulp Physical Properties

Figures 4.8 to 4.13 demonstrate the physical properties of laboratory handsheets made from the treated pulps. Figure 4.8 shows that pulp brightness decreased after beating because of the decrease in the scattering coefficient (Cond1). The hydrogen peroxide only controls (Cond2) were relatively bright as compared to the untreated samples. Free radical CMT resulted in a decrease in the brightness of all pulp samples, which was probably due to the formation of a colored chelator-iron complex during treatment. Increased chemical dosage would likely cause greater amounts of the complex to form and this is the likely cause of the lower brightness values.

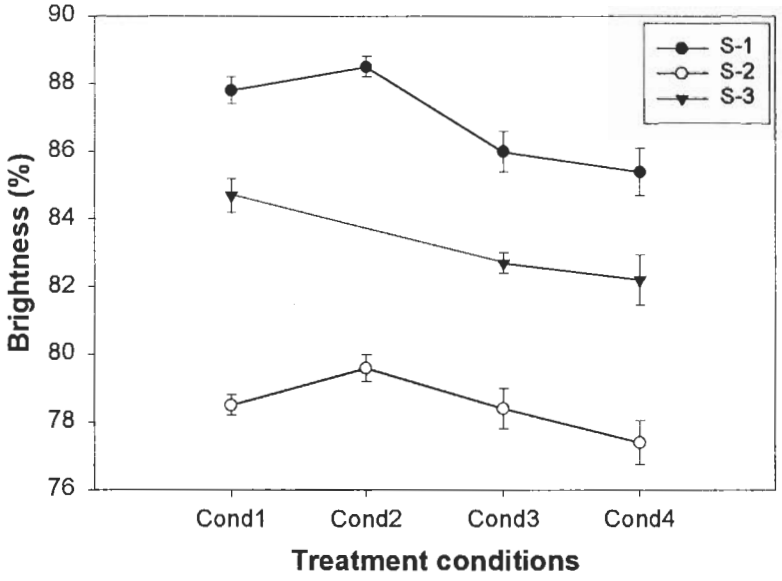

Figure 4.8. Comparison of TAPPI Brightness of Pulp Samples Treated at Different Conditions. Cond1: untreated; Cond2: H_2O_2 control; Cond3: low chemical concentration; Cond4: high chemical concentration.

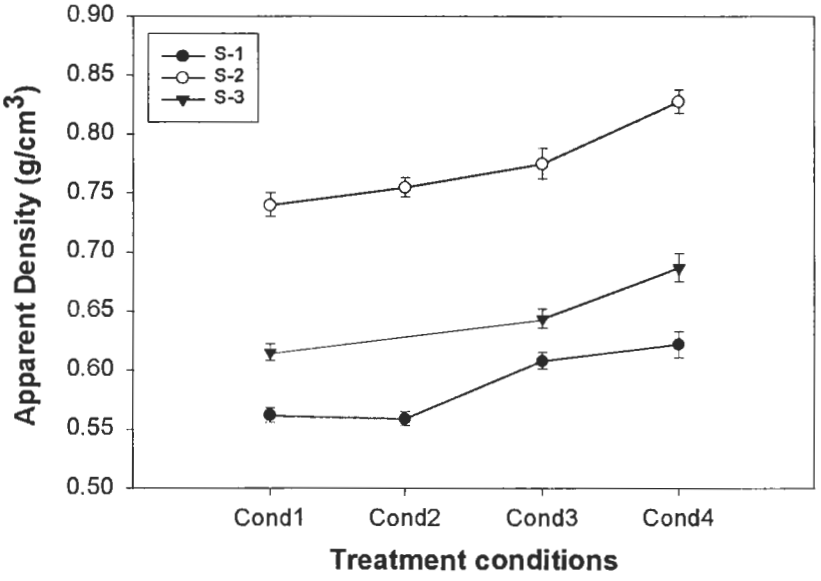

Figure 4.9. Development of Sheet Density with CMT. Cond1: untreated; Cond2: H_2O_2 control; Cond3: low chemical concentration; Cond4: high chemical concentration.

Figure 4.9 shows that compared to unbeaten pulp (sample S-1), the density of the handsheets increases after beating (samples S-2 and S-3). This occurs because during beating, the fiber primary wall is removed and the secondary wall is exposed, allowing fibers to bond more tightly after drying. Free radical treatments also resulted in sheet densification for all pulp samples in a dose dependent fashion. The density of a pulp is a measure of how collapsible or flexible the fibers are. Therefore, an increase in pulp density implies that enhanced fiber collapse and fiber packing capacity has been caused by CMT. Usually an increase in density is associated with greater paper sheet strength and in this work, three mechanical properties were studied: tensile index, tear index, and wet zero-span breaking length. Figure 4.10 presents the effect of CMT on paper tensile index.

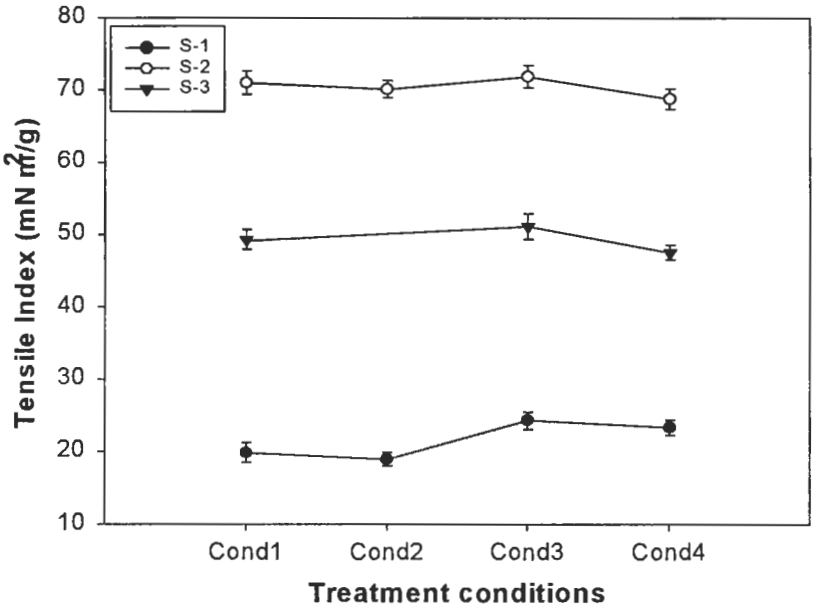

Figure 4.10. The Effect of Chelator Mediated Free Radical Treatment on Pulp Tensile Strength. Cond1: untreated; Cond2: H_2O_2 control; Cond3: low chemical concentration; Cond4: high chemical concentration.

For the unbeaten fiber sample S-1, a significant (see Appendix E for details) increase in the tensile strength of the sheet was apparent after free radical treatment. There was no statistical evidence that the mean tensile strength differed in the other two treatment groups (S-2 and S-3) at the 95% confidence level. A possible explanation for this tensile strength increase is that increased fibrillation on the fiber surface resulting from the CMT increased the internal fiber bonding of treated fibers.

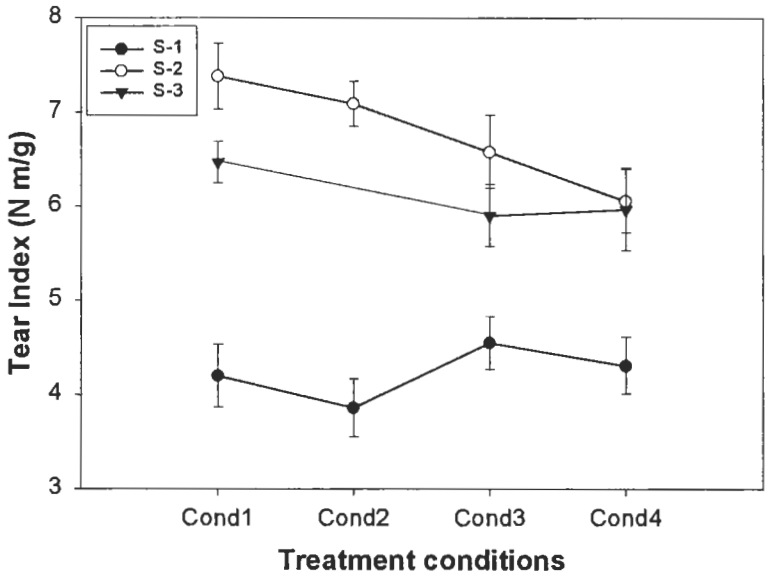

Figure 4.11. The Effect of Mediated Free Radical Treatment on Pulp Tear Strength. Cond1: untreated; Cond2: H_2O_2 control; Cond3: low chemical concentration; Cond4: high chemical concentration.

The tear index (Figure 4.11) of samples S-2 and S-3 decreased approximately 17% and 7% respectively when Cond4 (high chemical dose treatment) was compared to the control (Cond1). This decrease was significant at the 95% confidence level (Appendix E). The decrease in tear index is probably due to fiber cutting by the free radical treatment, which could potentially lead to more shorter and weaker fibers. Unlike

the beaten samples, S-1 displays a statistically insignificant increase in tear index at low chemical charge (Cond3). This may occur because surface lignin on the fiber protects the interior fiber layers from extensive degradation during exposure to CMT.

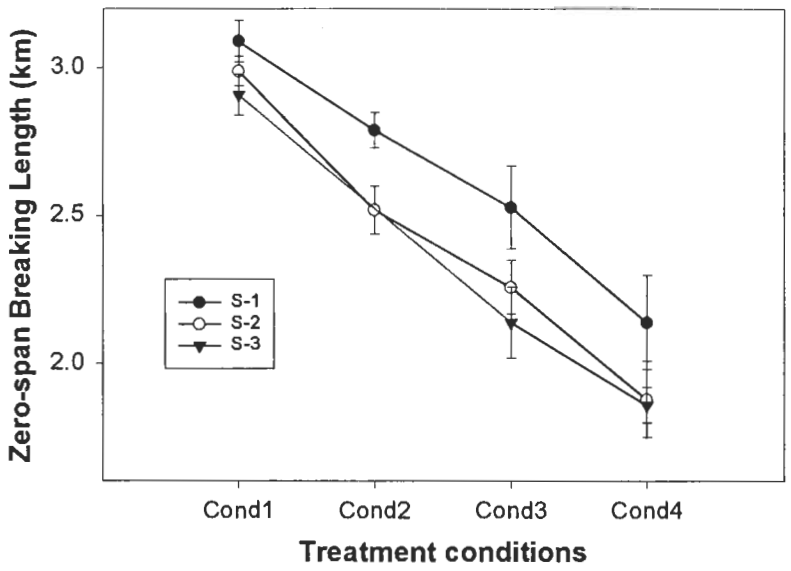

Figure 4.12. The Effect of Mediated Free Radical Treatment on Pulp Wet Zero-Span Tensile Strength. Cond1: untreated; Cond2: H_2O_2 control; Cond3: low chemical concentration; Cond4: high chemical concentration.

A substantial decreases in the wet zero-span breaking length (ZBL) (Figure 4.12) after CMT and peroxide treatment was observed. It is clear that the reduction is a function of chemical exposure in the treatment. Samples without treatment (Cond1) displayed the highest ZBL, hydrogen peroxide alone (Cond2) caused about 10% reduction in ZBL, while low and high chemical concentration treatments (Cond3 and Cond4) caused approximately 16% and 30% ZBL losses, respectively.

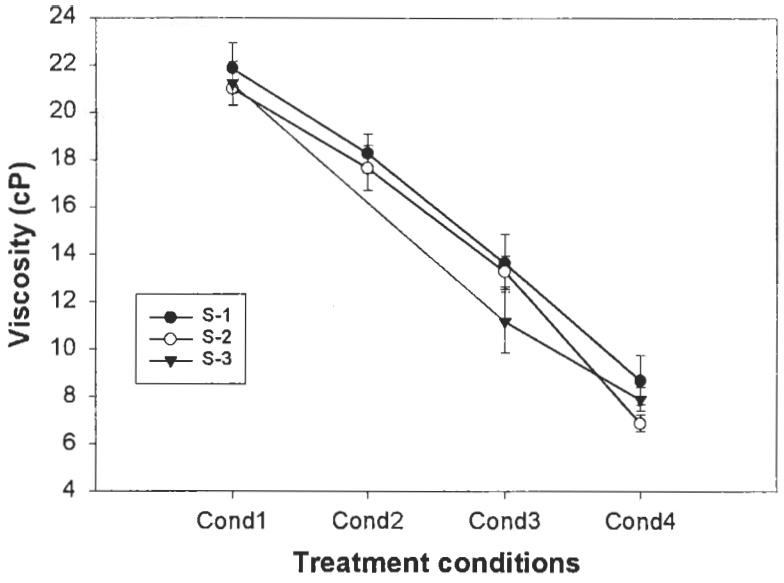

Figure 4.13. The Effect of Mediated Free Radical Treatment on Pulp Viscosity. Cond1: untreated; Cond2: H_2O_2 control; Cond3: low chemical concentration; Cond4: high chemical concentration.

Pulp viscosity data (Figure 4.13) confirm the intrinsic fiber strength loss observed in the zero-span breaking length tests and show a similar pattern to that data. The decrease in intrinsic fiber strength and pulp viscosity indicate that fiber disintegration and fiber damage had occurred as the result of the free radical activity in CMT. It was clear from this data that, although fiber flexibility and sheet consolidation had improved, fiber strength loss would limit applicability of this system unless further study on reaction conditions suggested a means to modify or control the CMT reactions. To facilitate our understanding of the reactions involved in the CMT process and the effect of the process on the pulp fiber, image analysis of the fibers after treatment was carried out.

4.4.5. Image Analysis

Direct evidence of changes in fiber morphology by the free radical treatment was obtained by environmental scanning electron microscopy (ESEM) and digital microscopy. In previous sections, we proposed that in the unbeaten fiber (S-1), a controlled free radical treatment might cause fibrillation of the fiber surface, which could potentially lead to increased tensile strength. Compared to the unbeaten, untreated control (Figure 4.14 and 4.16), unbeaten fiber treated with the CMT system (Cond3) displayed more fibril material on the fiber surface (Figure 4.15 and 4.17).

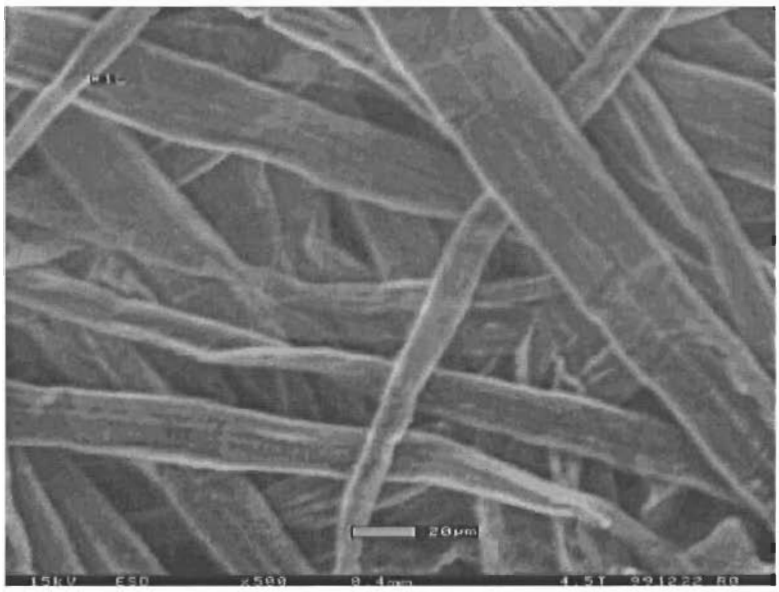

Figure 4.14. ESEM Micrograph of Untreated (Cond1) Unbeaten Pulp (S-1).

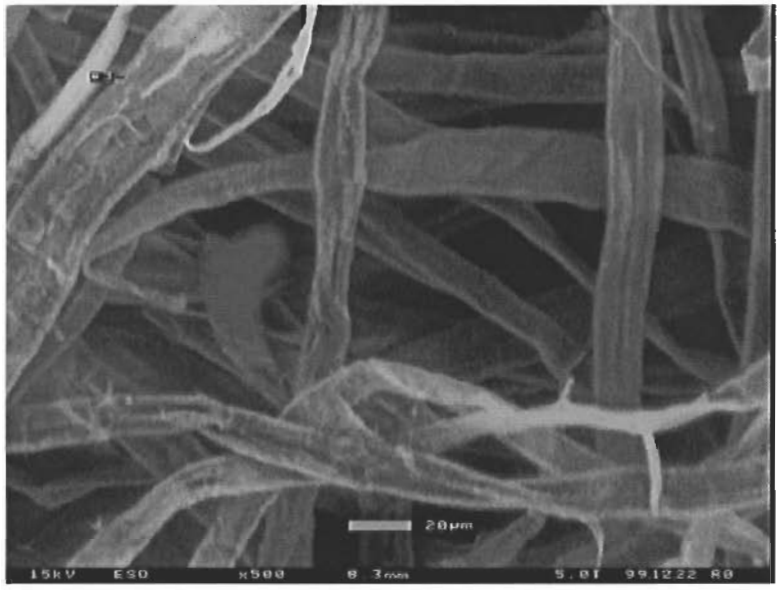

Figure 4.15. ESEM Micrograph of Unbeaten Pulp (S-1) Treated with Low CMT Chemical Concentrations (Cond3).

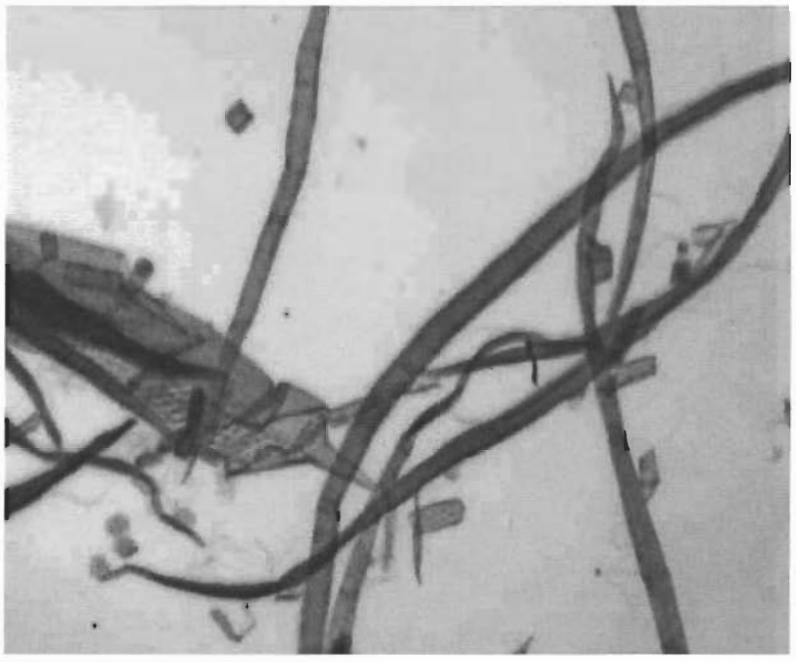

Figure 4.16. Photomicrograph of Untreated (Cond1) Unbeaten Pulp (S-1).

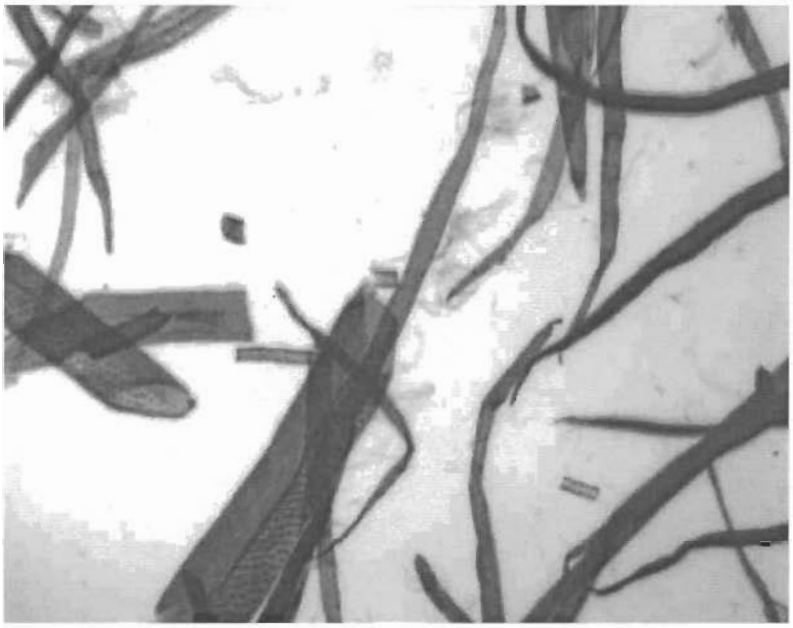

Figure 4.17. Photomicrograph of Unbeaten Pulp (S-1) Treated with Low CMT Chemical Concentrations (Cond3).

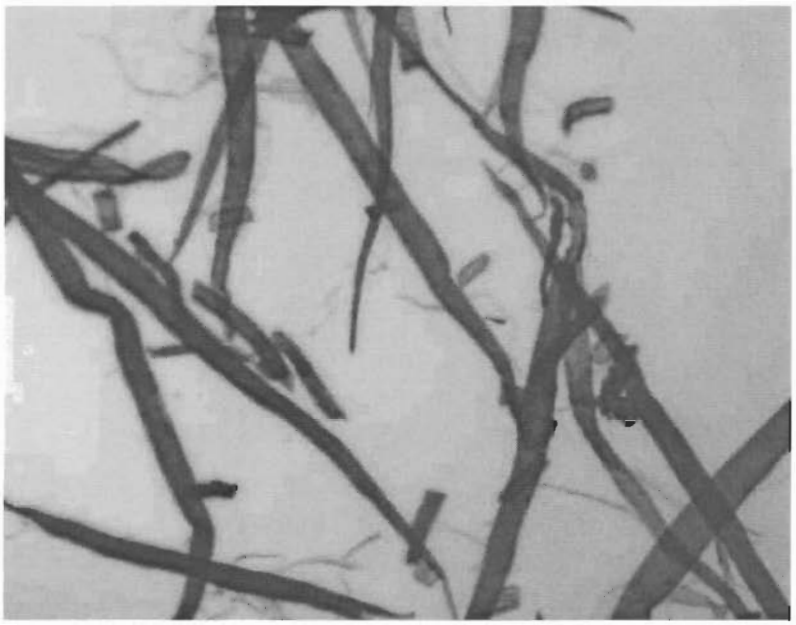

Figure 4.18. Photomicrograph of Unbeaten Pulp (S-1) Treated with High CMT Chemical Concentrations (Cond4).

Figure 4.19. Photomicrograph of Untreated (Cond1) Well-beaten Pulp (S-2).

Compared to the unbeaten fibers (S-1) treated with the low concentration CMT system (Figure 4.17), fiber treated at high chemical concentrations (Cond4) shows not only surface fibrillation, but also fiber fracture (Figure 4.18), which confirms the drastic decrease in fiber strength and viscosity after an 'over dose' of free radical treatment.

Figure 4.19 shows a light microscope image of a pulp sample after 45 minutes of beating (S-2, Cond1). Significant amounts of fibrils and fines material were generated during beating. ESEM images also taken of the same fiber sample (Figure 4.20), show the same surface fracture and fibrillation.

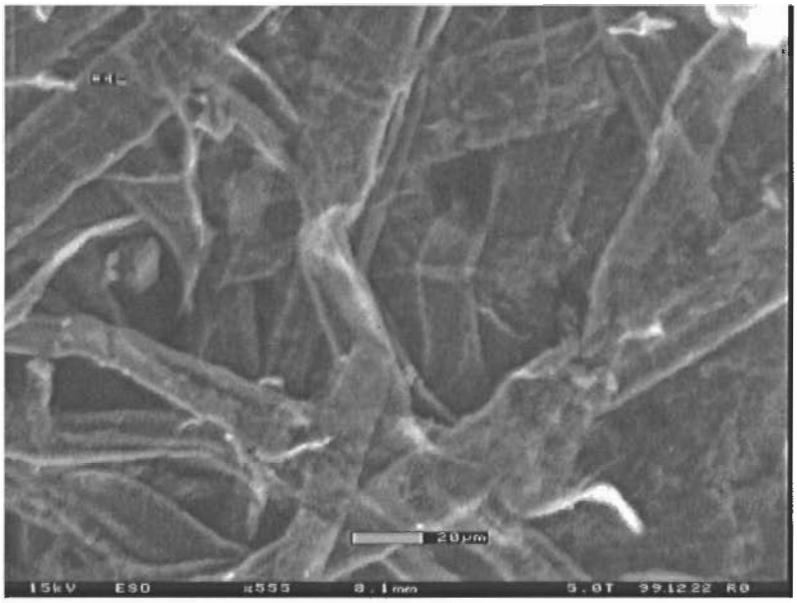

Figure 4.20. ESEM Micrograph of Untreated (Cond1) Well Beaten Pulp (S-2).

Figure 4.21 shows an ESEM micrograph of well-beaten fibers treated with low CMT chemical concentrations (Cond3). Compared to the untreated fibers shown in Figure 4.20, fibers collapse and bond more tightly to each either after treatment (Figure 4.21). A light microscope image of the same fibers (Treatment S-2, Cond3) is shown in Figure 4.22.

Figure 4.21. ESEM Micrograph of Well-beaten Fibers (S-2) Treated with Low CMT Chemical Concentrations (Cond3).

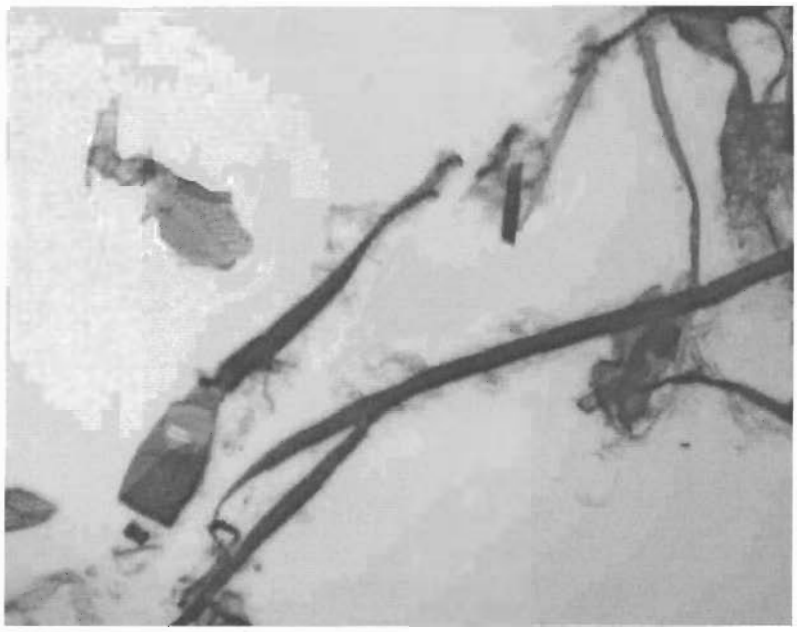

Figure 4.22. Microscope Image of Well-beaten Fibers (S-2) Treated with Low CMT Chemical Concentrations (Cond3).

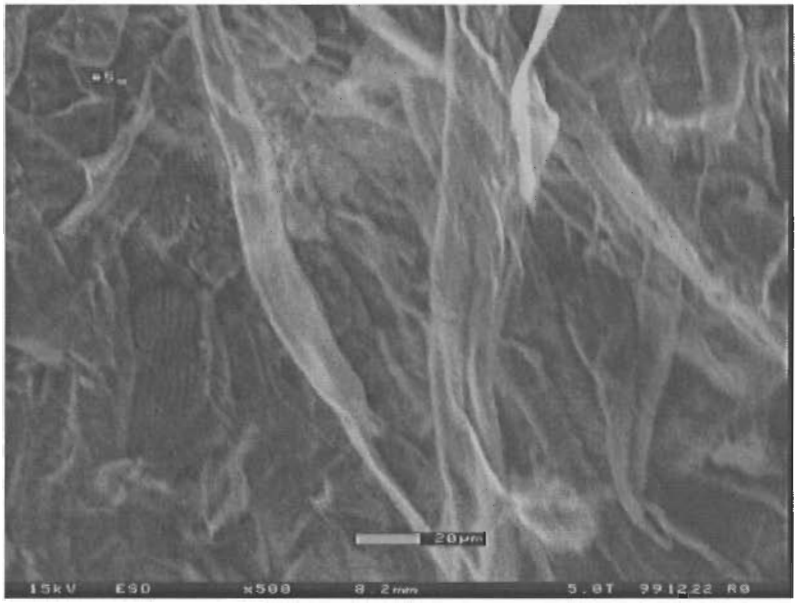

Figure 4.23. ESEM Micrograph of Well-beaten Fibers (S-2) Treated with High CMT Chemical Concentrations (Cond4).

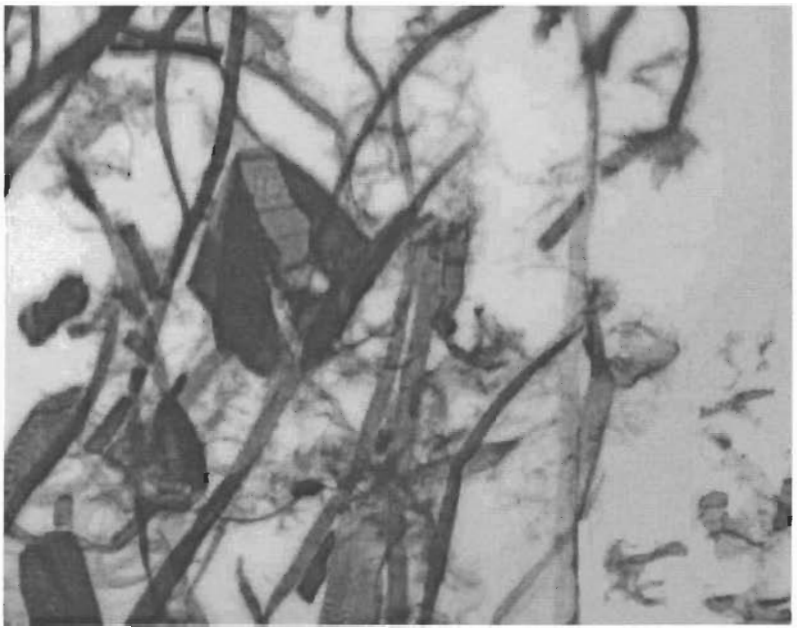

Figure 4.24. Microscope Image of Well-beaten Fibers (S-2) Treated with High CMT Chemical Concentrations (Cond4).

Treatment with high CMT chemical concentrations (Cond4) causes significant surface modification and fines production for well-beaten fibers (S-2) (Figure 4.23 and 4.24). It can be observed that fibers were more collapsed and more fines material and flakes were generated after intensified free radical treatment, which confirms the increased fines content and sheet density described above. However, treatment with peroxide alone or with low CMT chemical concentrations resulted in limited fiber surface fibrillation and fracture, as a result there are less improvements in sheet consolidation and less damage to strength properties.

4.5. Conclusions

The work presented here overviews the effect of chelator mediated free radical treatment (CMT) on fiber properties and shows the treatment effect varies with the nature of the pulp (its fines content and degree of beating) as well as the CMT chemical concentration. We observed that beaten and unbeaten fibers reacted differently when treated with the CMT system.

1. In general, intensified free radical treatment (Cond4) causes severe fiber damage and disintegration of both beaten and unbeaten fibers. A decrease in pulp freeness, intrinsic fiber strength and pulp viscosity occurs when fibers are treated with high concentration of CMT.
2. Free radical treatment results in concurrent sheet densification in a concentration dependent fashion. Fibers become more flexible and easier to collapse after free radical treatment, which is confirmed by the increased sheet density and by direct microscopic observations.

3. Under relatively mild reaction conditions (Cond3), a freeness increase can be observed in beaten fiber stock (S-2) after free radical treatment. There is also a reduced loss in mechanical properties if fibers are treated with lower CMT chemical concentrations.
4. For unbeaten fibers (S-1), an increase of tensile strength occurs after CMT. One possible reason is fiber surface hydrolysis caused by free radical activity. This results in fibrillation of the fiber surface, which consequently increases fiber to fiber bonding.
5. For beaten fibers (S-2), a relatively mild exposure to CMT (Cond3) causes a reduction in fines and small fibril materials. Fines and fiber surface fibrils may be preferentially attacked by the free radicals because of their high specific surface area and accessibility.
6. Although the preferential hydrolysis of fines by cellulase enzymes has been reported previously (Jackson *et al.* 1993; Sarkar *et al.* 1995; Stork and Preira 1995), little research has been carried out on study the interaction between oxygen based free radicals and cellulose fibers and fines. The hydroxyl radical is a very active oxidant and usually exhibits non-specificity in reactions, and therefore should react indiscriminately with both fibers and fines. However, the free hydroxyl radical is so active and short lived in the environment (half life = 10^{-9} s), it must be generated within five to ten molecular diameters of potential reactants in order to oxidize the substrate effectively (Dreosti 1991; Cadenas 1995). Therefore, the result of free radical treatment may vary depending on the diffusion and mixing of the free radical generating reactants. Based on experimental results presented here as well as similar

treatments using cellulase enzymes, we can speculate that chelators and Fenton reagent chemicals are more likely to attack microfibril and fines because of their higher surface to weight ratio. Therefore, a properly controlled CMT could potentially serve to remove colloidal materials quickly with limited damage to the longer fiber.

7. The ESEM and light microscope observations as well as the COD measurements confirm that during treatment, fines and fibrils may be broken down to smaller components, and potentially sugars that are removed during the following washing stage. Fiber surface fibrillation and disintegration may occur in longer fibers. Under treatment conditions where small fibers are being produced faster than they are consumed, freeness levels can be expected to decrease with reaction time. For the same reason, freeness increases occur when there are more fines and fibril components being removed from the pulp slurry than are being created. Since fines are hydrophilic, their reduction renders the fibers less hydrophilic and improves the rates of drainage.
8. Despite the results showing severe fiber damage occurs when fibers are treated with high concentration of CMT, the work presented here shows that there might be potential application of a properly controlled CMT system for certain applications. For example, it is possible to improve sheet consolidation and network packing by treating low-grade coarse pulp fibers with a CMT system. Additional work is needed to explore how the CMT system may be better controlled to minimize fiber damage and exploit the low cost potential for pulp flexibility enhancements and pulp drainage enhancements. One possibility is to link the chelator to a substrate (less expensive

than an enzyme) that is large enough to keep it from penetrating into the fiber cell wall. Then we could maintain the free radical generating system on the surface of the fiber so as to minimize the less desirable fiber strength loss. We also could make the chelator to have higher affinity for specific chemical groups, by this way we may limit the generation of free radicals near target fiber area.

REFERENCES

Agosin, E., Jarpa, S., Rojas, E., and Espejo, E., 1989. Solid-state fermentation of pine sawdust by selected brown-rot fungi. *Enz. Microbial Technol.* 11:511-517.

Appel, H.M., 1993. Phenolics in ecological interactions: The importance of oxidation. *J. Chem. Ecol.* 19:1521-1552.

Aust, S.D., 1991. Transition metals in oxidative stress: An overview. In: Davies, K.J.A. (Ed.), *Oxidative damage and repair.* Pergamon Press, Oxford, UK, pp. 802-807.

Backa, S., Gierer, J., and Martin, D., 1992. Hydroxyl radical activity in brown-rot fungi studied by a new chemiluminescence method. *Holzforschung.* 46(1):61-67.

Backa, S., Gierer, J., and Martin, D., 1993. Hydroxyl radical activity associated with the growth of white-rot fungi. *Holzforschung.* 47(3):181-187.

Beinert, H., 1972. Flavins and flavoproteins, including iron-sulfur proteins. In: Swartz, H.M., Bolton, J.R. and Borg, D.C., (Eds.), *Biological Application of Electron Spin Resonance.* Wiley-Interscience, NY.

Berenbaum, M.R., 1995. Metabolic detoxification of plant pro-oxidants. In: Ahmad, S. (Ed.), *Oxidative Stress and Antioxidant Defenses in Biology.* Chapman and Hall, NY.

Bhat, G.R., Heitmann, J.A., and Joyce, W.T., 1991. Novel techniques for enhancing the strength of secondary fiber. *Tappi J.* 74(9):151-157.

Buettner, G.R., 1985. Spin trapping of hydroxyl radical. In: Greenwald, R.A., (Ed.), *CRC Handbook of Methods for Oxygen Radical Research.* Boca Raton, FL.

Cadenas, E., 1995. Mechanism of oxygen activation and reactive oxygen species detoxification. In: Ahmad, S. (Ed.), *DNA and Free Radicals.* Ellis Horwood, Chichester, UK.

Chandhoke, V., 1991. Iron-binding compounds produced by the brown-rot fungus *Gloeophyllum Trabeum. Thesis Ph.D.*, University of Maine.

Chandhoke, V., Goodell, B., Jellison, J., and Fekete, F.A., 1992. Oxidation of KTBA by iron-binding compounds produced by the wood-decaying fungus *Gloeophyllum Trabeum. FEMS Microbiol. Lett.* 90:236-266.

Chopard, C., 1992. Spin-trapping in biological systems. In: Catoire, B. (Ed.), *Electron Spin Resonance (ESR) Applications in Organic and Bioorganic Materials.* Springer-Verlag, Berlin.

Cobb, C.E., 1982. The non-enzymatic decomposition of cellulose by brown-rot fungus *Gloeophyllum trabeum*. *Thesis M.S.*, Michigan Tech. University.

Cohen, G., 1985. The Fenton Reaction. In: Greenwald, R.A. (Ed.), *CRC Handbook of Methods for Oxygen Radical Research*. Boca Raton, FL.

Cowan, J.A., 1993. *Inorganic Biochemistry: An Introduction.* VCH, NY.

Cowling E.B., 1961. Comparative biochemistry of the decay of sweetgum sapwood by white-rot and brown-rot fungi. *Technical bulletin No.1258.* Washington, D.C., USA: U.S. Department of Agriculture. 79pp.

Cowling, E.B. and Brown, W., 1969. Structural features of cellulosic materials in relation to enzymatic hydrolysis. *Adv. Chem. Ser.* 95:152-187.

Daniels, M.J., 1992. Using biological enzymes in paper making. *Paper Technology.* (6): 14-17.

Darlington, W.B., 1992. *TAPPI 1992 Pulping Conference Proceedings,* Tappi Press, Atlanta.

Dreosti, I.E., 1991. Free radical pathology and the genome. In: Dreosti, I.E. (Ed.), *Trace Elements, Micronutrients, and Free Radicals.* Humana Press, Clifton, NJ, pp.149-170.

Eriksson, L.A., Heitmann, J.A., and Venditti, R.A., 1997. Drainage and strength properties of OCC and ONP using enzymes with refining. *1997 TAPPI Proceedings of the Recycling Symposium.* TAPPI Press, Atlanta, pp.423-433.

Fekete, F.A., Chandhoke, V., and Jellison, J., 1989. Iron-binding compounds produced by wood-decaying basidiomycetes. *Appl. Environ. Microbiol.* 55:2720-2722.

Freiermuth, B., Garrett, M., and Jokinen, O., 1994. The use of enzymes in the production of release papers. *Paper Technology* (4):21-23.

Fridovich, I., 1976. Oxygen radicals, hydrogen peroxide, and oxygen toxicity. In: Pryor, W.A. (Ed.), *Free radicals in biology (Vol. 1)*. Academic Press. NY.

Gelvan, D. *et al.,* 1991. Small chelators and the nature of the metal ion in site-specificity of ·OH damage. In: Davies, K.J.A. (Ed.), *Oxidative damage and repair.* Oxford: Pergamon Press. p.825-830.

Gibbs, C.R., 1976. Characterization and application of ferrozine iron reagent as a ferrous iron indicator. *Anal. Chem.* 48:1197-1201.

Gierer, M.J., Jansbo, K., and Reitberger, T., 1989. *Holzforschung,* 43:391.

Goodell, B., Jellison, J., Enoki, A., Liu, J., Lu, J., Tanaka, H., Paszczynski, A., and Fekete, F., 1994. Redox reactions associated with oxidative degradation mediated by fungal biochelators from *G. trabeum.* Presented at FPS 1994 Meeting at Portland, ME.

Goodell, B., Jellison, J., Liu, J., Daniel, G., Paszczynski, A., Fekete, F., Krishnamurthy, S., Lu, J., and Xu, G., 1997. Low molecular weight chelators and phenolic compounds isolated from wood decay fungi and their role in the fungal biodegradation of wood. *Journal of Biotechnology.* 53:133-162.

Goodell, B., and Jellison, J., 1998. Chapter 15: the role of biological metal chelators in wood degradation and in xenobiotic degradation. In: Bruce, A. and Palfreyman, J.W. (Eds.), *Forest Products Biotechnology.* Taylor & Francis, Bristol, PA.

Green, F., Larsen, M.J., Winandy, J.E., and Highley, T.L., 1991. Role of oxalic acid in incipient brown-rot decay. *Mater. Org.* 26:191-213.

Gutteridge, J.M.C., and Rago, S., 1986. Copper + zinc and manganese superoxide dismutases inhibit deoxyribose degradation by the superoxide-driven Fenton reaction at two different stages. *Biochem. J.* 234:225-228.

Halliwell, B., 1965. Catalytical decomposition of cellulose under biological conditions. *Biochem. J.* 95:518-536.

Halliwell, B., and Gutteridge, J.M.C., 1984. Role of iron in oxygen radical reactions. *Meth. Enzymol.* 105:47-56.

Halliwell, B., and Gutteridge, J.M.C., 1988. Iron as a biological prooxidant. *ISI Atlas of Science, Biochemistry.* 1: 48-52.

Halliwell, B. and Gutteridge, J.M.C., 1989. Free radicals in biology and medicine, 2nd ed. Oxford: Clarendon Press.

Hamilton, F. (Ed.), 1987. Secondary fibers and non-wood pulping. *Pulp and Paper Manufacture.* 3: 159.

Hartwig, R.C., and Loepper, R.H., 1993. Evaluation of soil iron. In: Barton, L.L. and Hemming, B.C. (Eds.), *Iron Chelation in Plants and Soil Microorganisms.* Academic Press, NY. pp.405-482.

Heise, O.U., Unwin, J.P., Klungness, J.H., Fineran, W.G., and Abubakr, S., 1996. Industrial scaleup of enzyme-enhanced deinking of nonimpact printed toners. *Tappi J.* 79(3):207-212.

Heitmann, J.A., Joyce, T.W., and Prasad, D.Y., 1992. Enzyme deinking of newsprint waste. *5th International Conference on Biotechnology in the Pulp and Paper Industry.* Vancouver. pp.175.

Highley T.L., 1980. Cellulose degradation by cellulase clearing and non-clearing brown-rot fungi. *Appl. Environ. Microbiol.* 40:1145-1147.

Hirano, T., Tanaka, H., and Enoki, A., 1995. Extracellular substance from the brown-rot basidiomycete *Tyromyces palustris* that reduces molecular oxygen to hydroxyl radicals and ferric iron to ferrous iron. *Mokuzai Gakkaishi.* 41:334-341.

Hyde, S.M., and Wood, P.M., 1995. A model for attack at a distance from the hyphae based on studies with the brown rot *Coniophora puteana*. *International Research Group on Wood Preservation* document no. IRG/95/10104.

Hyde, S.M., and Wood, P.M., 1997. A mechanism for production of hydroxyl radicals by the brown-rot fungus *Coniophora puteana*: Fe(III) reduction by cellobiose dehydrogenase and Fe(II) oxidation at a distance from the hyphae. *Microbiology.* 143:259-266.

Illman, B.L. and Highley, T.L., 1989. Decomposition of wood by brown-rot fungi. In: O'Rear C. E., and Llewellyn (Eds.), *Biodeterioration Research 2.* Plenum Press, NY, pp. 484-465.

Illman, B.L., Meinholtz, D.C., and Highley, T.L., 1988. Generation of hydroxyl radical by the brown-rot fungus *Postia placenta*. *International Research Group on Wood Preservation* document no. IRG/WP/1360.

Jackson, S.L., Heitmann, J.A., and Joyce, W.T., 1993. Enzymatic modification of secondary fiber. *Tappi J.* 76(3):147-154.

James, R.O., and Healy, T.Y., 1972. *J. Colloid Interface Sci.* 40(1):42.

Janzen, E.G., and Blackburn, B.J., 1969. Detection and identification of short-lived free radicals by electron spin resonance trapping techniques (spin trapping). Photolysis of organolead, -tin, and –mercury compounds. *J. Amer. Chem. Soc.* 91:4481.

Jeffries, T.W., and Klungness, J.H., 1994. Comparison of enzyme-enhanced with conventional deinking of xerographic and laser-printed paper. *Tappi J.* 77(4):173-179.

Jeffries, T.W., and Viikari, L., (Eds.) 1996. *Enzymes for Pulp and Paper Processing.* American Chemical Society Symp. Ser. Vol. 655. ACS, Washington, DC.

Jellison, J., Chandhoke, V., Goodell, B., and Fekete, F., 1991a. The isolation and immunolocalization of iron-binding compounds produced by *Gloeophyllum trabeum*. *Appl. Microbiol. Biotechnol.* 35:805-809.

Jellison, J., Chandhoke, V., Goodell, B., Fekete, F., Hayashi, N., Ishihara, M., and Yamamoto, K., 1991b. The action of siderophores isolated from *Gloeophyllum trabeum* on the structure and crystallinity of cellulose. *International Research Group on Wood Preservation Series.* Boc 5607, S-114 86. Stockholm, Sweden. Document IRG/WP 1479.

Jellison, J., Smith, J., and Shortle, W.C., 1992. Cation analysis of wood degraded by white and brown-rot fungi. *International Research Group on Wood Preservation* Document no. IRG/WP/1552.

Jellison, J., Connolly, J., Goodell, B., Doyle, B., Illman, B., Fekete, F., and Ostrofsky, A., 1997. The role of cations in the biodegradation of wood by the brown-rot fungi. *Int. Biodeteriot. Biodegrad.* 39:165-179.

Jobbins, J.M., and Frank, N.E., 1997. Enzymatic deinking of mixed office waste: process condition optimization. *Tappi J.* 80(9): 73-78.

Kalyanaraman, B., Morehouse, K.M., and Mason, R.P., 1991. An electron paramagnetic resonance study of the interactions between the adriamycin semiquinone, hydrogen peroxide, iron-chelators, and radical scavengers. *Arc. Biochem. Biophys.* 286:164-170.

Kantelinen, A., Jokinen, O., and Pere, J., 1997. The mechanism of cellulase / hemicellulase treatment for improved drainage. *1997 TAPPI Biological Sciences Symposium Proceedings.* TAPPI, Atlanta, pp. 267.

Kerem, Z., Jensen, K.A., and Hammel, K.E., 1999. Biodegradation mechanism of the brown rot basidiomycete *Gloeophyllum trabeum*: evidence for an extracellular hydroquinone-driven fenton reaction. *FEBS Letters.* 446:49-54.

Kirk, T.K., Ibach, R., Mozuch, M.D., Conner, A.H., and Highley, T., 1991. Characteristics of cotton cellulose depolymerized by a brown-rot fungus, by acid, or by chemical oxidants. *Holzforschung.* 45:239-244.

Koenigs, J.W., 1972. Production of extracellular H_2O_2 and peroxidase by brown-rot fungi. *Phytopathology.* 62:100-110.

Koenigs. J.W., 1974. Production of hydrogen peroxide by wood-rotting fungi in wood and its correlation with weight loss, depolymerization, and pH changes. *Arch. Microbio.* 99:129-145.

Koppenol, W.H., and Butler, J., 1985. *Adv. Free Radical Bio. Med.* 1:91.

Knudsen, O., Young, J.D., and Yang, J.L., 1998. Long term use of enzymatic deinking at STORA Dalum plant. In: *Proceedings of the 7th International Conference on Biotechnology of the Pulp and Paper Industry.* Vancouver, BC.

Laughton, M.J., and Tagesson, C., 1989. Antioxidant and pro-oxidant actions of the plant phenolics quercetin, gossypol and myricetin. *Biochemical Pharmacology.* 38(17):2859-2865.

Lind, J., and Merényi, G., 1997. Hydroxyl radical induced viscosity loss in cellulose fibers. *J. of Wood Chem. and Tech.* 17(1&2):111-117.

Lopez-Goni, I., Moriyon, I., and Conner, M., 1992. Identification of 2,3-dihydroxybenzoic acid as a *brucella abortus* siderophore. *Infection and Immunity.* 60(11):4496-4503.

Lu, J., 1994. The role of the high affinity iron chelators isolated from wood decay fungus *Gloeophyllum trabeum* in one electron oxidation reactions and in hydroxyl radical production. *Thesis M.S.,* University of Maine.

Mansfield, S.D., Wong, K.K.Y., Jone, E.D., and Saddler, J.N., 1996. Modification of Douglas-fir mechanical and kraft by enzyme treatment. *Tappi J.* 79(8):125-132.

Mansfield, S.D., Dickson, A.R., and Saddler, J.N., 1998. Improving paper properties by a selective enzymatic treatment of coarse pulp fibers. In: *Proceedings of the 7th International Conference on Biotechnology of the Pulp and Paper Industry.* Vancouver, BC, pp. A189.

McBride D., 1994. High-density kneading system offers alternative to conventional deinking. *Advances in Paper Recycling.* Miller Freeman Books, San Francisco, CA .

McKinney, R.W.J., 1995. Wastepaper preparation and contaminant removal. In: McKinney, R.W.J. (Ed), *Technology of Paper Recycling.* Blackie Academic & Professional, Glasgow, UK.

Mentasti, E., Pelizzetti, E. and Baiocchi, C., 1997. Electron-transfer reactions of benzene-1,2-diols with hexachloroiridate-(IV) in acidic perchlorate media. *Journal of the Chemical Society Dalton transactions.* 24:132-135.

Moran, B.R., 1996. Enzyme treatment improves refining efficiency, recycled fiber freeness. *Pulp & Paper.* (9):119-121.

Moran, J.F., 1997. Complexes of iron with phenolic compounds from soybean nodules and other legume tissues: prooxidant and antioxidant properties. *Free Radical Biology & Medicine.* 22(5): 961-870.

Nagarajan, R., and Sarkar, J.M., 1996. Evaluation of drainage improvement by enzyme-polymer treatment. *1996 Papermakers Conference, TAPPI Proceedings.* Philadelphia, p.475-480.

Neilands, J.B., (Ed.) 1974. *Microbial Iron Metabolism.* Academic Press, NY.

Paszczynski, A., Crawford, R., Funk, D., and Goodell, B., 1999. De novo synthesis of 4,5-dimethoxycatechol and 2,5-dimethoxyhydroquinone by the brown-rot fungus *Gloeophyllum trabeum*. *Appl. Environ. Microbiol.* 65(2):674-679.

Patriarca, P., 1971. *Arch. Biochem. Biophys.* 145:255.

Perkins, M.J., 1980. Spin trapping. *Adv. Phys. Org. Chem.* 17:1-17.

Pommier, J.C., Fuentes, J.L., and Goma, G., 1989. Using enzymes to improve the process and the product quality in the recycled paper industry. Part 1: the basic laboratory work. *Tappi J.* 72(6):187-191.

Prasad, D.Y., 1993. Enzymatic deinking of laser and xerographic office wastes. *Appita* 46(4):289.

Puntarulo, S., and Sarkanen, K.V., 1988. Effect of oxygen concentration on microsomal oxidation of ethanol and generation of oxygen radicals. *Biochem. J.* 251:787.

Quick, T.H., and Hodgson, K.T., 1986. *Tappi J.* 69(3):102.

Reese, E.T., Siu, R.G.H., and Levinson, H.S., 1950. The biological degradation of soluble cellulose derivatives and its relationship to the mechanism of cellulose hydrolysis. *J. Bacteriol.* 59:485-497.

Reese, E.T., 1977. Degradation of polymeric carbohydrate by microbial enzymes. In: Loweus, F.A. and Rumeckles, V.C.(Eds.), *The Structure, Synthesis, and Biodegradation of Wood - Recent Adv. Phytochem.* Vol. 11. Plenum Press, NY.

Rowley, D.A., and Halliwell, B., 1983. Formation of hydroxyl radicals from hydrogen peroxide and iron salts by superoxide- and ascorbate- dependent mechanisms: relavance to the pathology of rheumatoid disease. *Clin. Sci.* 64:649-653.

Rutledge-Cropsey, K., Klungness, J.H., and Abubark, S.M., 1998. Performance of enzymatically deinked recovered paper on paper machine runnability. *Tappi J.* 81(2):148-151.

Sarkar, J.M., Cosper, D.R., and Hartig, E.J., 1995. Applying enzymes and polymers to enhance the freeness of recycled fiber. *Tappi J.* 78(2):89-95.

Schmidt, C.T., Whitten, B.K., and Nicholas, D.D., 1981. A proposed role for oxalic acid in non-enzymatic wood decay brown-rot fungi. *Am.Wood Preservers Assoc.* 77:157-164.

Shimada, M., Ma, D.B., and Akamatsu, Y., 1994. A proposed role of oxilic acid in wood decay systems of wood-rotting basidiomycetes. *FEMS Microbiol. Rev.* 131:285.

Shinde, R.F., and Hayward, C., 1991. EPR studies of iron substitution in the molecular sieve VPI-5. *J. Phys. D: Appl. Phys.* 24:1486-1488.

Shao, Y., 1997. A study of the non-enzymatic low molecular weight agent Gt-chelator isolated from *Gloeophyllum trabeum*: mechanisms of wood degradation by brown-rot fungi. *MS thesis,* University of Maine. Maine.

Smith, A.W., and Freeman, S., 1990. Characterization of siderophore from *Acinetobacter calcoaceticus*. *FEMS Microbiol. Lett.* 70:29-32.

Stookey, L.L., 1970. Ferrozine: a new spectrophotometric reagent for iron. *Analytical Chemistry.* 42(7):779-781.

Stork, R., Preira, H. *et al.,* 1995. Upgrading recycled pulps using enzymatic treatment. *Tappi J.* 78(2):79-87.

Sulzberger, B., and Laubsher, H., 1995. Reactivity of various types of iron(III) (hydr)oxides towards light-induced dissolution. *Mar. Chem.* 50:103-115.

Tanaka, N., Itakura, S., and Enoki, A., 1999. Hydroxyl radical generation by an extracellular low-molecular-weight substance and phenol oxidase activity during wood degradation by the white-rot basidiomycete *Phanerochaete chrysosporium*. *Holzforschung.* 53(1):21-28.

Tanaka, N., Akamatsu, Y., Hattori, T., and Shimada, M., 1994. Effect of oxalic acid on the oxidative breakdown of cellulose by the Fenton Reaction. *Wood Research.* 81:8-10.

TAPPI, 1992. *TAPPI Test Methods*. TAPPI Press, Atlanta, Georgia.

Vidotti, R.M., Johnson, D.A., and Thompson, E.V., 1992. *1992 Pulping Conference Proceedings.* TAPPI PRESS, Atlanta, Georgia.

Vidotti, R.M., Johnson, D.A., and Thompson, E.V., 1993. Repulping and flotation studies of photocopied and laser-printed office waste paper. Part I: repulping and image analysis. *Progress in Paper Recycling.* 8:30-39.

Walker, C., Dinus, R., McDonough, T.J., and Eriksson, K.-E.L., 1995. Evaluating three iron-based biomimetic compounds for their selectivity in a polymeric model system for pulp. *Tappi J.* 78(6):103-109.

Weil, J.A., Bolton, J.R., and Wertz, J.E., 1996. *Electron Paramagnetic Resonance: Elemental Theory and Practical Applications.* John Wiley & Sons, 2nd Ed., New York.

Wertz, B., and Bolton, C., 1972. *Electron Spin Resonance.* Springer-Verlag, Berlin.
Winterbourn, C.C., 1991. Free radical biology of iron. In: Dreosti, I.E. (Ed.), *Trace Elements, Micronutrients, and Free Radicals.* Humana Press, Inc., Clifton, NJ, pp.231.

Xu, G., 1996. Cellulose degradation mediated by chelators isolated from *Gloeophyllum trabeum*: mechanism of wood degradation by brown-rot fungi. *MS thesis*, University of Maine. Maine.

Xu, J., and Jordan, B.B., 1988. Mechanism of the oxidation of 2,3-dihydroxybenzoic acid by iron(III). *Inorganic Chemistry.* 27:4563-4566.

Yang, J.L., Ma, J., and Eriksson, K.-E.L., 1996. Enzymatic deinking of recycled fibers – development of the enzymatic process. *Proceedings of Sixth International Conference of Biotechnology in the Pulp and Paper Industry,* Vienna, Austria, pp.157-162.

Zareba, M., Bober, A., Zecca, L., and Sarna, T., 1995. The effect of a synthetic neuromelanin on yield of free hydroxyl radicals generated in model systems. *Bioch. Biophys Acta.* 1271:343-348.

Zepp, R.G., Faust, B.C., and Hoigne, J., 1992. Hydroxyl radical formation in aqueous reactions (pH 3-8) of iron(II) with hydrogen peroxide: The photo-Fenton reaction. *Environ. Sci. Technol.* 26:313-319.

Zeyer, C., Rucker, J.W., Joyce, T.W., and Heitmann, J.A., 1996. Performance study of enzymatic deinking using cellulase/hemicellulase blends. *Proceedings of Sixth International Conference of Biotechnology in the Pulp and Paper Industry,* Vienna, Austria, pp.169-172.

Zeyey, C., Joyce, T.W., Heitmann, J.A., and Rucker, J.W., 1994. Factors influencing enzyme deinking of recycled fiber. *Tappi J.* 77(10):169-177.

Zollner, H.K., and Schroeder, L.R., 1997. Enzymatic deinking of non-impact printed white office paper with α-amylase. *1997 Recycling Symposium.* TAPPI Press, Atlanta, Georgia, pp. 403-408.

Zollner, H.K., and Schroeder, L.R., 1998. Enzymatic deinking of non-impact printed white office paper with α-amylase. *Tappi J.* 81(3):166-170.

APPENDICES

Appendix A. Standard Curve of Ferrozine Assay.

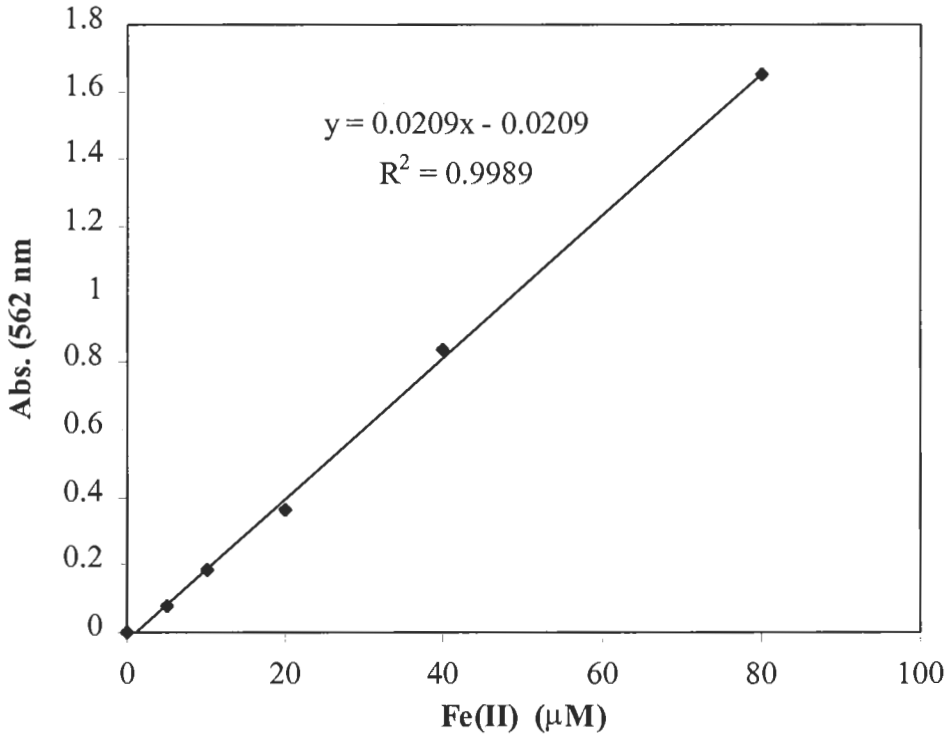

Figure A.1. Standard Curve of Ferrozine Assay. Ferrozine reagent (1.0 mM) was incubated with different concentrations of Fe(II) at pH 4.0 (acetate buffer, 100 mM). Readings at 52 nm were made 5 minutes after the Ferrozine reagent was added.

Appendix B. A Sample of the Standard Printed Sheet.

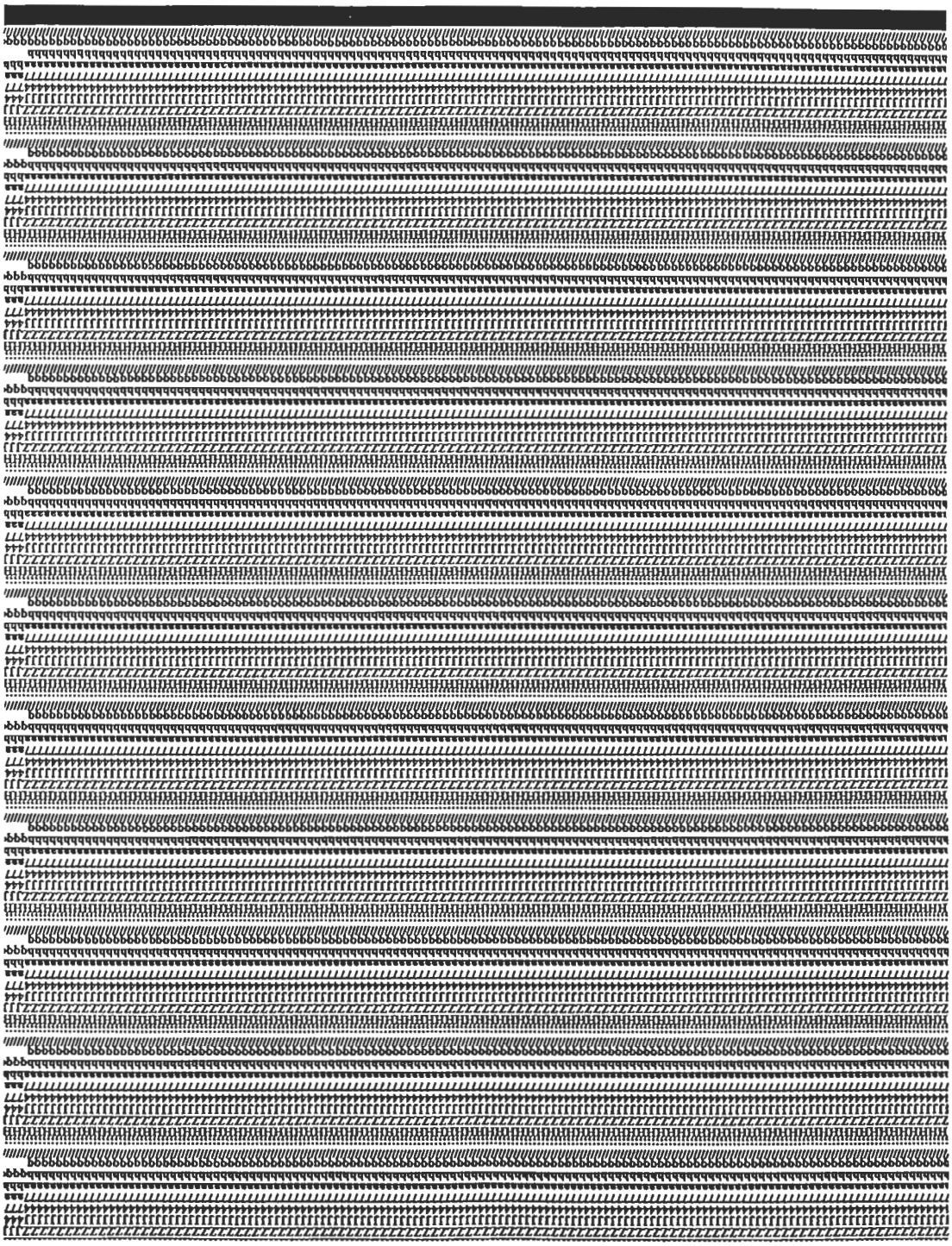

Appendix C. A Sample of the Spec *Scan® Image Analysis Output.

Apogee Systems, Inc.

Spec*Scan 2000 - V.1.2.25

Fri 7-Aug-1998 14:21

Scanner Settings: Tappi Count, 600 dpi, 6" rd, 80%
Grade Identification: Qian
Load / Reel Number: A-1

4 sheets 6-inch round
Total Area Scanned: 0.055072 sq.m.

Resolution: 600 dots/inch
Threshold: 158 (80.0%+ 0.0)
256-shade Grayscale mode
Normal Image Mode
Scan-to-Screen

Sheet Number	Speck Data Count	Area	PPM	Overall Gray Ave.	StdDev	Dirt Grayscale 2σ Min	Mode	2σ Max	Ave.	Fiber Grayscale 2σ Min	Mode	2σ Max	Ave.
1	49	4.62	335.6	199.49	6.26	52	157	158	116.8	188	199	211	199.5
2	48	4.61	335.2	199.94	6.26	52	158	158	116.8	188	200	212	200.0
3	46	4.49	325.8	200.14	6.30	51	158	158	116.7	188	201	212	200.2
4	48	4.58	332.6	199.71	6.28	51	157	158	116.7	188	199	212	199.7
Sample	191	18.30	332.3	199.82	6.28	51	157	158	116.7	188	200	212	199.9

Categories:	Min Avg. Gray	Max Avg. Gray	Min Meas. Area	Max Meas. Area	Count	Area (sq.mm)	Calculated Count (in 1 sq.meter)	PPM	Average Grayscale	Darkest Grayscale	Average Size (sq.mm)
0-39 GSV	0	39	0.020	99999							
40-79 GSV	40	79	0.020	99999							
80-119 GSV	80	119	0.020	99999	141	13.088	2560	237.7	106.06	31.00	0.093
120-129 GSV	120	129	0.020	99999	64	4.054	1162	73.6	123.88	63.00	0.063
130-139 GSV	130	139	0.020	99999	54	2.622	981	47.6	134.39	88.00	0.049
140-149 GSV	140	149	0.020	99999	50	1.966	908	35.7	143.02	107.00	0.039
150-159GSV	150	159	0.020	99999							
160-169GSV	160	169	0.020	99999							
170-255 GVV	170	255	0.020	99999							
Total > 0.02 sq mm	0	255	0.020	99999	309	21.729	5611	394.6	120.68	31.00	0.070

Sample Grayscale Brightness Analysis:

	99% Min	Mode	99% Max
Dirt Content:	38	157	158
Fiber Content:	184	200	215
Overall	184	200	215

Overall Grayscale Brightness = 199.8 = 78.4%
Overall Grayscale Std Deviation = 6.3 = 2.5%
Std.Dev. of Sheet Overall Ave. = 0.3 = 0.1%

Dirt Count Summary:

	All Sizes	>=0.040
Number of Specks:	191	191
Avg. Speck Area:	0.0958	0.0958
Median Speck Area:	0.0761	0.0761
Total Area (sq.mm):	18.30	18.30
Parts Per Million:	332.3	332.3
StdDev of Sheet PPM:	4.52	4.52
Count in 1 sq.m:	3468	3468
Counting Precision:	7.24	7.24

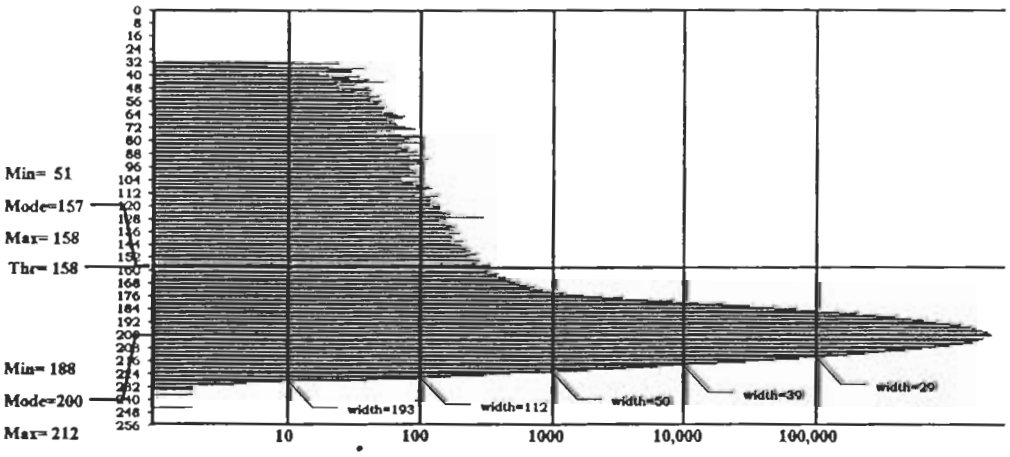

Overall Grayscale Brightness = 199.8 = 78.4%
Overall Grayscale Std Deviation = 6.3 = 2.5%

Apogee Systems, Inc.

Spec*Scan 2000 - V.1.2.25

Fri 7-Aug-1998 14:21

Scanner Settings: Tappi Count, 600 dpi, 6" rd, 80%
Grade Identification: Qian
Load / Reel Number: A-1

Resolution: 600 dots/inch
Threshold: 158 (80.0%+ 0.0)
256-shade Grayscale mode
Normal Image Mode
Scan-to-Screen

4 sheets 6-inch round
Total Area Scanned: 0.055072 sq.m.

Dirt Content Histogram	Dirt Spot Size	Sample Count	Sample Area (sq.mm)	Sample Count (in 1 sq.meter)	Sample PPM	Cumulative Count	Cumulative Area (sq.mm)	Cumulative Cum. PPM
	>= 5.000	0						
	3.00	0						
	2.50	0						
	2.00	0						
	1.50	0						
	1.00	0						
	0.80	0						
	0.60	0						
4	0.40	4	1.867	73	33.9	4	1.867	33.9
	0.30	0						
	0.25	0						
4	0.20	4	0.862	73	15.7	8	2.729	49.6
19	0.15	19	3.208	345	58.2	27	5.937	107.8
37	0.10	37	4.364	672	79.2	64	10.301	187.0
9	0.09	9	0.849	163	15.4	73	11.151	202.5
15	0.08	15	1.271	272	23.1	88	12.421	225.5
19	0.07	19	1.446	345	26.3	107	13.867	251.8
14	0.06	14	0.903	254	16.4	121	14.771	268.2
38	0.05	38	2.118	690	38.5	159	16.889	306.7
32	0.04 TAPPI	32	1.410	581	25.6	191	18.299	332.3
320								
	Totals ->	191	18.299	3468	332.3			

Categories:	Min Avg. Gray	Max Avg. Gray	Min Meas. Area	Max Meas. Area	Count	Area (sq.mm)	Calculated Count (in 1 sq.meter)	Calculated PPM	Average Grayscale	Darkest Grayscale	Average Size (sq.mm)
0-39 GSV	0	39	0.020	99999							
40-79 GSV	40	79	0.020	99999							
80-119 GSV	80	119	0.020	99999	141	13.088	2560	237.7	106.06	31.00	0.093
120-129 GSV	120	129	0.020	99999	64	4.054	1162	73.6	123.88	63.00	0.063
130-139 GSV	130	139	0.020	99999	54	2.622	981	47.6	134.39	88.00	0.049
140-149 GSV	140	149	0.020	99999	50	1.966	908	35.7	143.02	107.00	0.039
150-159GSV	150	159	0.020	99999							
160-169GSV	160	169	0.020	99999							
170-255 GVV	170	255	0.020	99999							
Total > 0.02 sq mm	0	255	0.020	99999	309	21.729	5611	394.6	120.68	31.00	0.070

Sample Grayscale Brightness Analysis:

	99% Min	Mode	99% Max
Dirt Content:	38	157	158
Fiber Content:	184	200	215
Overall	184	200	215

Overall Grayscale Brightness = 199.8 = 78.4%
Overall Grayscale Std Deviation = 6.3 = 2.5%
Std.Dev. of Sheet Overall Ave. = 0.3 = 0.1%

Dirt Count Summary:

	All Sizes	>=0.040
Number of Specks:	191	191
Avg. Speck Area:	0.0958	0.0958
Median Speck Area:	0.0761	0.0761
Total Area (sq.mm):	18.30	18.30
Parts Per Million:	332.3	332.3
StdDev of Sheet PPM:	4.52	4.52
Count in 1 sq.m:	3468	3468
Counting Precision:	7.24	7.24

Appendix D. Statistical Analysis of the Deinking Results.

D.1. ANOVA analysis of Freeness data.

D.2. ANOVA analysis of Fiber Length Measurement data.

D.3. ANOVA analysis of Brightness data.

D.4. ANOVA analysis of Tensile Strength data.

D.5. ANOVA analysis of Tear Strength data.

D.6. ANOVA analysis of Wet Zero-span Tensile Strength data.

Table D.1. ANOVA Analysis of Freeness Data.

```
Effects coding used for categorical variables in model.

Categorical values encountered during processing are:  SAMPLE$ (3 levels)
   C-1, T-1, T-2

Dep Var: FREENESS   N: 9   Multiple R: 0.896   Squared multiple R: 0.804

                          Analysis of Variance

Source             Sum-of-Squares   df  Mean-Square     F-ratio       P

SAMPLE$                   182.833    2       91.417      10.233       0.017

Error                      44.667    5        8.933
```

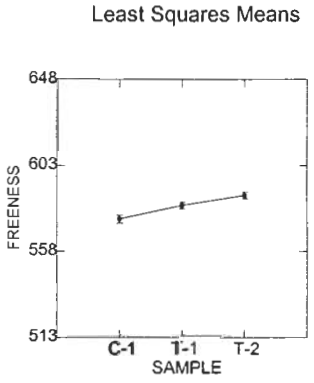


```
Durbin-Watson D Statistic     2.697
First Order Autocorrelation  -0.510
COL/
ROW SAMPLE$
  1  C-1
  2  T-1
  3  T-2
Using least squares means.
Post Hoc test of FREENESS
```

```
Tukey HSD Multiple Comparisons.
Matrix of pairwise comparison probabilities:

                    1          2          3
          1         1.000
          2         0.107      1.000
          3         0.014      0.167      1.000
```

Table D.2. ANOVA Analysis of Fiber Length Measurement Data.

```
Categorical values encountered during processing are:
SAMPLE$ (3 levels)
   C-1, T-1, T-2

Dep Var: LEN_W_W   N: 9   Multiple R: 0.694   Squared multiple R: 0.482

                          Analysis of Variance

Source            Sum-of-Squares   df  Mean-Square     F-ratio       P

SAMPLE$                    0.000    2        0.000       2.794       0.139

Error                      0.000    6        0.000
```

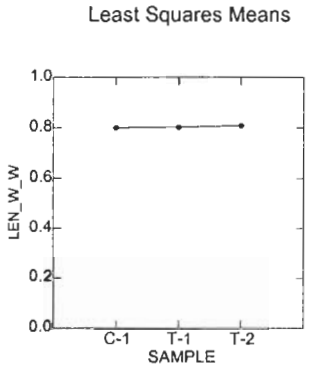


```
Durbin-Watson D Statistic     2.403
First Order Autocorrelation  -0.207
COL/
ROW SAMPLE$
  1  C-1
  2  T-1
  3  T-2
Using least squares means.
Post Hoc test of LEN_W_W

Using model MSE of 0.000 with 6 df.
Matrix of pairwise mean differences:

                    1          2          3
          1         0.000
          2         0.002      0.000
          3         0.009      0.007      0.000

Tukey HSD Multiple Comparisons.
Matrix of pairwise comparison probabilities:

                    1          2          3
          1         1.000
          2         0.864      1.000
          3         0.139      0.268      1.000
```

Table D.3. ANOVA Analysis of Brightness Data.

```
Categorical values encountered during processing are:
SAMPLE$ (4 levels)
   C-1, Copy, T-1, T-2

Dep Var: BRIGHTNESS   N: 12   Multiple R: 0.943   Squared multiple R: 0.889

                          Analysis of Variance
Source              Sum-of-Squares   df  Mean-Square     F-ratio       P

SAMPLE$                     25.545    3        8.515      18.627       0.001

Error                        3.200    7        0.457
```

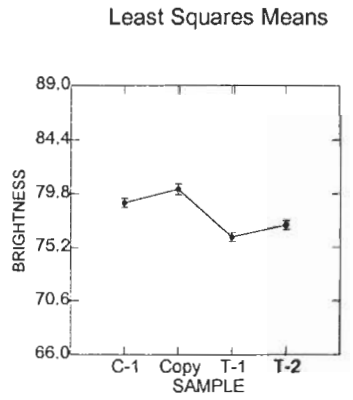


```
Durbin-Watson D Statistic     3.340
First Order Autocorrelation  -0.674
COL/
ROW SAMPLE$
  1  C-1
  2  Copy
  3  T-1
  4  T-2
Using least squares means.
Post Hoc test of BRIGHTNESS
```

```
Using model MSE of 0.457 with 7 df.
Matrix of pairwise mean differences:

                    1          2          3          4
          1       0.000
          2       1.167      0.000
          3      -2.900     -4.067      0.000
          4      -1.900     -3.067      1.000      0.000

Tukey HSD Multiple Comparisons.
Matrix of pairwise comparison probabilities:

                    1          2          3          4
          1       1.000
          2       0.312      1.000
          3       0.005      0.001      1.000
          4       0.042      0.007      0.343      1.000
```

Table D.4. ANOVA Analysis of Tensile Strength Data.

```
-------------------------------------------------------------------------------
Categorical values encountered during processing are:
SAMPLE$ (3 levels)
   C-1, T-1, T-2

Dep Var: TENSILE   N: 9   Multiple R: 0.487   Squared multiple R: 0.237

                          Analysis of Variance
Source            Sum-of-Squares   df  Mean-Square     F-ratio       P

SAMPLE$                    7.132    2        3.566       0.931       0.445

Error                     22.993    6        3.832
-------------------------------------------------------------------------------
```

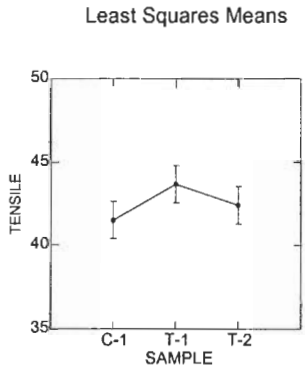


```
Durbin-Watson D Statistic     2.357
First Order Autocorrelation  -0.358
COL/
ROW SAMPLE$
  1  C-1
  2  T-1
  3  T-2
Using least squares means.
Post Hoc test of TENSILE
-------------------------------------------------------------------------------
Using model MSE of 3.832 with 6 df.
Matrix of pairwise mean differences:

                    1           2           3
          1       0.000
          2       2.170       0.000
          3       0.900      -1.270       0.000

Tukey HSD Multiple Comparisons.
Matrix of pairwise comparison probabilities:

                    1           2           3
          1       1.000
          2       0.418       1.000
          3       0.844       0.720       1.000
-------------------------------------------------------------------------------
```

Table D.5. ANOVA Analysis of Tear Strength Data.

```
Categorical values encountered during processing are:
SAMPLE$ (3 levels)
   C-1, T-1, T-2

Dep Var: TEAR   N: 9   Multiple R: 0.208   Squared multiple R: 0.043

                          Analysis of Variance

Source            Sum-of-Squares   df  Mean-Square     F-ratio       P

SAMPLE$                    0.270    2        0.135       0.135       0.876

Error                      6.000    6        1.000
```

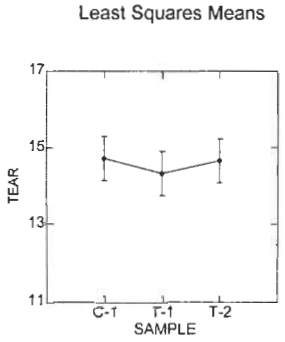


```
Durbin-Watson D Statistic     2.833
First Order Autocorrelation  -0.500
COL/
ROW SAMPLE$
  1  C-1
  2  T-1
  3  T-2
Using least squares means.
Post Hoc test of TEAR
```

```
Using model MSE of 1.000 with 6 df.
Matrix of pairwise mean differences:

                    1          2          3
          1       0.000
          2      -0.390      0.000
          3      -0.050      0.340      0.000

Tukey HSD Multiple Comparisons.
Matrix of pairwise comparison probabilities:

                    1          2          3
          1       1.000
          2       0.884      1.000
          3       0.998      0.910      1.000
```

Table D.6. ANOVA Analysis of Wet Zero-span Tensile Strength Data.

```
Categorical values encountered during processing are:
SAMPLE$ (3 levels)
   C-1, T-1, T-2

Dep Var: ZERO_SPAN   N: 9   Multiple R: 0.807   Squared multiple R: 0.651

                          Analysis of Variance

Source            Sum-of-Squares   df  Mean-Square     F-ratio       P

SAMPLE$                    0.113    2        0.057       5.592       0.043

Error                      0.061    6        0.010
```

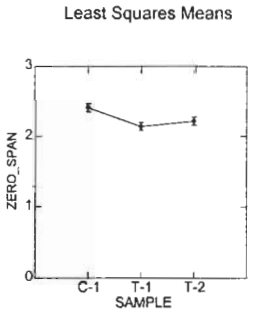


```
Durbin-Watson D Statistic     2.942
First Order Autocorrelation  -0.553
COL/
ROW SAMPLE$
  1  C-1
  2  T-1
  3  T-2
Using least squares means.
Post Hoc test of ZERO_SPAN
```

```
Using model MSE of 0.010 with 6 df.
Matrix of pairwise mean differences:

                    1          2          3
          1       0.000
          2      -0.267      0.000
          3      -0.210      0.077      0.000

Tukey HSD Multiple Comparisons.
Matrix of pairwise comparison probabilities:

                    1          2          3
          1       1.000
          2       0.040      1.000
          3       0.059      0.641      1.000
```

Appendix E. Statistical analysis of the CMT treatment results.

E.1. ANOVA analysis of Fines Content data.

E.2. ANOVA analysis of Freeness data.

E.3. ANOVA analysis of Brightness data.

E.4. ANOVA analysis of Density data.

E.5. ANOVA analysis of Tensile Strength data.

E.6. ANOVA analysis of Tear Strength data.

E.7. ANOVA analysis of Wet Zero-span Tensile Strength data.

E.8. ANOVA analysis of Viscosity data.

Table E.1. ANOVA Analysis of Fines Content Data.

a: S-1

```
Categorical values encountered during processing are:
SAMPLE$ (4 levels)
   Cond1, Cond2, Cond3, Cond4

Dep Var: FINES_CONT (S-1)  N: 12  Multiple R: 0.944   Squared multiple R: 0.892
                          Analysis of Variance

Source             Sum-of-Squares   df  Mean-Square     F-ratio       P
SAMPLE$                     2.551    3        0.850       7.236       0.058
Error                       0.310    3        0.103
```

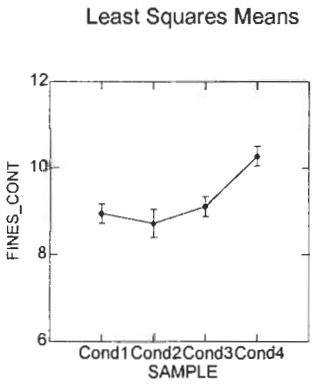


```
Durbin-Watson D Statistic     2.764
COL/
ROW SAMPLE$
  1  Cond1
  2  Cond2
  3  Cond3
  4  Cond4
Using least squares means.
Post Hoc test of FINES_CONT
Using model MSE of 0.103 with 3 df.
Matrix of pairwise mean differences:

                    1          2          3          4
          1       0.000
          2      -0.225      0.000
          3       0.165      0.390      0.000
          4       1.330      1.555      1.165      0.000

Tukey HSD Multiple Comparisons.
Matrix of pairwise comparison probabilities:

                    1          2          3          4
          1       1.000
          2       0.934      1.000
          3       0.950      0.766      1.000
          4       0.074      0.084      0.103      1.000
```

Table E.1. Cont'd

b: S-2

```
Categorical values encountered during processing are:
SAMPLE$ (4 levels)
   Cond1, Cond2, Cond3, Cond4

Dep Var: FINES_CONT (S-2)  N: 12  Multiple R: 0.954   Squared multiple R: 0.911

                          Analysis of Variance

Source              Sum-of-Squares   df  Mean-Square     F-ratio       P
SAMPLE$                     40.447    3       13.482      16.961   0.005
Error                        3.974    5        0.795
```

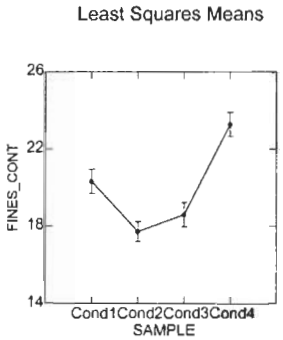


```
Durbin-Watson D Statistic     2.575
First Order Autocorrelation  -0.412
COL/
ROW SAMPLE$
  1  Cond1
  2  Cond2
  3  Cond3
  4  Cond4
Using least squares means.
Post Hoc test of FINES_CONT

Using model MSE of 0.795 with 5 df.
Matrix of pairwise mean differences:

                    1          2          3          4
          1     0.000
          2    -2.593      0.000
          3    -1.725      0.868      0.000
          4     2.955      5.548      4.680      0.000

Tukey HSD Multiple Comparisons.
Matrix of pairwise comparison probabilities:

                    1          2          3          4
          1     1.000
          2     0.083      1.000
          3     0.322      0.722      1.000
          4     0.073      0.004      0.012      1.000
```

Table E.1. Cont'd

c: S-3

```
Categorical values encountered during processing are:
SAMPLE$ (3 levels)
   Cond1, Cond3, Cond4
1 case(s) deleted due to missing data.

Dep Var: FINES_CONT (S-3)  N: 9   Multiple R: 0.869   Squared multiple R: 0.755

                        Analysis of Variance

Source            Sum-of-Squares   df  Mean-Square     F-ratio       P
SAMPLE$                    8.824    2        4.412       7.684       0.030
Error                      2.871    5        0.574
```

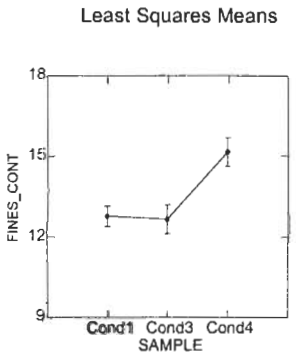


```
Durbin-Watson D Statistic     3.171
First Order Autocorrelation  -0.721
COL/
ROW SAMPLE$
  1  Cond1
  2  Cond3
  3  Cond4
Using least squares means.
Post Hoc test of FINES_CONT

Using model MSE of 0.574 with 5 df.
Matrix of pairwise mean differences:

                    1          2          3
          1       0.000
          2      -0.108      0.000
          3       2.387      2.495      0.000

Tukey HSD Multiple Comparisons.
Matrix of pairwise comparison probabilities:

                    1          2          3
          1       1.000
          2       0.985      1.000
          3       0.033      0.048      1.000
```

Table E.2. ANOVA Analysis of Freeness Data.

a: S-1

```
Categorical values encountered during processing are:
SAMPLE$ (4 levels)
   Cond1, Cond2, Cond3, Cond4

Dep Var: CSF (S-1)  N: 12   Multiple R: 0.450   Squared multiple R: 0.202
                          Analysis of Variance

Source              Sum-of-Squares   df  Mean-Square     F-ratio       P
SAMPLE$                     78.433    3       26.144       0.507   0.691
Error                      309.167    6       51.528
```

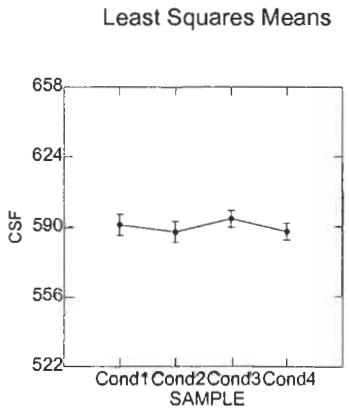


```
Durbin-Watson D Statistic     3.150
First Order Autocorrelation  -0.587
COL/
ROW SAMPLE$
  1  Cond1
  2  Cond2
  3  Cond3
  4  Cond4
Using least squares means.
Post Hoc test of CSF
Using model MSE of 51.528 with 6 df.
Matrix of pairwise mean differences:

                1          2          3          4
        1   0.000
        2  -3.500      0.000
        3   3.000      6.500      0.000
        4  -3.333      0.167     -6.333      0.000

Tukey HSD Multiple Comparisons.
Matrix of pairwise comparison probabilities:

                1          2          3          4
        1   1.000
        2   0.959      1.000
        3   0.966      0.760      1.000
        4   0.954      1.000      0.713      1.000
```

Table E.2. Cont'd

b:S-2

```
Categorical values encountered during processing are:
SAMPLE$ (4 levels)
   Cond1, Cond2, Cond3, Cond4

Dep Var: CSF (S-2) N: 12   Multiple R: 0.920   Squared multiple R: 0.847

                          Analysis of Variance
Source              Sum-of-Squares   df  Mean-Square     F-ratio       P
SAMPLE$                   1791.233    3      597.078      11.086       0.007
Error                      323.167    6       53.861
```

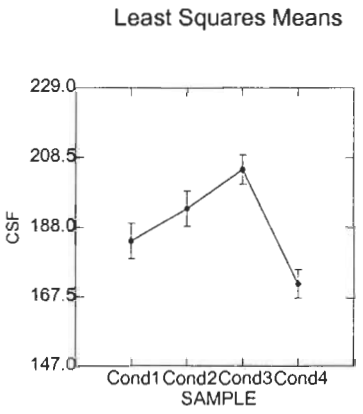


```
Durbin-Watson D Statistic     2.429
First Order Autocorrelation  -0.258
COL/
ROW SAMPLE$
  1  Cond1
  2  Cond2
  3  Cond3
  4  Cond4
Using least squares means.
Post Hoc test of CSF

Using model MSE of 53.861 with 6 df.
Matrix of pairwise mean differences:

                    1           2           3           4
          1       0.000
          2       9.500       0.000
          3      21.000      11.500       0.000
          4     -12.667     -22.167     -33.667       0.000
Tukey HSD Multiple Comparisons.
Matrix of pairwise comparison probabilities:

                    1           2           3           4
          1       1.000
          2       0.598       1.000
          3       0.073       0.392       1.000
          4       0.323       0.060       0.005       1.000
```

Table E.2. Cont'd

c:S-3

```
Categorical values encountered during processing are:
SAMPLE$ (3 levels)
   Cond1, Cond3, Cond4

Dep Var: CSF (S-3)   N: 9   Multiple R: 0.844   Squared multiple R: 0.713

                        Analysis of Variance

Source            Sum-of-Squares   df  Mean-Square     F-ratio       P
SAMPLE$                  641.667    2      320.833       8.694       0.013
Error                    258.333    7       36.905
```

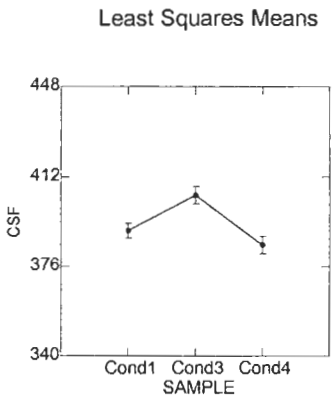


```
Durbin-Watson D Statistic     3.283
First Order Autocorrelation  -0.646
COL/
ROW SAMPLE$
  1  Cond1
  2  Cond3
  3  Cond4
Using least squares means.
Post Hoc test of CSF

Using model MSE of 36.905 with 7 df.
Matrix of pairwise mean differences:

                    1           2           3
          1       0.000
          2      14.167       0.000
          3      -5.833     -20.000       0.000

Tukey HSD Multiple Comparisons.
Matrix of pairwise comparison probabilities:

                    1           2           3
          1       1.000
          2       0.043       1.000
          3       0.460       0.012       1.000
```

Table E.3. ANOVA Analysis of Brightness Data.

a: S-1

```
Categorical values encountered during processing are:
SAMPLE$ (4 levels)
   Cond1, Cond2, Cond3, Cond4

Dep Var: BRIGHTNESS (S-1) N: 12   Multiple R: 0.899   Squared multiple R: 0.809
                          Analysis of Variance

Source              Sum-of-Squares   df  Mean-Square     F-ratio       P
SAMPLE$                     15.487    3         5.162      11.284       0.003
Error                        3.660    8         0.457
```

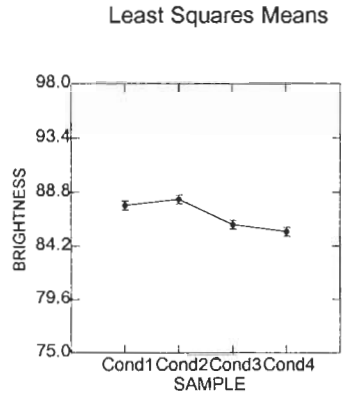


```
Durbin-Watson D Statistic     3.172
First Order Autocorrelation  -0.590
COL/
ROW SAMPLE$
  1  Cond1
  2  Cond2
  3  Cond3
  4  Cond4
Using least squares means.
Post Hoc test of BRIGHTNESS

Using model MSE of 0.457 with 8 df.
Matrix of pairwise mean differences:

                    1          2          3          4
          1       0.000
          2       0.533      0.000
          3      -1.633     -2.167      0.000
          4      -2.233     -2.767     -0.600      0.000
Tukey HSD Multiple Comparisons.
Matrix of pairwise comparison probabilities:

                    1          2          3          4
          1       1.000
          2       0.772      1.000
          3       0.071      0.018      1.000
          4       0.016      0.005      0.707      1.000
```

Table E.3. Cont'd.

b: S-2

```
Categorical values encountered during processing are:
SAMPLE$ (4 levels)
   Cond1, Cond2, Cond3, Cond4

Dep Var: BRIGHTNESS (S-2) N: 12   Multiple R: 0.848   Squared multiple R: 0.719

                              Analysis of Variance
Source              Sum-of-Squares   df  Mean-Square     F-ratio       P
SAMPLE$                      8.929    3        2.976       5.122   0.043
Error                        3.487    6        0.581
```

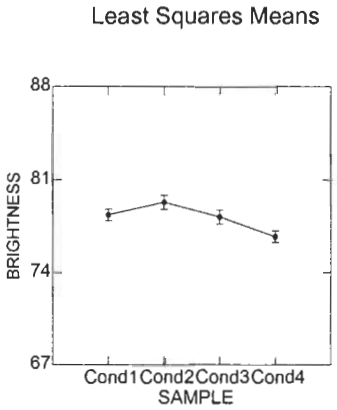


```
Durbin-Watson D Statistic     2.437
First Order Autocorrelation  -0.370
COL/
ROW SAMPLE$
  1  Cond1
  2  Cond2
  3  Cond3
  4  Cond4
Using least squares means.
Post Hoc test of BRIGHTNESS
Using model MSE of 0.581 with 6 df.
Matrix of pairwise mean differences:

                    1          2          3          4
          1     0.000
          2     0.933      0.000
          3    -0.167     -1.100      0.000
          4    -1.667     -2.600     -1.500      0.000
Tukey HSD Multiple Comparisons.
Matrix of pairwise comparison probabilities:

                    1          2          3          4
          1     1.000
          2     0.573      1.000
          3     0.995      0.520      1.000
          4     0.127      0.037      0.237      1.000
```

Table E.3. Cont'd.

c: S-3

```
Categorical values encountered during processing are:
SAMPLE$ (3 levels)
   Cond1, Cond3, Cond4

Dep Var: BRIGHTNESS (S-3)  N: 9   Multiple R: 0.927   Squared multiple R: 0.860
                          Analysis of Variance

Source              Sum-of-Squares   df  Mean-Square     F-ratio       P

SAMPLE$                      3.105    2        1.553       6.129       0.140

Error                        0.507    2        0.253
```

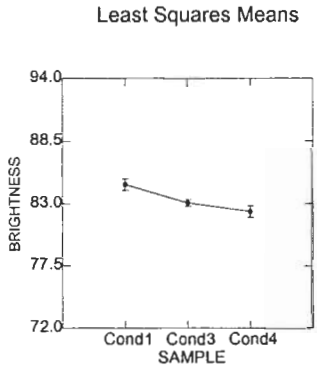


```
Durbin-Watson D Statistic     3.123
First Order Autocorrelation  -0.561
COL/
ROW SAMPLE$
  1  Cond1
  2  Cond3
  3  Cond4
Using least squares means.
Post Hoc test of BRIGHTNESS

Using model MSE of 0.253 with 2 df.
Matrix of pairwise mean differences:

                    1           2           3
          1       0.000
          2      -1.633       0.000
          3      -2.400      -0.767       0.000

Tukey HSD Multiple Comparisons.
Matrix of pairwise comparison probabilities:

                    1           2           3
          1       1.000
          2       0.188       1.000
          3       0.138       0.511       1.000
```

Table E.4. ANOVA Analysis of Density Data.

a: S-1

```
-------------------------------------------------------------------------------
Categorical values encountered during processing are:
SAMPLE$ (4 levels)
   Cond1, Cond2, Cond3, Cond4

Dep Var: DENSITY (S-1)  N: 12   Multiple R: 0.983   Squared multiple R: 0.966
                              Analysis of Variance

Source              Sum-of-Squares   df  Mean-Square     F-ratio       P
SAMPLE$                      0.010    3        0.003      65.756       0.000
Error                        0.000    7        0.000
-------------------------------------------------------------------------------
```

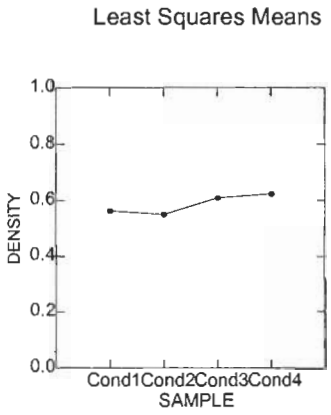


```
Durbin-Watson D Statistic     3.069
First Order Autocorrelation  -0.544
COL/
ROW SAMPLE$
  1  Cond1
  2  Cond2
  3  Cond3
  4  Cond4
Using least squares means.
Post Hoc test of DENSITY
-------------------------------------------------------------------------------
Using model MSE of 0.000 with 7 df.
Matrix of pairwise mean differences:
                      1           2           3           4
             1      0.000
             2     -0.013       0.000
             3      0.046       0.059       0.000
             4      0.060       0.073       0.014       0.000

Tukey HSD Multiple Comparisons.
Matrix of pairwise comparison probabilities:

                      1           2           3           4
             1      1.000
             2      0.272       1.000
             3      0.000       0.000       1.000
             4      0.000       0.000       0.155       1.000
-------------------------------------------------------------------------------
```

Table E.4. Cont'd

b: S-2

```
Categorical values encountered during processing are:
SAMPLE$ (4 levels)
   Cond1, Cond2, Cond3, Cond4
Dep Var: DENSITY (S-2)  N: 12  Multiple R: 0.985   Squared multiple R: 0.970
                        Analysis of Variance

Source            Sum-of-Squares   df  Mean-Square     F-ratio       P
SAMPLE$                    0.011    3        0.004      42.718       0.002
Error                      0.000    4        0.000
```

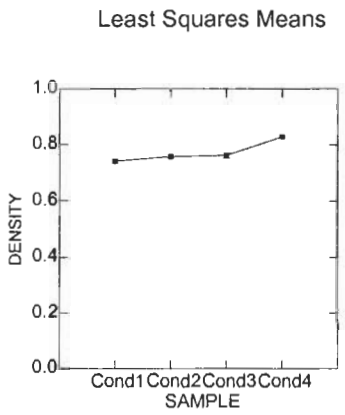


```
Durbin-Watson D Statistic     3.105
First Order Autocorrelation  -0.569
COL/
ROW SAMPLE$
  1  Cond1
  2  Cond2
  3  Cond3
  4  Cond4
Using least squares means.
Post Hoc test of DENSITY

Using model MSE of 0.000 with 4 df.
Matrix of pairwise mean differences:
                    1          2          3          4
          1     0.000
          2     0.016      0.000
          3     0.020      0.004      0.000
          4     0.086      0.070      0.066      0.000

Tukey HSD Multiple Comparisons.
Matrix of pairwise comparison probabilities:

                    1          2          3          4
          1     1.000
          2     0.402      1.000
          3     0.392      0.983      1.000
          4     0.002      0.004      0.012      1.000
```

Table E.4. ANOVA Analysis of Density Data.

c: S-3

```
------------------------------------------------------------------------------
Categorical values encountered during processing are:
SAMPLE$ (3 levels)
   Cond1, Cond3, Cond4

Dep Var: DENSITY (S-3)  N: 9   Multiple R: 0.963   Squared multiple R: 0.928
                          Analysis of Variance

Source              Sum-of-Squares   df  Mean-Square     F-ratio       P
SAMPLE$                      0.004    2        0.002      25.635       0.005
Error                        0.000    4        0.000
------------------------------------------------------------------------------
```

Least Squares Means

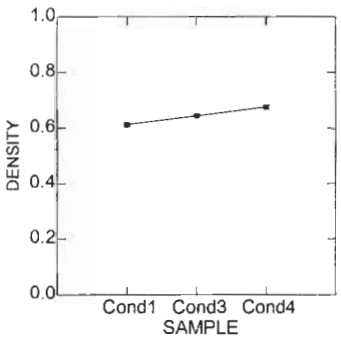


```
Durbin-Watson D Statistic     2.032
First Order Autocorrelation  -0.143
COL/
ROW SAMPLE$
  1  Cond1
  2  Cond3
  3  Cond4
Using least squares means.
Post Hoc test of DENSITY
------------------------------------------------------------------------------

Using model MSE of 0.000 with 4 df.
Matrix of pairwise mean differences:

                    1           2           3
          1         0.000
          2         0.032       0.000
          3         0.063       0.031       0.000

Tukey HSD Multiple Comparisons.
Matrix of pairwise comparison probabilities:

                    1           2           3
          1         1.000
          2         0.036       1.000
          3         0.004       0.038       1.000
------------------------------------------------------------------------------
```

Table E.5. ANOVA Analysis of Tensile Strength Data.

a: S-1

```
Categorical values encountered during processing are:
SAMPLE$ (4 levels)
   Cond1, Cond2, Cond3, Cond4

Dep Var: TENSILE (S-1)   N: 12   Multiple R: 0.973   Squared multiple R: 0.946
                         Analysis of Variance

Source              Sum-of-Squares   df  Mean-Square     F-ratio       P
SAMPLE$                     44.419    3      14.806      41.070       0.000
Error                        2.524    7       0.361
```

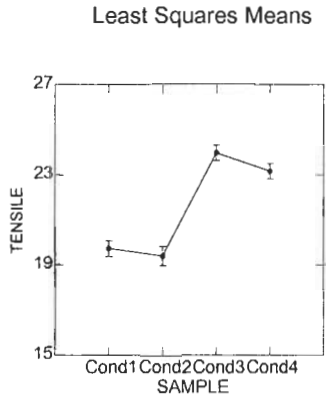


```
Durbin-Watson D Statistic     3.018
First Order Autocorrelation  -0.546
COL/
ROW SAMPLE$
  1  Cond1
  2  Cond2
  3  Cond3
  4  Cond4
Using least squares means.
Post Hoc test of TENSILE

Using model MSE of 0.361 with 7 df.
Matrix of pairwise mean differences:
                1           2           3           4
        1   0.000
        2  -0.338       0.000
        3   4.257       4.595       0.000
        4   3.440       3.778      -0.817       0.000

Tukey HSD Multiple Comparisons.
Matrix of pairwise comparison probabilities:

                1           2           3           4
        1   1.000
        2   0.923       1.000
        3   0.000       0.000       1.000
        4   0.001       0.001       0.406       1.000
```

Table E.5. Cont'd

b: S-2

```
-------------------------------------------------------------------------------
Categorical values encountered during processing are:
SAMPLE$ (4 levels)
   Cond1, Cond2, Cond3, Cond4
Dep Var: TENSILE (S-2)   N: 12   Multiple R: 0.848   Squared multiple R: 0.718
                              Analysis of Variance

Source            Sum-of-Squares   df  Mean-Square     F-ratio       P
SAMPLE$                   14.744    3        4.915       5.101   0.043
Error                      5.781    6        0.963
-------------------------------------------------------------------------------
```

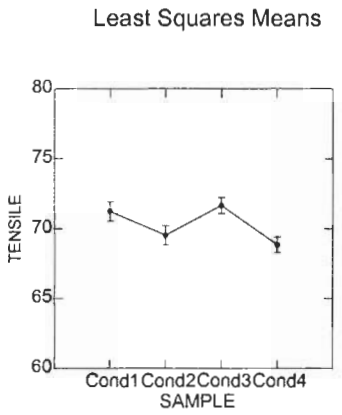


```
Durbin-Watson D Statistic     3.097
First Order Autocorrelation  -0.559
COL/
ROW SAMPLE$
  1  Cond1
  2  Cond2
  3  Cond3
  4  Cond4
Using least squares means.
Post Hoc test of TENSILE
-------------------------------------------------------------------------------
Using model MSE of 0.963 with 6 df.
Matrix of pairwise mean differences:

                1          2          3          4
        1   0.000
        2  -1.700      0.000
        3   0.428      2.128      0.000
        4  -2.378     -0.678     -2.807      0.000

Tukey HSD Multiple Comparisons.
Matrix of pairwise comparison probabilities:

                1          2          3          4
        1   1.000
        2   0.386      1.000
        3   0.961      0.183      1.000
        4   0.130      0.871      0.048      1.000
-------------------------------------------------------------------------------
```

Table E.5. Cont'd

c: S-3

```
Categorical values encountered during processing are:
SAMPLE$ (3 levels)
   Cond1, Cond3, Cond4

Dep Var: TENSILE (S-3)  N: 9   Multiple R: 0.734   Squared multiple R: 0.539
                          Analysis of Variance

Source              Sum-of-Squares   df  Mean-Square     F-ratio       P
SAMPLE$                      8.672    2        4.336       2.927       0.144
Error                        7.407    5        1.481
```

Least Squares Means

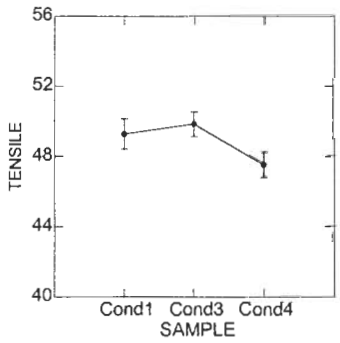


```
Durbin-Watson D Statistic     2.832
First Order Autocorrelation  -0.420
COL/
ROW SAMPLE$
  1  Cond1
  2  Cond3
  3  Cond4
Using least squares means.
Post Hoc test of TENSILE
```

```
Using model MSE of 1.481 with 5 df.
Matrix of pairwise mean differences:

                    1          2          3
          1       0.000
          2       0.557      0.000
          3      -1.770     -2.327      0.000

Tukey HSD Multiple Comparisons.
Matrix of pairwise comparison probabilities:

                    1          2          3
          1       1.000
          2       0.874      1.000
          3       0.331      0.139      1.000
```

Table E.6. ANOVA Analysis of Tear Strength Data.

a: S-1

```
------------------------------------------------------------------------------
Categorical values encountered during processing are:
SAMPLE$ (4 levels)
   Cond1, Cond2, Cond3, Cond4

Dep Var: TEAR (S-1)   N: 12   Multiple R: 0.662   Squared multiple R: 0.438
                          Analysis of Variance

Source            Sum-of-Squares   df  Mean-Square     F-ratio       P
SAMPLE$                    0.329    3        0.110       1.559       0.294
Error                      0.422    6        0.070
------------------------------------------------------------------------------
```

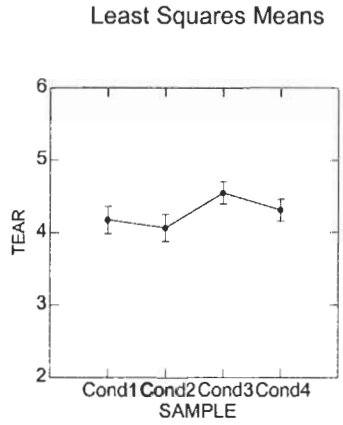


```
Durbin-Watson D Statistic     3.284
First Order Autocorrelation  -0.693
COL/
ROW SAMPLE$
  1  Cond1
  2  Cond2
  3  Cond3
  4  Cond4
Using least squares means.
Post Hoc test of TEAR
------------------------------------------------------------------------------
Using model MSE of 0.070 with 6 df.
Matrix of pairwise mean differences:
                    1           2           3           4
              1     0.000
              2    -0.110       0.000
              3     0.375       0.485       0.000
              4     0.138       0.248      -0.237       0.000

Tukey HSD Multiple Comparisons.
Matrix of pairwise comparison probabilities:

                    1           2           3           4
              1     1.000
              2     0.974       1.000
              3     0.468       0.284       1.000
              4     0.937       0.742       0.707       1.000
------------------------------------------------------------------------------
```

Table E.6. Cont'd

b: S-2

```
Categorical values encountered during processing are:
SAMPLE$ (4 levels)
   Cond1, Cond2, Cond3, Cond4

Dep Var: TEAR (S-2)  N: 12  Multiple R: 0.926   Squared multiple R: 0.858
                          Analysis of Variance

Source            Sum-of-Squares   df  Mean-Square     F-ratio       P
SAMPLE$                    2.134    3        0.711      12.091       0.006
Error                      0.353    6        0.059
```

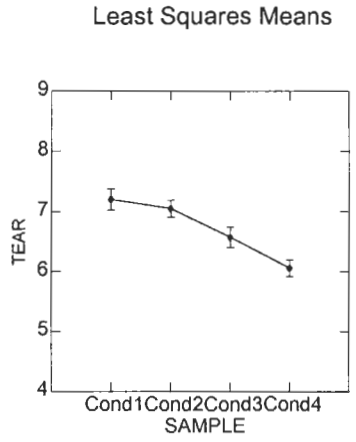


```
Durbin-Watson D Statistic     3.107
First Order Autocorrelation  -0.626
COL/
ROW SAMPLE$
  1  Cond1
  2  Cond2
  3  Cond3
  4  Cond4
Using least squares means.
Post Hoc test of TEAR
-------------------------------------------------------------------------------
Using model MSE of 0.059 with 6 df.
Matrix of pairwise mean differences:
                    1          2          3          4
             1    0.000
             2   -0.153      0.000
             3   -0.630     -0.477      0.000
             4   -1.143     -0.990     -0.513      0.000
Tukey HSD Multiple Comparisons.
Matrix of pairwise comparison probabilities:

                    1          2          3          4
             1    1.000
             2    0.896      1.000
             3    0.140      0.238      1.000
             4    0.008      0.010      0.196      1.000
-------------------------------------------------------------------------------
```

Table E.6. ANOVA Analysis of Tear Strength Data.

c: S-3

```
Categorical values encountered during processing are:
SAMPLE$ (3 levels)
   Cond1, Cond3, Cond4
Dep Var: TEAR (S-3)  N: 9   Multiple R: 0.674   Squared multiple R: 0.454
                        Analysis of Variance

Source              Sum-of-Squares   df  Mean-Square     F-ratio       P
SAMPLE$                      0.587    2        0.293       2.495   0.163
Error                        0.706    6        0.118
```

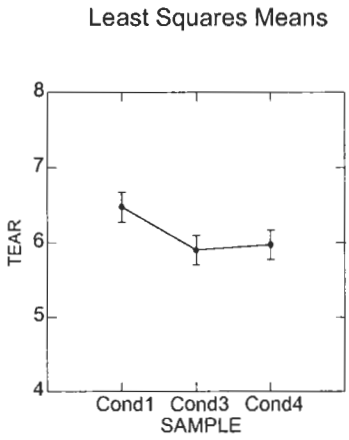


```
Durbin-Watson D Statistic     1.655
First Order Autocorrelation  -0.035
COL/
ROW SAMPLE$
  1  Cond1
  2  Cond3
  3  Cond4
Using least squares means.
Post Hoc test of TEAR
```

```
Using model MSE of 0.118 with 6 df.
Matrix of pairwise mean differences:

                    1          2          3
          1       0.000
          2      -0.573      0.000
          3      -0.503      0.070      0.000

Tukey HSD Multiple Comparisons.
Matrix of pairwise comparison probabilities:

                    1          2          3
          1       1.000
          2       0.182      1.000
          3       0.249      0.966      1.000
```

Table E.7. ANOVA Analysis of Wet Zero-span Tensile Strength Data.

a: S-1

```
Categorical values encountered during processing are:
SAMPLE$ (4 levels)
   Cond1, Cond2, Cond3, Cond4

Dep Var: ZERO_SPAN (S-1) N: 12   Multiple R: 0.927   Squared multiple R: 0.860
                                 Analysis of Variance
Source              Sum-of-Squares   df  Mean-Square     F-ratio       P
SAMPLE$                      0.659    3        0.220      16.405       0.001
Error                        0.107    8        0.013
```

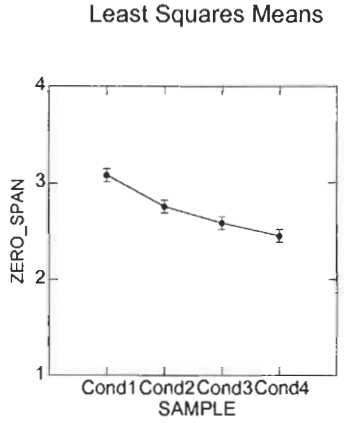


```
Durbin-Watson D Statistic     2.273
First Order Autocorrelation  -0.201
COL/
ROW SAMPLE$
  1  Cond1
  2  Cond2
  3  Cond3
  4  Cond4
Using least squares means.
Post Hoc test of ZERO_SPAN
Using model MSE of 0.013 with 8 df.
Matrix of pairwise mean differences:
                        1           2           3           4
             1          0.000
             2         -0.323       0.000
             3         -0.493      -0.170       0.000
             4         -0.627      -0.303      -0.133       0.000

Tukey HSD Multiple Comparisons.
Matrix of pairwise comparison probabilities:

                        1           2           3           4
             1          1.000
             2          0.037       1.000
             3          0.004       0.340       1.000
             4          0.001       0.050       0.527       1.000
```

Table E.7. Cont'd

b: S-2

```
Categorical values encountered during processing are:
SAMPLE$ (4 levels)
   Cond1, Cond2, Cond3, Cond4

Dep Var: ZERO_SPAN (S-2) N: 12   Multiple R: 0.961   Squared multiple R: 0.924
                                 Analysis of Variance

Source              Sum-of-Squares   df  Mean-Square     F-ratio       P
SAMPLE$                      1.844    3        0.615      24.471       0.001
Error                        0.151    6        0.025
```

Least Squares Means

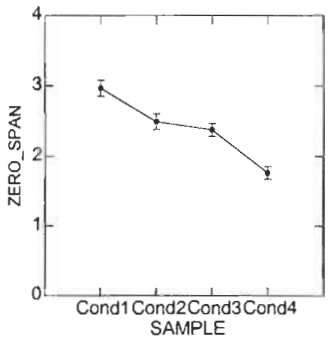


```
Durbin-Watson D Statistic     1.499
First Order Autocorrelation   0.247
COL/
ROW SAMPLE$
  1  Cond1
  2  Cond2
  3  Cond3
  4  Cond4
Using least squares means.
Post Hoc test of ZERO_SPAN
```

```
Using model MSE of 0.025 with 6 df.
Matrix of pairwise mean differences:
                        1           2           3           4
             1          0.000
             2         -0.475       0.000
             3         -0.590      -0.115       0.000
             4         -1.207      -0.732      -0.617       0.000
Tukey HSD Multiple Comparisons.
Matrix of pairwise comparison probabilities:

                        1           2           3           4
             1          1.000
             2          0.086       1.000
             3          0.025       0.855       1.000
             4          0.001       0.009       0.012       1.000
```

Table E.7. Cont'd

c: S-3

```
Categorical values encountered during processing are:
SAMPLE$ (3 levels)
   Cond1, Cond3, Cond4

Dep Var: ZERO_SPAN (S-3) N: 9   Multiple R: 0.960   Squared multiple R: 0.922
                                Analysis of Variance

Source            Sum-of-Squares   df  Mean-Square     F-ratio       P
SAMPLE$                    1.729    2        0.864      35.537       0.000
Error                      0.146    6        0.024
```

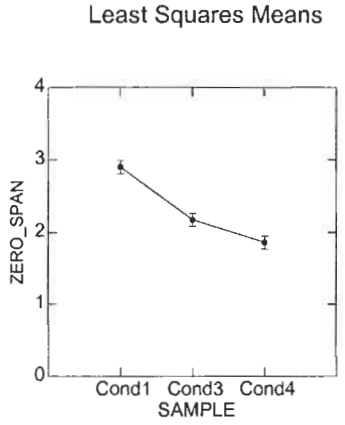


```
Durbin-Watson D Statistic     2.618
First Order Autocorrelation  -0.460
COL/
ROW SAMPLE$
  1  Cond1
  2  Cond3
  3  Cond4
Using least squares means.
Post Hoc test of ZERO_SPAN
```

```
Using model MSE of 0.024 with 6 df.
Matrix of pairwise mean differences:

                    1          2          3
          1       0.000
          2      -0.730      0.000
          3      -1.047     -0.317      0.000

Tukey HSD Multiple Comparisons.
Matrix of pairwise comparison probabilities:

                    1          2          3
          1       1.000
          2       0.003      1.000
          3       0.000      0.104      1.000
```

Table E.8. ANOVA Analysis of Viscosity Data.

a: S-1

```
Categorical values encountered during processing are:
SAMPLE$ (4 levels)
   Cond1, Cond2, Cond3, Cond4
Dep Var: VISCOSITY (S-1) N: 12   Multiple R: 0.985   Squared multiple R: 0.969
                                 Analysis of Variance

Source              Sum-of-Squares   df  Mean-Square     F-ratio       P
SAMPLE$                    226.021    3       75.340      63.373       0.000
Error                        7.133    6        1.189
```

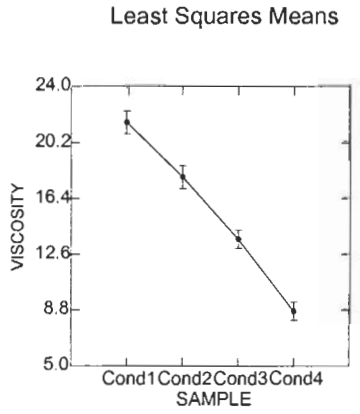


```
Durbin-Watson D Statistic     3.040
First Order Autocorrelation  -0.537
COL/
ROW SAMPLE$
  1  Cond1
  2  Cond2
  3  Cond3
  4  Cond4
Using least squares means.
Post Hoc test of VISCOSITY
-------------------------------------------------------------------------------
Using model MSE of 1.189 with 6 df.
Matrix of pairwise mean differences:
                        1           2           3           4
             1        0.000
             2       -3.710       0.000
             3       -7.940      -4.230       0.000
             4      -12.880      -9.170      -4.940       0.000

Tukey HSD Multiple Comparisons.
Matrix of pairwise comparison probabilities:

                        1           2           3           4
             1        1.000
             2        0.054       1.000
             3        0.001       0.021       1.000
             4        0.000       0.000       0.006       1.000
-------------------------------------------------------------------------------
```

Table E.8. Cont'd

b:S-2

```
Categorical values encountered during processing are:
SAMPLE$ (4 levels)
   Cond1, Cond2, Cond3, Cond4

Dep Var: VISCOSITY (S-2) N: 12   Multiple R: 0.996   Squared multiple R: 0.992
                                 Analysis of Variance

Source              Sum-of-Squares   df  Mean-Square     F-ratio       P
SAMPLE$                    266.105    3       88.702     250.934       0.000
Error                        2.121    6        0.353
```

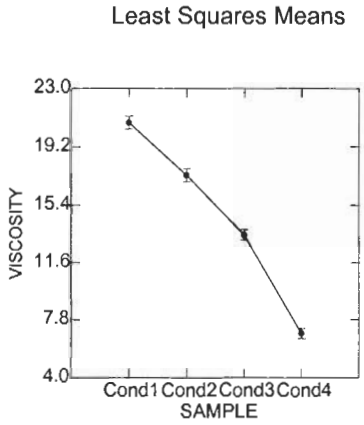


```
Durbin-Watson D Statistic     2.686
First Order Autocorrelation  -0.381
COL/
ROW SAMPLE$
  1  Cond1
  2  Cond2
  3  Cond3
  4  Cond4
Using least squares means.
Post Hoc test of VISCOSITY
-------------------------------------------------------------------------------
Using model MSE of 0.353 with 6 df.
Matrix of pairwise mean differences:
                    1           2           3           4
             1      0.000
             2     -3.425       0.000
             3     -7.348      -3.923       0.000
             4    -13.885     -10.460      -6.537       0.000

Tukey HSD Multiple Comparisons.
Matrix of pairwise comparison probabilities:

                    1           2           3           4
             1      1.000
             2      0.005       1.000
             3      0.000       0.001       1.000
             4      0.000       0.000       0.000       1.000
-------------------------------------------------------------------------------
```

Table E.8. Cont'd

c:S-3

```
Categorical values encountered during processing are:
SAMPLE$ (3 levels)
   Cond1, Cond3, Cond4

Dep Var: VISCOSITY (S-3) N: 9   Multiple R: 0.989   Squared multiple R: 0.978
                              Analysis of Variance

Source            Sum-of-Squares   df  Mean-Square     F-ratio       P
SAMPLE$                  271.842    2      135.921     136.157       0.000
Error                      5.990    6        0.998
```

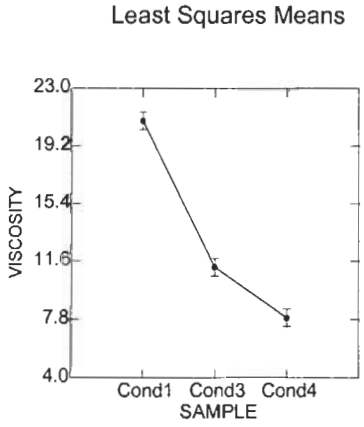


```
Durbin-Watson D Statistic     2.968
First Order Autocorrelation  -0.501
COL/
ROW SAMPLE$
  1  Cond1
  2  Cond3
  3  Cond4
Using least squares means.
Post Hoc test of VISCOSITY
Using model MSE of 0.998 with 6 df.
Matrix of pairwise mean differences:

                    1          2          3
          1       0.000
          2      -9.660      0.000
          3     -12.950     -3.290      0.000

Tukey HSD Multiple Comparisons.
Matrix of pairwise comparison probabilities:

                    1          2          3
          1       1.000
          2       0.000      1.000
          3       0.000      0.016      1.000
```

Biography of the Author

Mr. Qian was born in Harbin, China and graduated from No.1 High School in Nanjing, China. He entered Nanjing Forest University, majoring in chemical engineering. He received his bachelor's degree with university honors in July, 1991, and subsequently attended the graduate school in Nanjing Forest University, graduating in 1994 with a master's degree in chemical engineering. As an assistant engineer, he had been working at the Institute of Chemical Engineering of Forest Products in Chinese Academy of Forestry from 1994 to 1996. In September 1996, Mr. Qian joined the graduate program in Wood Science and Technology at the University of Maine, where he worked as a graduate research assistant. Yuhui Qian is a candidate for the Master of Science degree in Forestry from The University of Maine in December, 2001.